

INDEX

Welcome	5
President, Committees and Organisation	7
Faculty	9
General Information.	11
ESHNR 2012 – Schedule.	17
Scientific Programme.	18
Abstracts	24
Oral Presentations	24
Thursday, September 13 th 2012	24
Friday, September 14 th 2012	34
Saturday, September 15 th 2012.	72
Poster List	82
Educational Poster	85
Scientific Poster	105
Acknowledgement	137

Low Radiation Dose CT Scanners



MiniCAT

The Xoran MiniCAT™ is a compact, upright volume computed tomography system designed for high-resolution bone window imaging of the sinuses, temporal bones and skull base. MiniCAT™ provides immediate access to images at the patient's point-of-care, resulting in a faster diagnosis and treatment.



xCAT ENT

The Xoran xCAT® ENT is a portable, volume computed tomography system designed for high-resolution bone window imaging of the sinuses, temporal bones and skull base. The portability of xCAT® ENT makes it ideal for use pre-, intra- and post-operatively to compare and confirm surgical plans and procedures.



Exklusive Partner:

Medical Diagnostic Systems GmbH

info@volumenct.org

www.volumenct.org

WELCOME

Dear Colleagues



It is a great pleasure to welcome you to the 25th Congress and Refresher Course of the European Society of Head and Neck Radiology which is organised in cooperation with the Deutsche Röntgengesellschaft e.V. (German Society of Radiology).

The scientific programme is designed under the motto "to look at head and neck radiology from various angles". Special focus is directed on the interdisciplinary approach to the orbit, f-MRI in ENT and vascular tumours and malformations. Further lectures at invitation cover such groups of themes as the post-therapeutic imaging, imaging strategies and possible findings depending on a leading symptom, selected regions (paranasal sinuses, jaw and oral cavity), state of newer and special techniques in 2012, compartment based image interpretation as well as pitfalls and challenges. In addition, you can test your head and neck knowledge in two interactive interpretation sessions with TED. Finally, basic knowledge will be presented in the ESHNR refresher course following a two-year-rhythm.

We are particularly glad about a lot of submissions for presenting own scientific results. 35 short oral presentations, 32 scientific and 22 educational posters will deliver insights into current trends of head and neck research, interesting cases and well prepared special topics.

You are warmly invited to attend our social programme offering a get-together at the congress venue immediately after the scientific programme of the first congress day, the social evening with the ESHNR award presentation at the Ring-Café on Friday, and a guided city tour of about one hour on Friday afternoon before the social evening or alternatively on Saturday afternoon. Take the opportunity to learn about Eastern Germany's most prospering city: Leipzig – a traditional trading town with a cosmopolitan atmosphere and a long history of education and culture.

On behalf of all organisers, I wish you a multifaceted congress with new impressions as well as a pleasant stay in Leipzig.

A handwritten signature in black ink that reads 'S. Kösling'.

Sabrina Kösling

President of 25th ESHNR Congress

Exploring new Routes

KARL STORZ Instruments



STORZ
KARL STORZ – ENDOSKOPE
THE DIAMOND STANDARD

KARL STORZ GmbH & Co. KG, Mittelstraße 8, D-78532 Tuttlingen/Germany, Phone: +49 (0)7461 708-0, Fax: +49 (0)7461 708-105, E-Mail: info@karlstorz.de
KARL STORZ Endoscopy America, Inc, 2151 E. Grand Avenue, El Segundo, CA 90245-5017, USA, Phone: +1-424-218-8100, Fax: +1-800-321-1304, E-Mail: info@kse.com
KARL STORZ Endoscopia Latino-America, 815 N. W. 57 Av., Suite No. 480, Miami, FL 33126-2042, USA, Phone: +1 305 262-8960, Fax: +1 305 262-89 86, E-Mail: info@ksela.com
KARL STORZ Endoscopy Canada Ltd., 2345 Argentea Road, Suite 100, Mississauga, Ontario L5N 8K4, Phone: +1 905 816-8100, Fax: +1 905 858-0933, E-Mail: info@karlstorz.ca
www.karlstorz.com

PRESIDENT, COMMITTEES AND ORGANISATION

Congress president

Sabrina Kösling

Martin-Luther-Universität Halle-Wittenberg
Klinik für Diagnostische Radiologie
E-Grube-Str. 40
06097 Halle (Germany)
sabrina.koesling@medizin.uni-halle.de

Local organising committee

Sylva Bartel-Friedrich (Halle/Germany)
Silvio Brandt (Halle/Germany)
Florian Dammann (Göppingen/Germany)
Holger Greess (Esslingen/Germany)
Marc Keberle (Paderborn/Germany)
Sabrina Kösling (Halle/Germany)
Thi Dao Nguyen (Halle/Germany)

Scientific committee

Sylva Bartel-Friedrich (Halle/Germany)
Minerva Becker (Geneva/Switzerland)
Christian Czerny (Vienna/Austria)
Erich Hofmann (Fulda/Germany)
Michael Lell (Erlangen/Germany)
Sabrina Kösling (Halle/Germany)
Martin Mack (Munich/Germany)
Berit Verbist (Leiden/Netherlands)

General Organisation

Deutsche Röntgengesellschaft e.V.

Office
Ernst-Reuter-Platz 10
10587 Berlin (Germany)
Telefon: 0049 / 30 / 916 070 0
eshnr@drg.de

Thinking ahead. Focused on life.



Kleinste Strukturen verdienen unsere beste Auflösung



Hochpräzise Röntgentechnologie für exzellente Diagnostik

Als favorisiertes System von HNO-Ärzten und Universitäten bietet Ihnen 3D Accuitomo 170 höchste Aufnahmequalität und größtmögliche Flexibilität in 9 unterschiedlichen Aufnahmevolumen (FOV). Mit einer Auflösung von mehr als 2lp/mm und einer Voxelgröße von 80µm erhalten Sie detaillierte Einblicke in alle Bereiche des Kopfes, einschließlich der feinsten Knochenstrukturen des Innenohres sowie der Anatomie der Nasennebenhöhlen. Sie profitieren von hochpräzisen Aufnahmen – für eine sichere Diagnose und optimale Behandlungsplanung. Erfahren Sie mehr über 3D Accuitomo 170 unter www.morita.de/hno



ic med EDV-Systemlösungen für die Medizin GmbH
Walther-Rathenau-Str. 4 | D-06116 Halle/Saale | www.ic-med.de
Tel.: 0345 2984190 | Fax: 0345 29841960 | info@ic-med.de

FACULTY

- Bartel-Friedrich, Sylva** (Halle/Germany)
- Bartsch, Andreas** (Heidelberg/Germany)
- Beale, Timothy** (London/United Kingdom)
- Becker, Minerva** (Geneve/Switzerland)
- Bisdas, Sotirios** (Tübingen/Germany)
- Bloching, Marc Boris** (Berlin/Germany)
- Borges, Alexandra** (Lisbon/Portugal)
- Brandt, Silvio** (Halle/Germany)
- Casselmann, Jan** (Bruges/Belgium)
- Czerny, Christian** (Vienna/Austria)
- Dammann, Florian** (Göppingen/Germany)
- Dubrulle, Frédérique** (Lille Cedex/France)
- Eggesbø, Heidi Beate** (Oslo/Norway)
- Ernemann, Ulrike** (Tübingen/Germany)
- Farina, Davide** (Brescia/Italy)
- Forsting, Michael** (Essen/Germany)
- Freling, Nicole** (Amsterdam/The Netherlands)
- Greess, Holger** (Esslingen/Germany)
- Hofmann, Erich** (Fulda/Germany)
- Imhof, Herwig** (Vienna/Austria)
- Jäger, Lorenz** (Saarbrücken/Germany)
- Kabala, Julian** (Bristol/United Kingdom)
- Karaman, Can** (Aydin/Turkey)
- Keberle, Marc** (Paderborn/Germany)
- Kösling, Sabrina** (Halle/Germany)
- Kress, Bodo** (Frankfurt am Main/Germany)
- Lell, Michael** (Erlangen/Germany)
- Lemmerling, Marc** (Gent/Belgium)
- Mack, Martin G.** (Munich/Germany)
- Maroldi, Roberto** (Brescia/Italy)
- Meltendorf, Christian** (Halle/Germany)
- Müller-Forell, Wibke** (Mainz/Germany)
- Nguyen, Thi Dao** (Halle/Germany)
- Olliff, Julie** (Birmingham/United Kingdom)
- Stippich, Christoph** (Basel/Switzerland)
- Trojanovska, Agnieszka** (Lublin/Poland)
- Verbist, Berit M.** (Leiden/The Netherlands)
- Werner, Jochen A.** (Marburg/Germany)



**“Sophistication and power in the datacenter.
 Simplicity and elegance at your fingertips.”**

iNtuitionCLOUD – Public and Private

TeraRecon is the first and only provider of true thin-client advanced visualization in the Cloud. Free evaluation accounts are available at www.terarecon.com/cloud.

The runaway success of the public iNtuitionCLOUD has proven the power and capability of TeraRecon’s cloud technology, which is completely self-contained and not reliant on any third-party service for cloud hosting services. As a result, an equally-capable **Private** iNtuitionCLOUD is possible, with all security and access controls remaining within the healthcare enterprise.



info@terarecon.com | www.terarecon.com | +49 69 9510 3520 | 0800 837 2732

iNtuition and the iNtuition logo are trademarks of TeraRecon, Inc. Copyright© 2012 TeraRecon, Inc. All rights reserved.
 072512AQ_A-ESHNR/CLOUD_A1

GENERAL INFORMATION

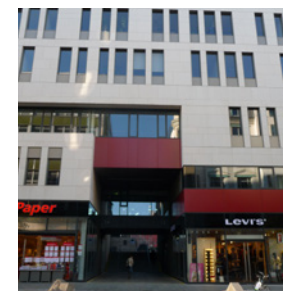
Congress Venue

The Congress will take place on the second floor of the main auditory building (Hörsaalgebäude) within the campus of the University of Leipzig. It is directly situated in Leipzig’s busy city centre and in walking distance of the main railway station and hotels of the inner city. The MDR High-Rise Building, which was part of the university complex in the past, is visible from nearly each point of the city and can be used as direction sign.

ADDRESS: Lecture hall building (Hörsaalgebäude) Universität Leipzig, Universitätsstr. 3, 04109 Leipzig



Congress Venue



Entrance from Grimmaische Str.



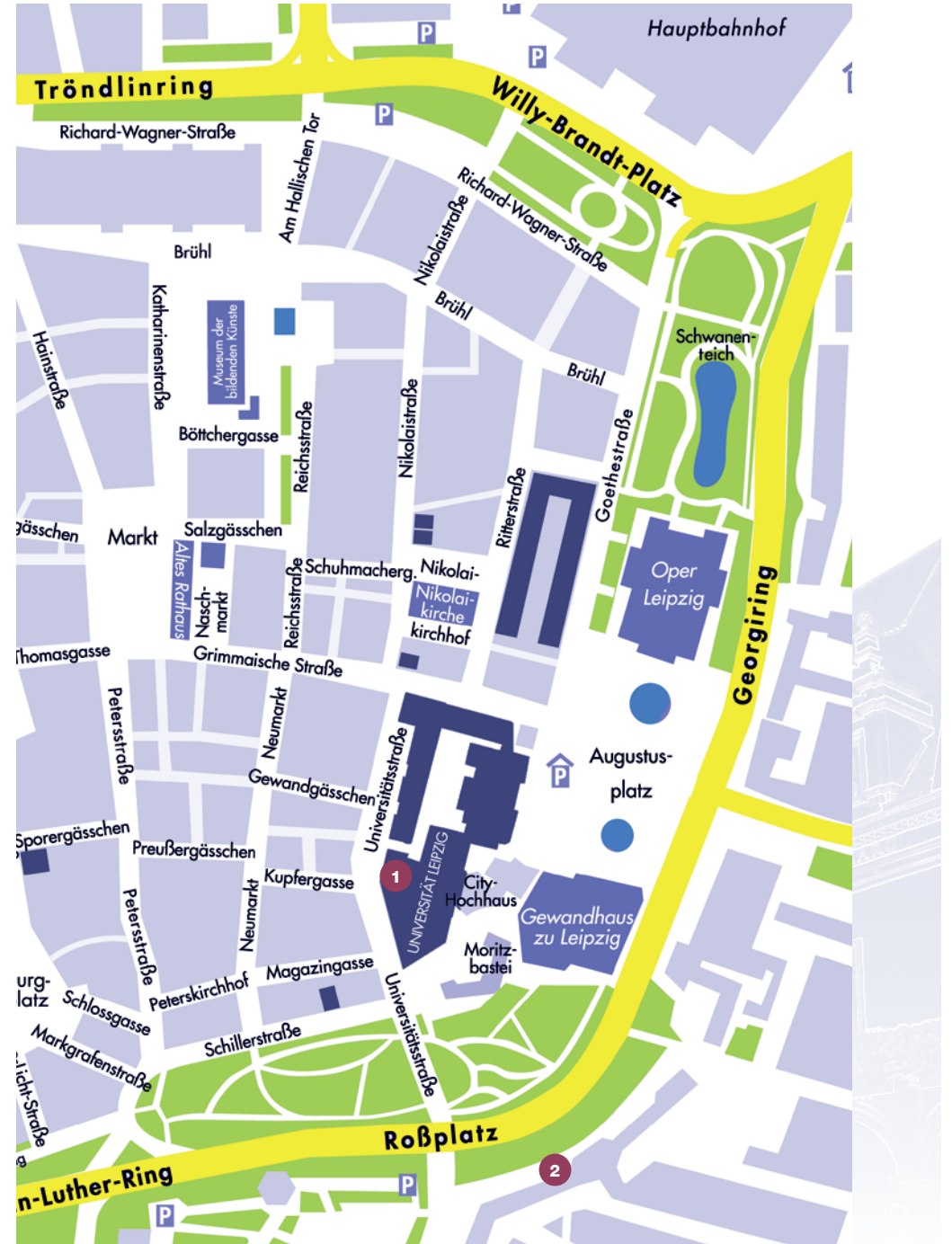
Entrance from Universitätsstr.

1

Lecture hall building (Hörsaalgebäude)
Universität Leipzig,
Universitätsstr. 3, 04109 Leipzig

2

Ring-Café, Roßplatz 8,
04103 Leipzig



Congress Language

The Congress language is English.

Congress Office / Registration/Bagde

The Congress Office is situated between the entrance doors of lecture hall 9.

Here you will receive your badge, the congress bag and the ticket for the social evening.

Opening hours

Thursday, September 13 th 2012	07.00 am – 6.00 pm
Friday, September 14 th 2012	07.30 am – 6.00 pm
Saturday, September 15 th 2012	07.30 am – 4.30 pm

You can register online until September 2nd, 2012.

Please note: On-site registration is possible, but only with paying cash in Euro (€).

Congress Fees, Payments, Cancellation, Refund-Policy

Registration Fee*	Early 31 st July 2012	1 st August 2012 – 2 nd September 2012	On-site (only cash)
Members of ESHNR	€ 300,00	€ 390,00	€ 390,00
Members of DRG	€ 300,00	€ 390,00	€ 390,00
Non Members	€ 370,00	€ 460,00	€ 460,00
Residents in training**	€ 200,00	€ 290,00	€ 290,00
Single Day Fee	€ 160,00	€ 160,00	€ 160,00
Social Evening	€ 60,00	€ 60,00	€ 60,00

* Fee includes: admittance to scientific sessions and exhibition, abstract book, refreshment during breaks, lunches, Get-together, guided city tour

** requires confirmation of the institution's head by way of proof

We kindly ask you to make all payments in Euro (€) prior to the congress. On-site you can only pay cash in Euro (€). Payment with credit or debit card will not be available.

Participants with outstanding payment are kindly ask to pay on-site. In case of recent payment take a written evidence of your payment with you. Otherwise the attendance of the congress will not be allowed.

In case of bank transfer by your organisation please make sure that your name and the key-word are indicated together with the money. If your organisation uses a block transfer for several participants it is necessary to include all relevant names. The online registration site is a secured site. Major credit cards such as VISA and EuroCard / MasterCard are accepted.

Full payment has to be received prior to the congress.

Cancellation of congress registration: written notification should be sent to the Organising Secretariat (platikanova@drg.de). Please note the following cancellation fees:

- » Until 5th August 2012: Full refund, no handling fee
- » From 6th August 2012 until 5th September 2012: Refund minus € 50,00 handling fee
- » After 5th September 2012: No refund

All refunds will be dealt with and paid back within 30 days after the congress.

There is no extra charge if in your stead a colleague will attend the congress.

Liability

In the case of Government intervention or regulation, military activity, strikes or any other circumstances that make it impossible or inadvisable for the ESHNR 2012 Annual Conference to take place at the time and place provided, the participant shall waive any claim for damage or compensation except the amount paid for registration after deduction of actual expenses incurred in connection with the congress and there shall be no future liability on the part of either party.

Industrial exhibition

Opening hours

Thursday, September 13 th 2012	09.30 am – 6.00 pm
Friday, September 14 th 2012	08.30 am – 6.00 pm
Saturday, September 15 th 2012	08.30 am – 2.00 pm

Breaks and Social Events

Coffee breaks (30 min) / Lunch time (1h)

Thursday, September 13 th 2012	10.30 am / 12.30 pm / 3.00 pm
Friday, September 14 th 2012	10.00 am / 12.30 pm / 3.30 pm
Saturday, September 15 th 2012	10.00 am / 1.00 pm / 4.00 pm

Social Events

Foyer lecture hall 9

Get-together	Thursday, September 13 th 2012	6.00 pm
Ring-Café, Roßplatz 8, 04103 Leipzig		
Social Evening	Friday, September 14 th 2012	7.30 pm

Certificate of attendance

Certificate of attendance can be obtained at the Congress office on Saturday from 11.00 am. If you booked a Single Day Ticket (Thursday or Friday) it can be obtained at the end of this day.

CME Credits

20 CME credits by Germany's Academy for Radiology and Medical Chamber of Saxony
18 European CME credits (ECMEC) by the European Accreditation Council for Continuing Medical Education (EACCME)

Guided City Tours

Please book your tour online via Congress-Homepage until September 1st, 2012.

www.eshnr2012.org – Social Programme

Each tour is limited to 25 participants.

There will be a limited supply of tickets on-site at the Congress-Office.

We offer tours to different themes on Friday and Saturday.

"Leipzig live – a city walk", "Ways to Johann Sebastian Bach" and "Music and Leipzig".

Meeting Point:

Main Entrance of the Lecture Hall Building (Hörsaalgebäude), Universitätsstraße

Friday, September 14th 2012

TIME: 06.15 pm

DURATION: ca. 1 hour

Saturday, September 15th 2012

TIME: 02.00 pm

DURATION: ca. 1 hour

Liability

The local organisers and the ESHNR are not liable for personal injury and loss or damage to private property.

Guideline for Speakers

The preview room is located on the second floor at the congress venue. There will be direction signs.

- » Please, submit your presentation (on USB-stick) in the preview room at the latest 1.5 hour before your session starts.
- » Please, choose a seat near the podium and do not leave the room before the session ends.
- » Please note that it is not possible to use your own laptops! All presentations have to be up-loaded in the congress IT-system. If you use an Apple computer, please bring your own adapter with you to the preview room.
- » Please, observe exactly your presentation time (invited lectures – besides TED sessions: 30 minutes including discussion; short oral presentations: 10 minutes including discussion). A lengthening cannot be accepted and chair-persons are requested to stop the presentation in such cases.
- » You are requested to come to the lecture room at the latest 5 minutes prior to start of the session. Please, identify yourself to the chairs.
- » Please, do not overload your presentation with too many images and please speak slowly.

ESHNR 2012 – SCHEDULE

September 13th–15th, 2012

	Thursday September, 13 th , 2012	Friday September, 14 th , 2012		Saturday September, 15 th , 2012	
	Lecture Hall 9	Lecture Hall 9	Lecture Hall 8	Lecture Hall 9	
08.00					08.00
08.30	OPENING CEREMONY	Current state of paranasal sinus imaging, pp 34	Special focus f-MRI in ENT, pp 39	Special focus Vascular malformations and tumour, pp 72	08.30
09.00	Special focus Multidisciplinary approach to the orbit, pp 24	Scientific presentations, pp 36			09.00
09.30		Scientific presentations, pp 36			09.30
10.00		Coffee break / Poster exhibition		Coffee break / Poster exhibition	10.00
10.30	Coffee break / Poster exhibition	Lesions of the jaw and oral cavity – role of radiology, pp 41	Newer techniques State in 2012, pp 47	Special focus Pitfalls and challenges, pp 74	10.30
11.00	Update your knowledge in post-therapeutic imaging, pp 25	Scientific presentations Jaw and cavity, pp 42	Scientific presentations Newer techniques, pp 48		11.00
11.30		Scientific presentations Jaw and cavity, pp 42	Scientific presentations Newer techniques, pp 48		11.30
12.00				Interactive image interpretation session with TED – neck, pp 76	12.00
12.30	Lunch / Poster exhibition	Lunch / Poster exhibition		CLOSING CEREMONY	12.30
13.00				Lunch	13.00
13.30	From symptoms to imaging strategies and findings, pp 26	Industrial Symposium Siemens Modern CT-Technology and Future of MRI			13.30
14.00				ESHNR Refresher Course 1 st part, p 77	14.00
14.30		Scientific presentations Varia, pp 53	Scientific presentations Temporal bone, pp 59		14.30
15.00	Coffee break / Poster exhibition				15.00
15.30	Scientific presentations Eye and Ear, pp 29	Coffee break / Poster exhibition			15.30
16.00	Interactive image interpretation session with TED – skull base, pp 33	Systematic approach for compartment based image interpretation, pp 64	Special techniques State in 2012, p 68	Coffee break / Poster exhibition	16.00
16.30				ESHNR Refresher Course 2 nd part, pp 79	16.30
17.00	GET-TOGETHER (Foyer Lecture Halls)	Scientific presentations, pp 66	Scientific presentations, pp 69		17.00
17.30		GENERAL MEMBER ASSEMBLY			17.30
18.00		GUIDED CITY TOURS			18.00
18.30		"Ways to Johann Sebastian Bach", "City of Leipzig" and "Music, Musicians and Leipzig"			18.30
19.00				14:00 – 15:00 Guided City tours	19.00
19.30				"Ways to Johann Sebastian Bach", "City of Leipzig" and "Music, Musicians and Leipzig"	19.30
20.00		Social Evening and Awards Ring-Café (Roßplatz 8)			20.00

SCIENTIFIC PROGRAMME

THURSDAY, SEPTEMBER 13TH, 2012

Lecture Hall 9

from 07.00	Registration		Page et seq
08.30 – 09.00	OPENING CEREMONY		
09.00 – 10.30	Special focus – multidisciplinary approach to the orbit	Chair: S Kösling / Halle (Germany), M Bloching / Berlin (Germany)	pp 24
09.00 – 09.30	When does the ophthalmologist need the radiologist and what does he want to know?	C. Meltendorf / Halle (Germany)	
09.30 – 10.00	Which points have to be clarified preoperatively?	M. Bloching / Berlin (Germany)	
10.00 – 10.30	The radiologist's answer – possibilities and limits in orbital imaging	W. Müller-Forell / Mainz (Germany)	
10.30 – 11.00	Coffee break / Poster viewing		
11.00 – 12.30	Update your knowledge in post-therapeutic imaging	Chair: F Dammann / Göppingen (Germany), M Lemmerling / Gent (Belgium)	pp 25
11.00 – 11.30	Paranasal sinuses	R. Maroldi / Brescia (Italy)	
11.30 – 12.00	Neck	M. Lell / Erlangen (Germany)	
12.00 – 12.30	Temporal bone	B. Verbist / Leiden (The Netherlands)	
12.30 – 13.30	Lunch / Poster viewing		
13.30 – 15.00	From symptoms to imaging strategies and findings	Chair: W Müller-Forell / Mainz (Germany), M Forsting / Essen (Germany)	pp 26
13.30 – 14.00	Tinnitus	M. Lemmerling / Gent (Belgium)	
14.00 – 14.30	Vertigo	E. Hofmann / Fulda (Germany)	
14.30 – 15.00	Facial Pain	J. Casselman / Bruges (Belgium)	
15.00 – 15.30	Coffee break / Poster viewing		
15.30 – 16.10	Short oral presentations: Eye and ear	Chair: N Freling / Amsterdam (The Netherlands), B Verbist / Leiden (The Netherlands)	pp 29
15.30 – 15.40	MR-Microscopy of the human eye – correlation with histology	Krueger PC et al / Greifswald (Germany)	
15.40- 15.50	Superior semicircular canal dehiscence: A simple classification system retrospectively applied to 598 consecutive temporal bone dehiscence CT examinations	Weindling S et al / Florida (United States of America)	
15.50 – 16.00	Aplasia of the cochlea: radiological findings and therapeutical options	Giesemann A et al / Hannover (Germany)	
16.00 – 16.10	Prevalence of labyrinthine ossification in CT and MR imaging of patients with acute deafness	Dirr F et al / Munich (Germany)	
16.10 – 17.00	Interactive image interpretation session with TED – skull base	S. Kösling / Halle (Germany)	pp 33
17.00 – 18.00	GET-TOGETHER		

Radiologie 360°



Von der Integration zur vernetzten Kommunikation

Agfa HealthCare bietet im Bereich der Radiologie ein umfassendes Portfolio an leistungsstarken Imaging- und IT-Lösungen mit einem vollständig integrierten Workflow für Diagnostik, Befundung und Demonstration.

Imaging- und IT-Lösungen von Agfa HealthCare ermöglichen in erster Linie Kostenersparnis sowie die Vereinfachung und Beschleunigung der Arbeitsabläufe in der Fachabteilung wie im ganzen Krankenhaus. Alles mit dem übergreifenden Ziel, die Qualität der Patientenversorgung zu verbessern.

Mit der Philosophie von Radiologie 360° stehen exzellent auf den gesamten Radiologie-Workflow abgestimmte, integrative und disziplinenübergreifende Systeme mit der geforderten Zukunftssicherheit zur Verfügung.

www.agfahealthcare.de

AGFA 
HealthCare

FRIDAY, SEPTEMBER 14TH, 2012

Parallel Sessions in Lecture Hall 9 and Lecture Hall 8

Page
et seq

LECTURE HALL 9

08.30 – 10.00	Current state of paranasal sinus imaging	Chair: H Imhof / Vienna (Austria), F Dubrulle / Lille (France)	pp 34
08.30 – 09.00	Benign lesions	H. Eggesbø / Oslo (Norway)	
09.00 – 09.30	Malignant lesions	J. Kabala / Bristol (United Kingdom)	
09.30 – 09.40	Radiology diagnosis of congenital cleft hard palate and alveolus	Petrovskaya V et al / Moscow (Russia)	
09.40 – 09.50	CT imaging of odontogenic infections involving the maxillary sinuses	Riis U et al / Oslo (Norway)	
09.50 – 10.00	CBCT in the detection of odontoma	Lo Casto A et al / Palermo (Italy)	

LECTURE HALL 8

08.30 – 10.00	Special focus – f-MRI in ENT	Chair: E Hofmann / Fulda (Germany), C Stippich / Basel (Switzerland)	pp 39
08.30 – 09.00	Basics and methods	C. Stippich / Basel (Switzerland)	
09.00 – 09.30	Clinical applications	A. Bartsch / Heidelberg (Germany)	
09.30 – 10.00	Central auditory processing disorders	S. Bartel-Friedrich, A Noll / Halle (Germany)	
10.00 – 10.30	<i>Coffee break / Poster viewing</i>		

LECTURE HALL 9

10.30 – 12.30	Lesions of the jaw and oral cavity – role of radiology	Chair: J Kabala / Bristol (United Kingdom), D Farina / Brescia (Italy)	pp 41
10.30 – 11.00	Jaw	H. Imhof / Vienna (Austria)	
11.00 – 11.30	Oral cavity	M. Mack / Munich (Germany)	
11.30 – 11.40	MRI based tumour volume measurements: An improved predictor of outcome in patients with oral cancer	Eley KA et al / Oxford (United Kingdom)	
11.40 – 11.50	Low-dose microfocus radiography in dental practice	Vasilyev A et al / Moscow (Russia)	
11.50 – 12.00	Bone density changes evaluated with Computer Tomography at interdental sites with horizontal bone loss	Dumitrescu AL et al / Bucharest (Romania)	
12.00 – 12.10	Quantitative computed tomography in jaw for detection of glucocorticoid-induced osteoporosis in miniature pigs by threshold-based bone density measurement	Kowald J et al / Regensburg (Germany)	
12.10 – 12.20	Head and neck findings in the postmortem imaging material in Linköping	Kovacovics B et al / Linköping (Sweden)	

FRIDAY, SEPTEMBER 14TH, 2012

Parallel Sessions in Lecture Hall 9 and Lecture Hall 8

Page
et seq

LECTURE HALL 8

10.30 – 12.30	Newer techniques – state in 2012	Chair: J Casselman / Bruges (Belgium), M Lell / Erlangen (Germany)	pp 47
10.30 – 11.00	Digital volume tomography (Cone beam CT)	L. Jäger / Saarbrücken (Germany)	
11.00 – 11.30	Physiological and metabolic imaging	S. Bisdas / Tübingen (Germany)	
11.30 – 11.40	Correlation between apparent diffusion coefficient and standardized uptake value in squamous cell carcinoma of the oral cavity and oropharynx	Preda L et al / Milano (Italy)	
11.40 – 11.50	Diffusion-weighted MRI and FDG PET/ CT in head and neck squamous cell carcinoma: is there any correlation between ADC and SUV values?	Varoquaux A et al / Genève (Switzerland)	
11.50 – 12.00	Can diffusion weighted imaging differentiate recurrent disease from reactive nodes in patients with treated head and neck squamous cell carcinoma?	Dudau C et al / London (United Kingdom)	
12.00 – 12.10	Dual metric differentiation of non-tumorous parotid gland diseases using high-resolution dynamic contrast-enhanced and diffusion weighted MRI	Busch J et al / Hamburg (Germany)	
12.10 – 12.20	Non-invasive differentiation of primary parotid gland tumors: does the combination of high-resolution dynamic contrast-enhanced MRI and diffusion-weighted imaging improve diagnostics?	Habermann CR et al / Hamburg (Germany)	

12.30 – 13.30 *Lunch / Poster viewing*

13.30 – 14.30	Industrial Symposium – Siemens AG	Chair: G Krombach / Gießen (Germany)	
13.30 – 14.00	Modern CT-Technology with focus on dose reduction in the head and neck area	M Lell / Erlangen (Germany)	
14.00 – 14.30	Creating the future of MRI: new developments for head and neck imaging	I Vallines / Erlangen (Germany)	

LECTURE HALL 9

14.30 – 15.30	Short oral presentations: Varia	Chair: H Eggesbø / Oslo NO, H Greess / Esslingen (Germany)	pp 53
14.30 – 14.40	Algorithm of radiologic examination of patients with diseases of lacrimal pathways	Privalova E et al / Moscow (Russia)	
14.40 – 14.50	Craniosynostosis and "Black Bone" MRI: An alternative to CT	Eley KA et al / Oxford (United Kingdom)	
14.50 – 15.00	Multimodality imaging in adolescent patients with advanced stage nasopharyngeal carcinoma, a single centre experience	Dudau C et al / London (United Kingdom)	
15.00 – 15.10	CT angiography of the external carotid artery branches in the neck: sufficient resolution to plan microvascular flap reconstruction procedures?	Kohler R et al / Genève (Switzerland)	
15.10 – 15.20	Origin and course of extracranial vertebral artery - CTA findings and embryologic considerations	Dürr N et al / Duisburg (Germany)	
15.20 – 15.30	Rektorzik's plexus – evaluation with contrast enhanced flat panel computed tomography and 3-DSA	Benndorf G / Houston (United States of America)	

FRIDAY, SEPTEMBER 14TH, 2012

Parallel Sessions in Lecture Hall 9 and Lecture Hall 8

Page
et seq

LECTURE HALL 8

14.30 – 15.30	Short oral presentations: Temporal bone	Chair: T Beale / London (UK), M Keberle / Paderborn (Germany)	pp 59
14.30 – 14.40	Are there substantial differences in spatial resolution of subtle temporal bone structures on CBCT and MDCT?	Pein K et al / Halle (Germany)	
14.40 – 14.50	The use of cone beam CT (CBCT) to determine intra-cochlear electrode positioning in human temporal bones	Beale T et al / London (United Kingdom)	
14.50 – 15.00	CT-based length assessments of cochlear implant (CI) electrodes in human temporal bone specimens, accuracy evaluation	Pomschar A et al / Munich (Germany)	
15.00 – 15.10	Quality control after cochlear implant surgery using cone beam CT	Pein K et al / Halle (Germany)	
15.10 – 15.20	Surgical relevance of the persistent petrosquamosal sinus	Giesemann A et al / Hannover (Germany)	
15.20 – 15.30	Prevalence of Chiari I malformation and cerebellar ectopia in patients with sensorial hearing loss	Haktanir A et al / Afyonkarahisar (Turkey)	
15.30 – 16.00	<i>Coffee break / Poster viewing</i>		

LECTURE HALL 9

16.00 – 17.30	Systematic approach for compartment based image interpretation	Chair: A Borges / Lisbon (Portugal), S Bartel-Friedrich / Halle (Germany)	pp 64
16.00 – 16.30	Suprahyoidal neck	F. Dubrulle / Lille (France)	
16.30 – 17.00	Infrahyoidal neck	N. Freling / Amsterdam (The Netherlands)	
17.00 – 17.10	Retropharyngeal calcific tendonitis of the longus colli muscle: a case report	Kontaki T et al / Kozani (Greece)	
17.10 – 17.20	Role of ultrasonography in characterising benign and malignant thyroid nodules	Elsayed A et al / Grimsby (United Kingdom)	
17.20 – 17.30	Ectopic parathyroid adenomas localized by dual-energy computed tomography	Kovacovics B et al / Linköping (Sweden)	

LECTURE HALL 8

16.00 – 17.30	Special techniques – state in 2012	Chair: J Olliff / Birmingham (UK), A Trojanowska / Lublin (Poland)	pp 68
16.00 – 16.30	Fibre tracking – can it help with head and neck problems?	M. Becker / Geneva (Switzerland)	
16.30 – 17.00	Imaging in computer-assisted head and neck surgery	F. Dammann / Göppingen (Germany)	
17.00 – 17.30	Improved in vivo visualisation and evaluation of endolymphatic hydrops using high field MRI in Menier's disease and correlation with audiovestibular function	Flatz WH et al / Munich (Germany)	
17.10 – 17.20	Comparison of true real-time MR imaging with radial k-s pace sampling to videofluoroscopy in the follow up evaluation of velopharyngeal dysfunction or insufficiency treated by surgery	Larson MC et al / Frankfurt (Germany)	
17.20 – 17.30	Detecting cholesteatoma on HASTE (nonechoplanar) diffusion-weighted MRI: the value of quantitative assessment using ADC values	Boyd E et al / London (United Kingdom)	
17.30 – 18.00	GENERAL ASSEMBLY		
18.15 – 19.15	GUIDED CITY TOURS		
FROM 19.30	SOCIAL EVENING AND AWARDS at Ring-Café (Rossplatz 8)		

SATURDAY, SEPTEMBER 15TH, 2012

Lecture Hall 9

Page
et seq

LECTURE HALL 9

08.30 – 10.00	Special focus - vascular malformations and tumours	Chair: M Mack / Munich (Germany), J Werner / Marburg (Germany)	pp 72
08.30 – 09.00	From the clinical point of view	J. Werner / Marburg (Germany)	
09.00 – 09.30	From the radiological point of view	U. Ernemann / Tübingen (Germany)	
09.30 – 10.00	Interventional possibilities	U. Ernemann / Tübingen (Germany)	
10.00 – 10.30	<i>Coffee break / Poster viewing</i>		
10.30 – 12:00	Pitfalls and challenges	Chair: R Maroldi / Brescia (Italy), M Becker / Geneva (Switzerland)	pp 74
10.00 – 11.00	Pseudolesions	C. Karaman / Aydın (Turkey)	
11.00 – 11.30	Difficult cases	J. Olliff / Birmingham (United Kingdom)	
11.30 – 12.00	Incidental findings – how to handle them?	T. Beale / London (United Kingdom)	
12.00 – 12.50	Interactive image interpretation session (TED) – Neck	D. Farina / Brescia (Italy)	pp 76
12.50 – 13.00	CLOSING CEREMONY		
13.00 – 14.00	<i>Lunch / Poster viewing</i>		
14.00 – 15.00	GUIDED CITY TOURS		
14.00 – 16.00	ESHNR Refresher Course – 1st part	Chair: C Karaman / Aidyn TR, C Czerny / Vienna (Austria)	pp 77
14.00 – 14.30	Thyroid and parathyroid glands	C. Czerny / Vienna (Austria)	
14.30 – 15.00	Nasopharynx: benign and malignant lesions	R. Maroldi / Brescia (Italy)	
15.00 – 15.30	Hypopharynx and larynx	M. Becker / Geneva (Switzerland)	
15.30 – 16.00	Salivary glands	N. Freling / Amsterdam (The Netherlands)	
16.00 – 16.30	<i>Coffee break / Poster viewing</i>		
16.30 – 18.30	ESHNR Refresher Course – 2nd part	Chair: B Kress / Frankfurt a. Main (Germany), DT Nguyen / Halle (Germany)	pp 79
16.30 – 17.00	Orbit and globe	W. Müller-Forell / Mainz (Germany)	
17.00 – 17.30	Trauma in the head and neck	B. Verbist / Leiden (The Netherlands)	
17.30 – 18.00	Temporomandibular joint	B. Kress Frankfurt a. Main / (Germany)	
18.00 – 18.30	Lymph nodes in the neck	A. Borges / Lisbon (Portugal)	

ABSTRACTS

Oral Presentations

Thursday, September 13th, 2012

Special focus – multidisciplinary approach to the orbit

13.09.2012, 09.00 – 10.30 am

Chairs: Sabrina Kösling, Halle (Germany) / Marc Boris Bloching, Berlin (Germany)

09.00 – 09.30 am

When does the ophthalmologist need the radiologist and what does he want to know?

Christian Meltendorf (Invited presentation)

Universitätsklinikum Halle (Saale), Universitätsklinik und Poliklinik für Augenheilkunde, Halle (Saale), Germany

09.30 – 10.00 am

Which points have to be clarified preoperatively?

Marc Boris Bloching (Invited presentation)

Helios-Klinikum Berlin, HNO-Klinik, Berlin, Germany

SUMMARY: Orbital and periorbital diseases represent a demanding challenge for the interdisciplinary cooperation because the orbit is located at the anatomical border between ophthalmology, ENT, maxillofacial surgery and neurosurgery. An accurate imaging and diagnosis by the radiological partners is the goal for correct treatment schedules and the indication and planning of surgical procedures. The knowledge of the possibilities of the other involved (orbital)–disciplines is fundamental for an optimal outcome of the patients. In this interdisciplinary lesson, representatives of the most important disciplines will show their point of view in the treatment of orbital diseases.

TAKE-HOME-POINTS: The basic knowledge of the diagnostics and treatment modalities of orbital inflammations, tumor diseases and trauma is arranged in a cooperative manner in reference to practical questions.

10.00 – 10.30 am

The radiologists answer – possibilities and limits in orbital imaging

Wibke Müller-Forell (Invited presentation)

Universitätsmedizin Mainz, Institut für Neuroradiologie, Mainz, Germany

Update your knowledge in post-therapeutic imaging

13.09.2012, 11.00 – 12.30 am

Chairs: Florian Dammann, Göppingen (Germany) / Marc Lemmerling, Gent (The Netherlands)

11.00 – 11.30 am

Paranasal sinuses

Roberto Maroldi (Invited presentation)

University of Brescia, Dipartimento di Specialità Chirurgiche, Scienze Radiologiche e Medico Forensi, Brescia, Italy

11.30 – 12.00 am

Neck

Michael Lell (Invited presentation)

Universitätsklinikum Erlangen, Radiologisches Institut, Erlangen, Germany

SUMMARY: Squamous cell carcinoma of the head and neck is often treated with radiation therapy primarily or additionally following surgical resection. To cover the resection defects, tissue flaps are frequently used, complicating the clinical detection of recurrent disease. Radiation treatment results in different tissue alterations (edema, scarring, incomplete resolution of non-viable tumor), creating a difficult clinical picture. Complications need to be detected and differentiated from normal therapy-associated changes. Radiological studies play a key role in this setting and the determination of patient management.

TAKE-HOME-POINTS: Signs of recurrent tumor, posttreatment changes, and associated complications will be discussed.

12.00 – 12.30 pm

Postoperative imaging of the temporal bone

Berit M. Verbist (Invited presentation)

Leiden University Medical Center, Dept of Radiology, C2S, Leiden, The Netherlands

SUMMARY: Many conditions which affect the function of the middle ear may require surgical intervention. Postoperative imaging will be requested either to evaluate complete removal of disease (eg in cholesteatoma) or because of new, persisting or recurrent complaints of the patient (eg vertigo after stapes replacement). Also inner ear diseases causing profound sensorineural hearing loss may be treated surgically to achieve hearing restoration by means of cochlear implantation. Postoperative imaging maybe required in case of malfunction. In this presentation different surgical procedures will be reviewed. The normal postoperative imag-

ing appearance of the most common surgical techniques and different types of prostheses will be shown. An overview of possible failures and complications will be given. It will be discussed whether CT or MRI should be performed to answer the clinical questions.

TAKE-HOME-POINTS: The audience will be shown how to:

- familiarize yourself with operation techniques and prosthetic material
- visualize and recognize postoperative complications.

From symptoms to imaging strategies and findings

13.09.2012, 13.30 – 15.00 pm

Chairs: Wibke Müller-Forell, Mainz (Germany) / Michael Forsting, Essen (Germany)

13.30 – 14.00 pm

Imaging patients with tinnitus

Marc Lemmerling (Invited presentation)

AZ Sint-Lucas Hospital Gent, Department of Radiology, Gent, Belgium

SUMMARY: Patients with tinnitus perceive sound in the ear in the absence of a corresponding external sound. Tinnitus can on one hand be classified as pulsatile (synchronous with the heartbeat) or non-pulsatile (continuous), on the other hand as objective or subjective. Non-pulsatile and subjective tinnitus are the more frequent variants. In case of pulsatile tinnitus CT

is the imaging method of choice, whereas MRI should first be used in case of non-pulsatile tinnitus. In the majority of patients with tinnitus imaging studies will find no explanation for their complaints. In case of pulsatile tinnitus one must exclude vascular neoplasms, other vascular anomalies, and otosclerosis. Glomus tumor (paraganglioma) is the most frequent vascular

mass that can cause tinnitus. A wide variety of vascular malformations can lead to tinnitus, such as AVMs and AVFs, aberrant carotid artery, persistent stapedial artery, dehiscent jugular vein, atherosclerotic disease, and rarely aneurysm, fibromuscular dysplasia, and carotid artery dissection. Some believe that vascular loops contacting the eighth cranial nerve at the brainstem root entry zone cause pulsatile tinnitus. In patients with non-pulsatile tinnitus vestibular schwannoma is the most important pathologic condition to consider. Other conditions that rarely cause tinnitus are MS, Chiari 1 malformation, and endolymphatic sac tumors.

TAKE-HOME-POINTS: 1. Non-pulsatile and subjective tinnitus are the most frequent variants. 2. CT is the imaging method of choice in case of pulsatile tinnitus, whereas MRI is preferred in non-pulsatile tinnitus. 3. In patients with pulsatile tinnitus one must exclude vascular neoplasms, other vascular anomalies, and otosclerosis. 4. In patients with non-pulsatile tinnitus vestibular schwannoma is the most important pathologic condition to consider.

14.00 – 14.30 pm

Vertigo

Erich Hofmann (Invited presentation)

Klinikum Fulda gAG, Kopfzentrum Klinikum Fulda, Fulda, Germany

SUMMARY: Vertigo is one of the most common clinical symptoms in an ENT radiologist's practice. The most common entities benign paroxysmal positioning vertigo (BPPV), vestibular neuropathy, and Menière's disease can mainly be diagnosed at physical or clinical examination of the patient and do not require imaging as a first line diagnostic tool. However, some life-threatening diseases can mimic innocuous conditions which creates a lot of uncertainty as to which patients to refer to neuroimaging. To use the appropriate imaging strategy, it may be useful to classify vertigo into ventral, peripheral and unclassifiable. Therefore, an experienced clinician is needed as a gatekeeper. In this con-

tribution, most diseases causing vertigo are presented encompassing peripheral (vestibular neuropathy, BPPV, Menière's disease, perilymph fistula, semicircular duct dehiscence, vestibular paroxysmia, pneumolabyrinth, labyrinthine hemorrhage, inflammatory inner ear disease) as well as central (stroke and other neurovascular disease, multiple sclerosis, neoplasias, malformations) pathology.

TAKE-HOME-POINTS: The Invited presentation concludes with some everyday diagnostic dilemmata.

14.30 – 15.00 pm

Facial Pain

Jan Casselman (Invited presentation)

Medische Beeldvorming AZ Sint-Jan Brugge, Departement Radiologie / RX-MBV, Bruges, Belgium

SUMMARY: Facial pain has many causes. The clinical presentation of the pain can help to differentiate different types of facial pain but often MR and CT are needed to detect or confirm the responsible lesion. The origin of the facial pain can be local and the pathology can then be in the dental, gingival, mucosal, salivary gland and sinus region. However, the cause is sometimes found a little further away like in case of TMJ disorders. Here myogenic and arthrogenic pain can be distinguished and imaging plays a major role in the latter group. Nerve involvement can also result in facial pain and the most frequently encountered involved nerves are the trigeminal nerve (V), intermediate nerve (VII) and glossopharyngeal nerve (IX) but SUNCT (Shortlasting Unilateral Neuralgiform Pain with Conjunctival injection and Tearing) also belongs to this group. In this group the trigeminal nerve is most frequently involved and trigeminal neuralgia (neurovascular conflict) and neuropathy must be distinguished as two different subgroups although many classifications with more subgroups have been proposed. Perineural tumor extension can be seen along all above mentioned nerves as well.

Connections between the three mentioned nerves exist and explain why the clinical signs are often indicating that at a different nerve is involved than the nerve which is really involved by the lesion. The facial pain can also be referred from the brain/meninges and other rare causes as carotidynia and Eagle syndrome must also be considered. Finally the diagnosis of persistent idiopathic facial pain is made when imaging remains negative, the pain is atypical and of obscure etiology (diagnosis of exclusion). In most of the above cases MR is the method of choice, however, many sinus and dental causes and the Eagle syndrome are best depicted on CT.

TAKE-HOME-POINTS:

- 1) MR is the imaging technique of choice to find the cause of facial pain, although CT is sometimes needed (dental, sinus, Eagle syndrome)
- 2) There are many causes of facial pain but patients with trigeminal neuralgia and neuropathy are most frequently referred for imaging
- 3) The brain, face and the upper part of the neck must be studied to include all regions where the potential lesion can be located.

Eye and ear (Short oral presentations)

13.09.2012, 15.30 – 16.10 pm

Chairs: Nicole Freling, Amsterdam (The Netherlands) / Berit M. Verbist, Leiden (The Netherlands)

15.30 – 15.40 pm

MR-Microscopy of the human eye correlation with histology

Paul-Christian Krueger (short oral presentation)

University Medicine Greifswald, Department of Interventional Radiology and Neuroradiology, Greifswald, Germany

Co-Authors: Langner S, Falke K, Guthoff R, Stachs O, Hosten N

OBJECTIVES: Magnetic resonance imaging (MRI) at 1.5 and 3 Tesla with small surface coils is a well-established procedure in the diagnosis of space-occupying lesions of the eye and orbital cavity. Until now histological examination has been required to reliably assess tumor extent and possible infiltration of surrounding structures. With ultra-high-field MRI, however, it has become possible to evaluate tumor morphology as well as infiltration into surrounding structures with sub-millimeter resolution. Using the example of different intraocular mass lesions this study describes the diagnostic prospects and potential of ultra-high-field MR microscopy.

MATERIALS AND METHODS: Ten human eyes with different space-occupying masses were examined ex vivo to compare the standard clinical examination (ultrasound) with ultra-high-field micro-MRI (7.1 Tesla, ClinScan, Bruker BioScan) using a small surface coil. Imaging parameters were: TE 48 ms; TR 2540 ms; slice thickness 500 µm; matrix size 512 x 512 pixels interpolated to 1024 x 1024 pixels; FOV 40 x 40 mm; in-plane resolution 39 x 39 x 500 µm/pixel; acquisition time 8:20 min per plane. Finally, the specimens were examined histologically, and the histological and MRI results were correlated.

RESULTS: Ultra-high-field MRI at 7.1 Tesla provided images of anatomical structures of the bulb as well as different benign and malignant intraocular masses with high resolution, enabling reliable assessment of tumor morphology and extent. Subsequent histological examination confirmed MRI findings regarding origin, internal structure and extent of the masses.

CONCLUSIONS: This study demonstrates the potential of MR microscopy for imaging small anatomical structures. The findings correlate strongly with histology, making MRI of central importance in determining tumor morphology, extent and potential infiltration of surrounding structures. This work was performed ex vivo, but with wider availability, ultra-high-field MR microscopy is expected to become an essential tool not only in experimental studies but also for daily routine.

15.40 – 15.50 pm

Superior semicircular canal dehiscence: a simple classification system retrospectively applied to 598 consecutive temporal bone dehiscence CT examinations

Steven Weindling (short oral presentation)

Mayo Clinic – Florida, Radiology,
Jacksonville Florida, USA

Co-Authors: Broderick D, Lundy L

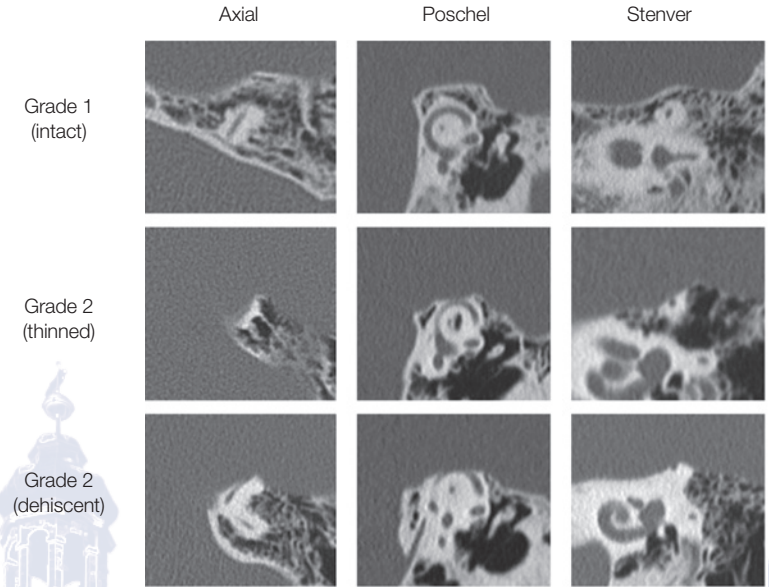
OBJECTIVES: To validate a proposed SCC dehiscence classification system for unifying the evaluation and reporting of Temporal Bone Dehiscence (TBD) CT exams.

MATERIALS AND METHODS: A sliver of bone remaining over the SSC roof excludes SSCD, yet true dehiscence may be difficult to distinguish from a severely thinned SSC bony roof on routine temporal bone CT. Newer multidetector CT helical techniques, including creation of overlapping, thin section, high resolution bone algorithm reconstructions in Poschl and Stenver planes, may improve visualization and localization of SCC roof bony defects. We created a SCCD classification system to provide a uniform approach for the evaluation and reporting of TBD CT exams. This classification system was then utilized by 2 experienced CAQ certified Neuroradiologists for independent, retrospective review of 498 consecutive tailored TBD CT studies performed at our institution between 11/2008–8/2010 for patients with symptoms consistent with SSCD. A consensus SSCD classification for all TB studies was then reached by comparing independent results with joint review of all discrepancies. Our SSC dehiscence classification system separates the SCC bony roof into 3 grades: Grade 0 (intact) – Bone, or air cells with intact overlying bone, covers the entire SCC roof; Grade 1 (thinned) – SCC bony roof thinned to ≤ 0.1 mm with converging bony margins from the SCC to the middle or posterior cranial fossa; Grade 2 (dehiscent) – Bone overlying a portion of the SCC

is clearly absent with parallel or diverging bony margins from the SCC to the middle or posterior cranial fossa. Grade 1 and 2 defect lengths were measured and localized to the anterior, middle and/or posterior thirds of the SCC roof.

RESULTS: Of 996 temporal bones imaged, 49 were excluded due to prior surgery, incomplete CT reformations or fracture. The 947 included temporal bones were classified by consensus as follows: Grade 0=88.5% (838/947); Grade 1=6.4% (61/947); Grade 2=5.1% (48/947). Interobserver agreement, as measured by a kappa of 0.6859, was substantial. SSC roof defects were distributed as follows: Anterior (gr. 1=28, gr. 2=15); Middle (gr. 1=46, gr. 2=32); Posterior (gr. 1=5; gr. 2=8). Of 61 grade 1 temporal bones, 1 patient had contralateral surgery, with 60 included contralateral bones classified as: grade 0=58% (35/60); grade 1=10% (6/60); grade 2=32% (19/60). Of 48 grade 2 temporal bones, 2 patients had contralateral TB surgery, with 46 included contralateral temporal bones classified as: grade 0=43% (20/46); grade 1=43% (20/46); grade 2 (bilateral dehiscence) =14% (6/46).

CONCLUSIONS: Our proposed SSCD classification system provided a structured methodology for reviewing and reporting SSCD CT results, and had good interobserver agreement. Improved characterization of SSC roof lesions using this classification may facilitate selection of optimal surgical candidates and best surgical approach.



15.50 – 16.00 pm

Aplasia of the cochlea: radiological findings and therapeutical options

Anja Giesemann (short oral presentation)

Medizinische Hochschule Hannover, Institut für Diagnostische und Interventionelle Neuroradiologie,
Hannover, Germany

Co-Authors: Kontorinis G, Giurgas A, Lanfermann H, Lenarz T, Götz F

OBJECTIVES: Radiological findings in cases of cochlear aplasia and evaluation of hearing outcome after CI-Implantation

MATERIALS AND METHODS: From a database with all CT-visible inner ear malformations admitted to a tertiary referral center between 1995 and 2011 all cases of cochlear aplasia were extracted. The CT- and MR-images were evaluated by two neuroradiologists. In cases of auditory implantation on the aplastic side the post-implantation performance and any relevant issues were recorded.

RESULTS: Twenty-eight ears with cochlear aplasia were found in 23 patients; bilateral in five, unilateral in 18 patients. The unilateral cases had contralaterally normal ears (two patients), cochlea hypoplasia (five patients), common cavity (six patients) and atresia of the internal auditory canal (one patient). Four patients (two with bilateral, two with unilateral cochlear aplasia) were treated with cochlear implants in the ipsilateral ear. One patient underwent auditory brainstem implantation. All implanted patients achieved speech perception but with limited vocabulary. The surgery was challenging and time demanding in all cases but was not related to any complications.

CONCLUSIONS: Aplasia of the cochlea is defined as the total absence of the cochlea, with a present, though malformed, vestibule. Although the hearing nerve cannot be identified, the post-implantation results suggest the existence of func-

tional hearing fibres in the remaining dysplastic inner ear structures. Hearing rehabilitation in such patients is very challenging and requires careful and individualized assessment; cochlear implantation may still be an option.

16.00 – 16.10 pm

Prevalence of labyrinthine ossification in CT and MR imaging of patients with acute deafness

Franziska Dirr (short oral presentation)

Ludwig Maximilian University Munich, Institute for Clinical Radiology, Munich, Germany

Co-Authors: Braun T, Hempel JM, Müller J, Ertl-Wagner B

OBJECTIVES: Labyrinthine ossification is a dreaded complication of inflammatory or destructive cochlear lesions: If cochlear implantation is chosen to treat an associated sensorineural hearing loss, labyrinthine ossification can compromise electrode insertion and even render it impossible in severe cases. The present study aimed to evaluate the prevalence of labyrinthine ossification in a cohort of patients with acute deafness.

MATERIALS AND METHODS: In a retrospective approach, 49 consecutive patients with unilateral sudden, at least severe sensorineural hearing loss were included in the study. Further inclusion criteria were either a HRCT of the temporal bone (isotropic spatial resolution at least 0.8 mm or below) or a high resolution CISS sequence (isotropic spatial resolution at least 1 mm or below). CT was performed in 15 (Definition Flash, Siemens Healthcare), and MR imaging in 41 patients (n=2 1.0 T Magnetom Harmony with 1.0 mm, n=27 1.5 T Magnetom Sonata or Symphony with 1.0 mm, n=8 1.5 T Magnetom Avanto with 0.6-0.7 mm and n=4 3.0 T Magnetom Verio with 0.5 mm spatial resolution; all Siemens Healthcare). Imaging had been performed after the onset of hearing loss with a median of approximately one week for CT and one month

for MRI. A standardized reading regarding the labyrinthine ossification was performed by an experienced head and neck radiologist blinded to the clinical symptoms.

RESULTS: Radiologic signs of labyrinthine ossification were present in 9 patients (8 CT and 1 MRI). 4 patients showed unilateral and 5 patients bilateral signs of labyrinthine ossification. In all unilateral cases, the deafened ear was affected. In the bilateral cases, symmetrical signs of labyrinthine ossification were observed in 3 cases, although the contralateral ear clinically still showed normacusis. For 4 patients with signs of labyrinthine ossification in CT, additional 1.5 T MRI with 1 mm spatial resolution was available, which showed no signs of labyrinthine ossification in all cases.

CONCLUSIONS: Signs of labyrinthine ossification were found in a surprisingly high rate (18 %) of patients with acute deafness. The data suggest HRCT of the temporal bone to be more sensitive to detect labyrinthine ossification than 1.5 T MRI with 1 mm spatial resolution, as neither of the patients with signs of labyrinthine ossification in CT had corresponding alterations in MRI. The relative diagnostic value of HRCT and MR imaging with 3T and a higher spatial resolution of

0.5 mm remains to be elucidated, though. As it currently is common practice only to perform MR imaging in most patients with acute deafness to exclude retrocochlear pathologies, the authors think that HRCT of the temporal bone should be considered in all patients with miss-

ing recovery of the acute deafness to exclude labyrinthine ossification and, in cases of early signs, to evaluate the patient further to facilitate early cochlear implantation before progression impedes electrode insertion.

Interactive image interpretation session with TED

13.09.2012, 16.10 – 17.00 pm

16.10 – 17.00 pm

Skull base

Sabrina Kösling (Invited presentation)

Universitätsklinikum Halle, Klinik für Diagnostische Radiologie, Halle (Saale), Germany

Current state of paranasal sinus imaging

14.09.2012, 08.30 – 10.00 am

Chairs: Herwig Imhof, Vienna (Austria) / Frédérique Dubrulle, Lille (France)

08.30 – 09.00 am

Benign lesions

Heidi Beate Eggesbø (Invited presentation)

University of Oslo (UiO), Faculty of Medicine,
Oslo, Norway

SUMMARY: Sinonasal imaging: Computed tomography (CT) is still regarded as the gold standard and workhorse in paranasal sinus imaging. Benign lesions of the paranasal sinuses show a wide spectrum from non-significant mucosal thickening and retention cysts to inflammatory and neoplastic conditions that require follow-up. CT findings that must alert for endoscopic examination and magnetic resonance (MR) imaging follow-up are advanced unilateral disease, remodelling or erosion of bone, and sinus opacifications with increased attenuation or micro-calcifications. In order to evaluate both bone and sinus opacifications adequately, the CT images must be reconstructed with both bone and soft tissue algorithms.

Mucosal thickening, retention cyst and polyps:

Mucosal thickening and retention cyst are the most common benign lesions found in the paranasal sinuses. Maxillary sinus mucosal thickening less than 4 mm is regarded as normal. The ethmoid sinuses are involved in the nasal cycle and mucosal lining up to 2 mm is normal, while in the frontal and sphenoid sinuses, the mucosal lining should not be seen at CT. Mucous retention cysts are due to obstruction of a seromucinous gland, while serous retention cysts have accumulation of fluid in the

submucosal layer and hence can be regarded as pseudocysts. Mucous retention cysts are most common, and found mainly in the maxillary sinuses. Polyps are, as serous retention cysts, due to the accumulation of fluid in the mucosa. Polyps most commonly originate from the ostiomeatal complex and seen as nasal polyps. Most polyps are benign, but simple polyps may also turn out to be malignant.

Mucocele and pyocele: Obstruction of any sinus ostium may cause retention of mucous and desquamated epithelium and is termed a mucocele when the sinus is expanded. By time, mucocele may expand and erode into the orbit or the brain. A mucocele may become superinfected and is then termed a pyocele.

Chronic rhinosinusitis: Chronic rhinosinusitis can be classified into five inflammatory patterns. The three first patterns are due to obstruction of the mucociliary clearance. 1) Infundibular pattern is caused by obstruction of the ethmoid infundibulum and only the maxillary sinus is involved. 2) Ostiomeatal complex pattern is caused by obstruction of the middle meatus and ipsilateral maxillary, anterior ethmoid and frontal sinuses are involved. 3) Sphenoethmoid recess pattern involve the posterior ethmoid and sphenoid

sinuses. 4) Polyposis pattern is recognized as panopacification with bulging and remodelling of the ethmoid walls, broadening of the ethmoid infundibulum and nasal cavity masses with outward convexity. 5) Sporadic pattern include all the rest as single polyps, cysts, postoperative mucosal thickening etc.

Fungal infection: Fungal infection must always be considered in chronic rhinosinusitis. The non-invasive forms are allergic fungal sinusitis (AFS) and fungus ball (mycetoma). AFS should be suspected when hyperattenuated sinus opacifications are seen on CT, while a fungus ball can be recognized by the scattered calcifications inside the opacification. In the invasive form, the hyphae pass through intact bone via blood vessels, and soft tissue masses can be identified in the fat plane outside the sinus walls, e.g. pre- or retroantral soft tissue swellings or swelling of the nasal septum, referred to as an eschar.

Sinonasal manifestations in patients with systemic disease: Sinonasal manifestations are described for several systemic diseases, e.g. cystic fibrosis, Wegener's granulomatosis, sarcoidosis and Samter's triad syndrome (aspirin sensitivity, asthma, sinonasal polyposis).

Benign neoplasms: Osteomas and inverted papillomas are the most common benign sinonasal neoplasms. An osteoma usually can be left untreated, unless interfering with the mucociliary

clearance or growing very large. Inverted papillomas (IP), named due to the mucosal infoldings into the stroma, are most commonly found in the ethmoid or maxillary sinuses. IP may display characteristic hyperostosis from the sinus wall where the tumour origin. IP can undergo malignant transformation. Fibrous dysplasia is commonly seen in the skull base, and when close to the sphenoid and ethmoid sinuses the lesion can interfere with mucociliary sinus clearance routes. Juvenile nasopharyngeal angiofibromas (JNA) are benign tumours of vascular origin. They arise from testosterone sensitive cells in the pterygoid plate in adolescence males. From the origin the angiofibromas can be locally aggressive growing in all directions via the pterygopalatine fossa: forward through the sphenopalatine foramen into the nasal cavity and nasopharynx, laterally through the pterygomaxillary fissure into the infratemporal fossa, posteriorly into the Vidian canal and foramen rotundum into the middle skull base. Further, large JNA will displace the maxillary sinus anteriorly and the sphenoid sinus upwardly. Two other rare benign sinonasal tumours that may be considered are schwannomas, characterized by a slow growing and remodeling the surrounding bone, and hemangiomas, classified as capillary, cavernous or mixed.

TAKE-HOME-POINTS: To be familiar with common benign paranasal sinus lesions with no need to follow-up and lesions that require follow-up.

09.00 – 09.30 am

Malignant lesions

Julian Kabala (Invited presentation)

UHB Bristol Royal Infirmary, Radiology,
Bristol, United Kingdom

SUMMARY: 80% of malignancy in the paranasal sinuses arise within the maxillary antra with most of the remainder arising in the fronto-ethmoid

area. About 75% of cancers are squamous cell carcinoma. Most of the others consist of adenocarcinoma (particularly in the ethmoid air

cells), lymphoma or salivary gland malignancies (adenoid cystic carcinoma in particular). A variety of rare malignancies may also be encountered including sarcoma, neurogenic tumours, plasmocytoma, melanoma and metastases. A histological diagnosis is usually achieved following endoscopic assessment. The primary aim of imaging is to determine the extent of the tumour, particularly in the areas that are difficult for the clinician to directly assess. For maxillary antral tumours the single most critical extension is posteriorly into the pterygopalatine fossa. From this site further extension may proceed posterosuperiorly into the middle cranial fossa and cavernous sinus (particularly via the foramen rotundum and vidian canal) and laterally via the pterygomaxillary fissure into the suprazygomatic masticator space (with further opportunity for intracranial spread for example via the foramen ovale). Fronto-ethmoid tumours often extend intracranially at an early stage, directly into the anterior cranial fossa. Tumours throughout the paranasal sinuses can access the orbit when sufficiently advanced. MRI is the standard modality for assessment of paranasal sinus malignancies by virtue of its ability

to differentiate tumour from benign processes (mucosal hypertrophy, retained secretions) and to demonstrate tumour extension along nerves and intracranially. CT is a powerful complementary modality with superior resolution and demonstration of subtle erosion of cortical bone.

TAKE-HOME-POINTS: Most malignancy arises in the paranasal sinuses and is most commonly squamous cell carcinoma. The primary aim of imaging is to determine the extent of the tumour in areas inaccessible to clinical and endoscopic examination. For maxillary antral tumours the single most critical extension is posteriorly into the pterygopalatine fossa which facilitates subsequent intracranial extension. Fronto-ethmoid tumours have a predilection for early intracranial extension. MRI is the standard modality for assessment of paranasal sinus malignancies by virtue of its ability to demonstrate the extent of tumour within soft tissues, particularly perineural and intracranial extension. CT is a powerful complementary modality particularly for the demonstration of subtle erosion of cortical bone.

09.30 – 09.40 am

Radiology diagnosis of congenital cleft hard palate and alveolus

Victoriya Petrovskaya (short oral presentation)

Clinic of Moscow State University of Medicine and Dentistry, Depart of Radiology, Moscow, Russia

Co-Authors: Blokhina N

OBJECTIVES: The diagnosis of Congenital Cleft pale and alveolus is early established and required a long-term treatment with various medical specialists. The most important part in reconstructive surgery is alveolar bone grafting and premaxillary fixation. Facial growth enhances teeth displacement, disocclusion, maxillary hypoplasia and craniofacial deformities. To outline the role of radiology assessment in patients with cleft palate and alveolus.

MATERIALS AND METHODS: Studies were performed in 102 patients with cleft palate and alveolus from 8-16year old. All patients were imaged with traditional radiology methods as orthopantomography, panoramic view with magnification, intraoral radiography and cone-beam computer tomography, multislice computer tomography microfocal radiography. The essay was performed before and after alveolar bone grafting at 1, 3, 6 and 9 month time.

RESULTS: Orthopantomography and panoramic radiographs with magnification detected 58 patients with unilateral fissured defects spread on the hard palate, 32 patients with bilateral defects of alveolar bone and palate with premaxillary displacement and 10 patients with hidden defects of hard palate. Microfocal radiography showed 9 patients with periodontitis granulosa, 15 patients with endodontic treatment, 26 patients with partly destructed cortical bone of a socket. In reconstructive surgery two types of bone graft were used, an autograft from iliac crest and autograft from mental region. In preoperative stage MSCT (n=42) and CBCT (n=58) were performed. The images allowed to determine the volume and size of bone defect, oronasal fistula, location of premaxilla, deformation of craniofacial region and disocclusion. High technique methods (MSCT, CBCT) allowed to plan the scale of surgical operation. 44 patients had sufficient amount of autograft bone from mental side, 56 patients had mental bone atrophy and in this cases cancellous bone from iliac crest was needed. 34 patients had defor-

mation of maxillary bone, sinus, and nasal cavity. They took the one-stage course with alveolar bone grafting and orthognathic surgery. In postoperative stage in 1,3,6 months the clinical results were proved with high technique radiology methods. MSCT (n=34) and CBCT (n=66) assessed bone formation and regeneration quality of alveolar bone, the size and shape of newly organized bone, placement of metal screws and state of donor site. To establish the rate of osseointegration in all patients Microfocal radiography was performed. It allowed to visualize the first signs of regeneration in the operation site. In 24 patients with cancellous autograft from iliac crest the bone regeneration was insufficient.

CONCLUSIONS: Multislice computer tomography and con-beam computer tomography helps to plan the reconstructive surgery and assess the postoperative results and autograft placement. Microfocal radiography is the selection method for regeneration assessment in patients with cleft palate and alveolar bone.

09.40 – 09.50 am

CT imaging of odontogenic infections involving the maxillary sinuses

Ulf Riis (short oral presentation)

Institute of Clinical Dentistry University of Oslo, Maxillofacial Radiology, Oslo, Norway

Co-Authors: Redfors M, Eggesbø HB, Larheim TA

OBJECTIVES: The learning objectives of this educational poster are to review and illustrate the computed tomographic (CT) features of odontogenic infections arising from a necrotic pulp in the maxillary molar teeth, and to show how odontogenic infections can proceed to the maxillary sinuses and mimic maxillary sinus disease. Further, to discuss CT imaging techniques of odontogenic infections. The maxillary molar teeth and the maxillary sinus have a close relation, and therefore, odontogenic disease in the upper jaw

often involves the maxillary sinuses. Infection is the most common odontogenic condition to cause maxillary sinus involvement. An infected tooth may form a direct pathway for bacteria and inflammatory agents into the jawbone and the maxillary sinuses. In the literature, it is reported odontogenic cause of maxillary sinus mucosal hyperplasia in 58–78%, and maxillary sinusitis in 4–47%. Infections most commonly originate from the soft tissue central in the tooth, referred to as the dental pulp. Caries and trauma are

the two major causes to formation of a necrotic dental pulp that is the first step to different odontogenic inflammatory conditions (Fig 1). Untreated, a necrotic pulp will proceed to an inflammatory lesion in the bone around the apex of the tooth, referred to as apical periodontitis. In the acute form, an apical periodontitis may turn into a periapical abscess, leading to pus and/or fistula formation that may further proceed to osteomyelitis. In the chronic form, granulation tissue mixed with inflammatory cells may develop into a periapical granuloma that may further proceed into a radicular cyst (apical cyst) due to entrapment and proliferation of epithelium. Radicular cysts are the most common of extrinsic lesions to involve the maxillary sinuses. Small radicular cysts can mimic retention cysts in the maxillary sinuses, but a radicular cyst can usually be differentiated from a retention cyst by the thin sclerotic border (Fig 2). However, an

infected radicular cyst bulging into the maxillary sinus may lose its characteristic sclerotic border and can therefore be difficult to differentiate from lesions originating in the maxillary sinuses. As the radicular cyst enlarges and displace the sinus floor superiorly, the cyst border can be difficult to distinguish from the floor of the sinus. In severe cases, radicular cysts may fill the whole sinus and therefore be misinterpreted as sinusitis or maxillary sinus tumour.

TAKE-HOME-POINTS: To be familiar with the CT features of odontogenic inflammatory conditions that may involve the maxillary sinuses or mimic maxillary sinus disease. To know the basic CT imaging technique that is necessary for revealing odontogenic disease.

To know the basic CT imaging technique that is necessary for revealing odontogenic disease.

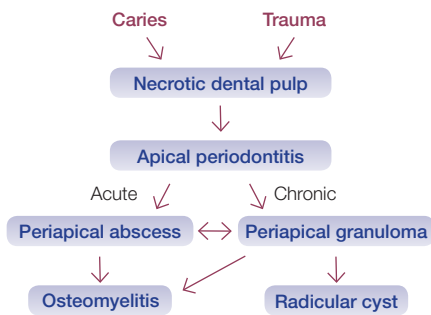


Fig 1 Flowchart of the development of odontogenic infections.

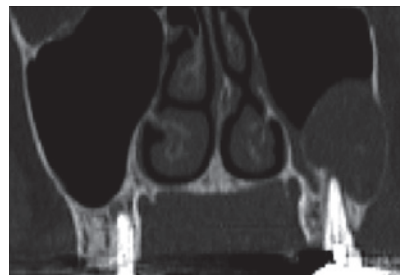


Fig 2 A radicular cyst is the most common extrinsic lesion to involve the maxillary sinus. This coronal CT demonstrates the thin sclerotic border that can help to differentiate at radicular cyst from a retention cyst arising in the maxillary sinus mucosa lining.

09.50 – 10.00 am

CBCT in the detection of odontoma

Antonio Lo Casto (short oral presentation)

DIBIMEF, Università degli Studi di Palermo, Sezione di Scienze radiologiche, Palermo, Italy

Co-Authors: Barreca F, Galbo L, Sergi M, Purpura P, La Tona G

OBJECTIVES: Odontoma is the most common among odontogenic tumors, representing 22- 23.9% of them. Impaction, aplasia, malformation, malpositioning, and devitalization of adjacent teeth are associated with 50-70% of odontomas. Two types of odontoma are distinguished, compound and complex. The typical features of compound odontoma are separate, rudimentary, closely positioned toothlike structures. When such buds form an amorphous and irregular conglomerate of dental tissue without a clear division, they are classified as complex odontoma. Both types are recognized more frequently in the permanent dentition, typically in the second or third decade of life. The anterior maxilla and the posterior part of the mandible are most commonly affected sites. CBCT findings in the detection of odontoma is reported.

MATERIALS AND METHODS: 5 patients (4 women, 1 man, ranging from 12 to 51 years) were studied by a CBCT device with 90 KV and 13 mA, 0,34 voxel size. Panoramic, cross sectional, multiplanar and 3D reformations were acquired.

RESULTS: 3 complex and 2 compound odontomas were found. Odontomas were located: 1 in the right maxilla, 2 in the left maxilla, 1 in the left mandible, 1 in the right mandible. In the patient with odontoma in the right maxilla, it was adjacent to the nasopalatin canal, caused the impaction of 11, with persistency of 51. Of the 2 odontomas in left maxilla, one was adjacent to the maxillary sinus floor, the other one was buccally erupted. The odontoma in the left mandible was contiguous to the mandibular canal wall.

RESULTS: Making a final diagnosis of odontoma only relying on panoramic or periapical radiographic appearance alone often presents a challenge, because odontomas can mimic other osseous or fibro-osseous lesions, and its recognition depends also on its position with respect to the x-ray beam incidence, due to overimposed adjacent anatomic structures or lesions, that can partially masquerade odontoma. Therefore, for differential diagnosis and treatment planning, the use of CBCT is highly recommended. CBCT in fact, thanks to tridimensional high resolution data acquisition, allows a correct identification of odontoma, avoiding overimposed structured noise, and of its relationship to contiguous anatomic structures.

CONCLUSIONS: Making a final diagnosis of odontoma only relying on panoramic or periapical radiographic appearance alone often presents a challenge, because odontomas can mimic other osseous or fibro-osseous lesions, and its recognition depends also on its position with respect to the x-ray beam incidence, due to overimposed adjacent anatomic structures or lesions, that can partially masquerade odontoma. Therefore, for differential diagnosis and treatment planning, the use of CBCT is highly recommended. CBCT in fact, thanks to tridimensional high resolution data acquisition, allows a correct identification of odontoma, avoiding overimposed structured noise, and of its relationship to contiguous anatomic structures.

Special focus – f-MRI in ENT

14.09.2012, 08.30 – 10.00 am

Chairs: Erich Hofmann, Fulda (Germany) / Christoph Stippich, Basel (Switzerland)

08.30 – 09.00 am

Basics and methods

Christoph Stippich (Invited presentation)

Universitätsspital Basel, Klinik für Radiologie und Nuklearmedizin, Basel, Switzerland

SUMMARY: This Invited presentation covers basic surface neuroanatomy of the human brain, functional- and imaging anatomy with a focus on the auditory system. The physiological, technical and experimental basics of functional MRI are summarized as well as preconditions for clinical applications: Blood oxygen level dependent contrast (BOLD), neurovascular coupling and hemodynamic response, paradigm designs and model based calculation of fMRI-signals, over-

lay procedures, strategies for analyzing data in individual patients and capabilities at 3.0 Tesla. The combination of fMRI with Diffusion Tensor Imaging (DTI) and tractography is highlighted.

TAKE-HOME-POINTS: Neuroanatomical basics; principles of BOLD-fMRI and DTI; preconditions for clinical application.

09.00 – 09.30 am

Clinical applications – Auditory FMRI of the Deaf?

Andreas Bartsch (Invited presentation)

Universitätsklinikum Heidelberg / Neurologische Klinik, Abteilung für Neuroradiologie, Heidelberg, Germany

SUMMARY: Stimulability of the auditory system is a prerequisite to successful cochlear implantation (CI). FMRI audiometry and promontory testing can demonstrate the integrity of the auditory system, even in virtually deaf CI candidates irrespective of their subjective hearing. These advanced FMRI applications are, in conjunction with each other and probabilistic tractography of

the acoustic radiation, useful to decide i) which ear should host the CI and ii) whether a different device implanted at the brainstem or midbrain level should be considered.

TAKE-HOME-POINTS: This talk illustrates actual decision-makings based on clinical cases.

09.30 – 10.00 am

fMRI in the Diagnostics of Auditory Processing Disorder

Sylva Bartel-Friedrich (Invited presentation)

Medizinische Fakultät der Martin-Luther-Universität Halle-Wittenberg, Klinik für Hals-, Nasen- und Ohrenheilkunde, Halle (Saale), Germany

Co-Authors: Kösling S, Noll A

SUMMARY: The term auditory processing disorder (APD; in German: auditive Verarbeitungs- und Wahrnehmungsstörung, AVWS) embraces various complex central auditory disorders. APD is a deficit in the perceptual processing of auditory information in the central nervous system [Bellis, 2004] and can be responsible for restrictions of auditory performance. Children with APD are able to hear beeps and tones with no difficulty and show normal pure-tone audiometry. However, speech is not processed in a normal way and this results in a variety of symptoms, such as the ability to discriminate speech against background noise or in poor acoustic environments. Given the frequent impairment of sound discrimination, reading and spelling may also be challenging. APD is specific to the auditory modality. However, it has symptoms in common with, and may be associated or co-occur with, attention deficit / hyperactivity disorder (AD/HD), language impairment, reading disability, learning disability, autism spectrum disorder, and reduced intellectual functioning. The differential diagnosis of APD from these related problems is therefore often challenging, yet important, since children with these disorders may exhibit similar behaviors but need additional assessment and care. The assessment tools should examine a variety of auditory skills, with particular attention to the following areas:

1. Sensation;
2. perception and discrimination of tones and speech sounds;
3. Localization;
4. auditory figure-ground;
5. phonemic awareness;

6. auditory memory;
7. dichotic listening.

Additionally, we have developed a functional magnetic resonance imaging (fMRI) test set in order to extend the diagnostic work-up to include imaging, and thus to improve both diagnostic performance and the monitoring of treatment outcome. Regarding interpretation of the results of testing, the diagnosis of APD may be considered if the following criteria are fulfilled: behavioral symptoms consistent across settings that correspond to APD; a consistent significant weakness (i.e., 2 standard deviations or more) on more than one audiological measure of APD that cannot be explained by other factors (e.g., cognition, attention, hearing impairment); inter- and intra-test patterns indicating APD, including ear differences on behavioral assessments and hemispheric differences on topographic physiologic tests. Additionally, a number of other considerations (e.g., medical history, genetic predisposition) must be taken into account. These considerations, in combination with test scores, are decisive for clinical impressions, interpretation and diagnosis. Intervention should encompass direct therapy, modification of the environment, compensatory strategies, teaching modifications, and, when indicated, improvement of the signal-to-noise ratio through an appropriate assistive listening device.

TAKE-HOME-POINTS: APD is a complex disorder, specific to the auditory modality. fMRI can contribute to the diagnostic work-up.

Lesions of the jaw and oral cavity – Role of radiology

14.09.2012, 10.30 – 12.30 pm

Chairs: Julian Kabala, Bristol (United Kingdom) / Davide Farina, Brescia (Italy)

10.30 – 11.00 am

Jaw

Herwig Imhof (Invited presentation)

Medizinische Universität Wien, Universitätsklinik für Radiodiagnostik, Vienna, Austria

SUMMARY: Imaging of the jaw include plain radiographs including intra- and/or extraoral techniques and panoramic radiography. In recent years CT, cone-beam CT (CBCT) and MRI have been used increasingly. The latter ones have been proven effective for differential diagnosis, determination of the extent of lesions and implantate planning. Discussed are the basic principles of Dental-CT and CBCT in implantology, and DD of cysts, common odontogenic tumors and bone-related lesions (fibrous dysplasia, osseous dysplasia).

TAKE-HOME-POINTS: 1. CBCT should be used only in high contrast small lesions, while low contrast lesions are preferably done with CT. 2. Jawbone lesions should be differentiated in radiolucent, mixed radiolucent and radiopaque, and complete radiopaque lesions, as well. 3. Next step in DD is to differentiate between lesions which are in contact with the tooth (teeth) or not. Eg. residual cysts, primordial cyst, ameloblastoma, fibrous dysplasia malignant neoplasma have typically no contact with the tooth.

11.00 – 11.30 am

Oral cavity

Martin G. Mack (Invited presentation)

Munich, Germany

SUMMARY: In the oral cavity and oropharynx the use of imaging should be restricted mainly to tumorous lesions. Only in rare cases of complicated parapharyngeal abscess, when concomitant inflammation of the parapharyngeal space is suspected, radiologic evaluation might be necessary to exclude an inflammatory spread to the parapharyngeal space and the carotid sheath respectively. Concerning tumor extension in malignomas of the oropharynx and oral cavity, the tumor margins as well as the grade of infiltration will affect the therapeutic management. In tumors of the anterior floor of the mouth or the tonsils, the infiltration of the mandible is an important point of

interest; in the tongue it is important to know the tumor has crossed the midline. In oropharyngeal cancer the tumor margins towards the tongue, the mandible and the parapharyngeal space influence the decision concerning an adequate therapeutic approach. Also in tumors of the base of the tongue and vallecula, the grade of infiltration determines, whether a surgical intervention is still sensible. In case an operation seems to be reasonable, the extent of the procedure will also depend on the size of the lesion as well as the depth of infiltrative growth.

11.30 – 11.40 am

MRI based tumour volume measurements: An improved predictor of outcome in patients with oral cancer

Karen A Eley (short oral presentation)

University of Oxford, Nuffield Department of Surgical Sciences, Oxford, United Kingdom

Co-Authors: Watt-Smith SR, Golding SJ

OBJECTIVES: The automatic upstaging of oral cavity tumours to T4a using the criteria of cortical bone invasion has been the subject of much debate. A potential method to enhance the TNM staging criteria is the incorporation of tumour volume (Tv) measurements which have been shown to be reliable predictors of outcome. The aim of this study was to determine the benefit of pre-treatment MRI based tumour volume measurements in patients presenting with SCC involving the oral cavity subsites most frequently associated with bone invasion the mandibular region and maxillary complex

MATERIALS AND METHODS: A retrospective study of all patients undergoing surgical resection for SCC of the retromolar trigone, mandible, floor of mouth (with bone involvement) (mandibular region), or maxillary sinus, maxilla, hard palate and maxillary gingiva (maxillary complex) between February 2001 and August 2011 was completed. Patients with a prior history of head and neck malignancy or radiation therapy to the head and neck

were excluded. In total, 101 patients met the inclusion criteria, and Tv measurements completed on their pre-treatment MRI using semi-automated methods of tumour segmentation.

RESULTS: The mean tumour volume was $12.79 \pm 24.31 \text{ cm}^3$ for maxillary complex tumours, and $5.73 \pm 7.30 \text{ cm}^3$ for mandibular region tumours. Independent samples t test was significant for increasing overall all-cause survival and decreasing tumour volume. Tv was stratified into 4 groups to correlate with the current TNM staging system. This resulted in down-staging of tumour stage in the majority of which has been classified as pT4 tumours. The Tv stratified groups were a more reliable predictor of outcome than the TNM staging.

CONCLUSIONS: MRI based tumour volume measurements appear to be a reliable predictor of outcome in patients with oral cavity SCC being more accurate than the clinical and pathological TNM staging in the cohort studied.

11.40 – 11.50 am

Low-dose microfocus radiography in dental practice

Alexandr Vasilyev (short oral presentation)

Clinic of Moscow State University of Medicine and Dentistry, Department of Radiology, Moscow, Russia

Co-Authors: Petrovskaya V, Potrahov E

OBJECTIVES: To estimate the possibilities of portable microfocus radiography in dentistry and maxillofacial surgery.

MATERIALS AND METHODS: There were examined one hundred forty patients, 5 to 50 years after endodontic treatment (n=40), cyst removal (n=30), implants installation (n=40),

bone grafting in patients with cleft alveolar bone (n=40). Imaging of treatment steps were performed by portable microfocal radiovisiograph Pardus-Stoma.

RESULTS: In 18 patients (range 5 to 13 years) low-dose microfocal radiovisiography allowed to assess the caries decay, periodontal tissue, structure of roots and furcation region in deciduous teeth, location and follicle structure. The method of microfocal X-ray was affective in choosing the right way of treatment: surgical treatment (n=6), endodontic treatment (n=12). 22 permanent teeth were viewed under X-ray control to assess periapical region, root canal preparation and filling. For cyst removal regular X-Ray control during the surgery was needed. Images were taken during removal of granulating tissue and filling material from the periapical zone. At the later stage of surgery the defect was filled with biomaterial. In postoperative stage, 1,3,6 months, 1year after the surgery, the bone imaging was performed and the historamm of new bone was created. In spite of careful implant planning the application of Microfocal radiovisiograph is necessary for the pa-

tients with the lack of bone, inadequate place in the jaw, foreign body in the region of future implantation and immediate implantation. X-Ray images were taken 3 times: before implant place creation, after place creation and after implant installation. At the beginning the microfocal radiovisiography assisted in measuring the size of alveolar bone, the distance between adjacent teeth and reveal bone changes. At the time of implant placement the location and depth of depth gauge were measured, where 9 patients had some changes of implant placement after. In patients with cleft alveolar bone application of portable microfocal radiovisiograph support to identify the structure of alveolar bone in the defect and near by teeth. In postoperative stage in one month after bone grafting it can be detected the first signs of osseointegration.

CONCLUSIONS: Low-dose microfocal radiovisiography is an affective method of diagnostics, which support to take images with high resolution and control the surgery in every steps, to have an influence on surgical operations, and thus, to reduce the postoperative complications.

11.50 – 12.00 am

Bone density changes evaluated with computer tomography at interradicular sites with horizontal bone loss

Alexandrina L. Dumitrescu (short oral presentation)

Dental Private Clinic,
Bucharest, Romania

Co-Authors: Zetu L, Teslaru S, Haba D

OBJECTIVES: The aim of the current study was to evaluate quantitatively bone density changes in the maxillary and mandibular interdental sites with horizontal bone loss.

MATERIALS AND METHODS: 29 individuals (17 females, mean age 40.44 years) participated in this study. Computer scans were performed

on a SOMATOM Emotion (Siemens), in Explora Center -RX in Iasi, Romania. After the CT images were stored in the computer sections of 0.5 mm thickness horizontal CT sections were selected to measure bone density of the interradicular and interdental septum.

RESULTS: There were no statistically significant differences between male and female subjects using t-test (466.33 ± 187.22 HU vs. 456.42 ± 188.29 HU) ($P > 0.05$). There were statistically significant differences of mean value and of bone density at specific bone depth levels in the interdental area between different age groups ($P=0.008$). At jaw level, no statistically significant differences between the right and left sides of the maxilla or mandible were detected ($P > 0.05$) but statistically significant differences of mean value and of bone density at specific bone depth levels between the maxilla and mandible were recorded (416.53 ± 195.15 vs. 529.64 ± 152.96 ; $P < 0.0001$). At tooth level, the multiple linear regression analyses showed mean alveo-

lar bone density value as well as particular values at different bone level as dependent variable, a strong association with age, gender, type of jaw, tooth type, presence of untreated caries, endodontic and prosthetic treatment and presence of periapical lesions. Significant differences in alveolar bone density were noted between participants with no alveolar bone loss and those with more than 2 mm alveolar bone resorption were observed in the first 1.5 mm bone depth.

CONCLUSIONS: Computer tomography allows early detection of changes in alveolar bone density and reveals an understanding of the bone changes during periodontal disease.

12.00 – 12.10 pm

Quantitative computed tomography in jaw for detection of glucocorticoid-induced osteoporosis in miniature pigs by threshold-based bone density measurement

Jan Kowald (short oral presentation)

University Hospital of Regensburg, Prof. Dr. med. Christian Stroszczynski, Institute of Diagnostic Radiology, Regensburg, Germany

Co-Authors: Estenfelder S, Stadlinger B, Hietschold V, Kuhlisch E, Stroszczynski C

OBJECTIVES: QCT of lumbar spine is an established method for assessment of bone density due to the fact that there is an extensive area of cancellous bone. Dental root measurements distort the density measurement of cancellous bone. Therefore extraction of this interference factor is required. The aim of this study was to detect glucocorticoid-induced loss of bone density in jaw by quantitative computed tomography. We used 27 adult female miniature pigs. Glucocorticoid-induced osteoporosis in lumbar spine of miniature pigs was shown in the past (Scholz-Ahrens et al., 2007). Bone density measurement in jaw was assessed by experimental software.

MATERIALS AND METHODS: In this study we used 27 adult female miniature pigs. Before intervention (t0), after 6 months (t6), and after 9 months (t9) bone density measurements in jaw and lumbar spine were performed. Caused by medicamentous intervention after baseline-CT decrease of bone density should be reached. For this study we developed an experimental software enabling the elimination of confounders. We determined thresholds that exclude dental roots and fatty bone marrow. Image evaluation ensued by imaging jaw bone in axial plane parallel to premolar surfaces amounting to dental roots. Measurement below dental roots was not achievable because of the mandibular nerve, maxillary and paranasal sinuses respectively. Images of CT-examinations were fused

by way of semiquantitative comparison. We defined regions of interest in cancellous bone limited by cortical bone, anterior and molar roots.

RESULTS: Mean bone density (BD) in mandible and maxilla decreased significantly with GC treatment. BD was -138,3 HU or -25.6% ($p < 0.001$) in mandible and -106.4 HU or 25.2% ($P < 0.001$) in maxilla after 9 months. Mean BD in lumbar vertebrae (L 1-3) decreased significantly after 6 months. BD was 38,0 HU or -9.7% ($p = 0.006$) in lumbar vertebrae 1, -39.7 HU or -10.6% in lumbar vertebrae 2 ($p = 0.006$)

and -36.1 HU or -9.9% in lumbar vertebrae 3 ($p = 0.005$). BD increased from t6 to t9. The result was, that there is no more significant difference as distinguished from baseline (lumbar vertebrae 1-3 (L1: $p > 0.999$, L2: $p = 0.982$, L3: $p = 0.993$)). At every time of measurement BD in mandibular was less than in maxilla (t0: $p < 0.001$ t6: $p = 0.007$ t9: $p = 0.043$).

CONCLUSIONS: In summary, we have shown a significant and persistent loss of bone in jaw. Thus the adult miniature pig is a suitable animal model for GC-induced osteoporosis in jaw.

Scholz-Ahrens KE, Dellling G, Stampa B, Helfenstein A, Hahne HJ, Acil Y, Timm W, Barkmann R, Hassenpflug J, Schrezenmeier J, & Gluer CC (2007). Glucocorticosteroid-induced osteoporosis in adult primiparous Gottingen miniature pigs: effects on bone mineral and mineral metabolism. *Am J Physiol Endocrinol Metab* 293, E385-E395.

12.10 – 12.20 pm

Head and neck findings in the postmortem imaging material in Linköping, Sweden

Beatrix Kovacsovics (short oral presentation)

University Hospital, Linköping, County Council of Östergötland, Department of Radiology, Linköping, Sweden

Co-Authors: Persson A, Wernvik E

OBJECTIVES: The center of Medical Imaging and Visualisation at University Hospital in Linköping Sweden in collaboration with the Swedish National Board of Forensic Medicine has developed a procedure for postmortem imaging (PM) that is now used routinely for forensic work since 2003. The first examinations were performed on a 16-slice scanner (Somatom Sensation 16, Siemens Medical solutions, Germany). The CT was replaced by a dual-source scanner (Somatom Definition, Siemens Germany) in 2006 and by more state-of-the-art dual-source scanner (Somatom Definition Flash, Siemens Germany) in 2009 and upgraded in 2012 with Stellant detectors. There is very little written on findings in the head and neck area in PM and our goal was to map the findings in this region in our material.

MATERIALS AND METHODS: Between November 2003 and September 2011 284 PM examinations were performed in Linköping. In 68 of them had the referral indicated possibility for damage in the head and neck area. Thirty-six of them had findings, twenty-six on skull, face and ten on the neck. In all but 5 cases the findings in the head and neck area was the cause of death. The cause of death was accident in seven cases, illness in one, suicide in two, unclear in one and homicide in twenty-five.

RESULTS: Those who died by accident (fall, drowning, explosion, swing set falling on the head) showed head neck findings comparable with injuries seen in everyday practice, ex zygomatium and blow in fractures, dislocated TMJ,

temporal bone and cervical spine fractures. In one case exsanguination after tonsillectomy was the cause of death. The bleeding following the unsuccessful emergency tracheotomy was a contributor to the death of a patient with ruptured aortic aneurysm. Nine of the homicide and suicide cases had damage on the neck which lead to death. One of them was strangled, one, who was shot, and had findings in the masticator space and the upper cervical spine. All seven exposed to stabbing with a knife had soft tissue injuries deep in the neck with connection to the airways. The facial fractures were much more extensive and often combined with skull trauma

in cases with blunt trauma to the head. Those who were shot in the head had no structure intact in the skull or the facial skeleton. The victim who was stabbed in the head, had intracranial bleeding but no trauma on the face.

CONCLUSIONS: Performing post mortem imaging provides significant input to the traditional physical autopsy. Many important findings can be discovered and provide valuable evidence and clues in the forensic investigation in the head and neck findings in post mortem imaging material together with state of the art image post processing will be demonstrated.

Newer techniques – state in 2012

14.09.2012, 10.30 – 12.30 pm

Chairs: Jan Casselman, Bruges (The Netherlands) / Michael Lell, Erlangen (Germany)

10.30 – 11.00 am

Digital volume tomography (Cone beam CT)

Lorenz Jäger (Invited presentation)

Privatärztliche radiologische Praxis Dr. Jäger & Partner, Saarbrücken, Germany

SUMMARY: Digital volume tomography (CBCT) is one of the fastest developing imaging technique at present. It was originally dedicated for dental radiology only. But now it made its way to diagnostic imaging in the field of ENT, Orthopedics and Surgery. The introduction of flat panel detectors and new post processing algorithms lead CBCT out of the dental niche to be established in diagnostic imaging of paranasal sinus, temporal bone, TMJ and the entire skull base. In ENT CBCT is getting more and more involved and is about to replace CT as an imaging technique of first choice in cases of examination of anatomical structures with high contrast.

Modern CBCT systems enable a superb anatomical resolution of 0.08 mm isotropic voxel size by using a tube voltage of only 90 kV and a tube-current of 5 to 10 mA. This high resolution volume data enables the reconstruction of images in any anatomical orientation without any gradually artifact. Images are stored in DICOM format and can be easily exported to RIS and PACS or to an imaging cloud.

Imaging technique will be presented as well as data management. The delineation of imaging anatomy will be demonstrated. Selected examples of pathology covering the field of ENT and dental diagnostic imaging will be given.

TAKE-HOME-POINTS: The major advantage of CBCT is the 3D diagnostic imaging of high contrast structures with an overwhelming anatomical resolution in combination with a minimum of x-ray dosage and a minimum of susceptibility to beam hardening artefacts due to prosthodontics.

11.00 – 11.30 am

Physiological and metabolic imaging

Sotirios Bisdas (Invited presentation)

Eberhard Karls Universität Tübingen, Diagnostische und Interventionelle Neuroradiologie, Tübingen, Germany

SUMMARY: Imaging of head and neck tumours has been in evolution in the last year. Improved hardware and software for computed tomography (CT) and magnetic resonance imaging (MRI) offer increases in the speed and resolution of imaging, and functional methods combined with anatomical imaging have been developed to enhance the diagnostic performance and assist the follow-up imaging. Tumour vascularization and evaluation of antiangiogenic and radiation therapies are based mainly on dynamic contrast-enhanced CT or MRI studies (perfusion studies), which shed light into the tumour microenvironment by estimating blood flow, blood volume and permeability-associated parameters in the pathological tissue. Perfusion studies have been shown to hold a predictive value for the long- and short-term assessment of the therapy response in tumour patients. Tumour metabolism is assessed by magnetic resonance spectroscopy and positron emission tomography, which is either with CT or MRI combined. Proton magnetic resonance spectroscopy is an upcoming modality and provides information about the molecular composition of tissue by studying subtle differences in resonance frequency of the protons embedded in different molecular structures. PET using the radiotracer [18F]fluoro-2-deoxy-glucose is the most commonly used metabolic imaging technology and its clinical value in the evaluation of the unknown

primary, and in the evaluation of recurrent or residual disease is established. Diffusion-weighted MRI, which estimates the diffusion restriction of water molecules in tumours and tumour-like lesions, is in combination with size and morphological criteria a predictor of presence of malignant lymph nodes. Initial reports indicate the use of diffusion-weighted imaging for response assessment after radiochemotherapy. Finally, in comparison with gadolinium containing chelates, the superparamagnetic iron oxide nanoparticles (SPION) show a more extensive shortening of T1 and T2 relaxation time, which results in higher sensitivity in imaging and the visualisation of single iron loaded cells at clinical field strengths.

TAKE-HOME-POINTS: Therefore, molecular imaging may potentially be applied in a variety of fields, among them oncology in order to enhance the detection of specific tumours by using over-expressed cellular markers as molecular targets. Specifically, ultra small SPION with prolonged blood half time can be used for the imaging of neck lymph nodes.

11.30 – 11.40 am

Correlation between apparent diffusion coefficient and standardized uptake value in squamous cell carcinoma of the oral cavity and oropharynx

Lorenzo Preda (short oral presentation)

Divisione di Radiologia
Milano, Italy

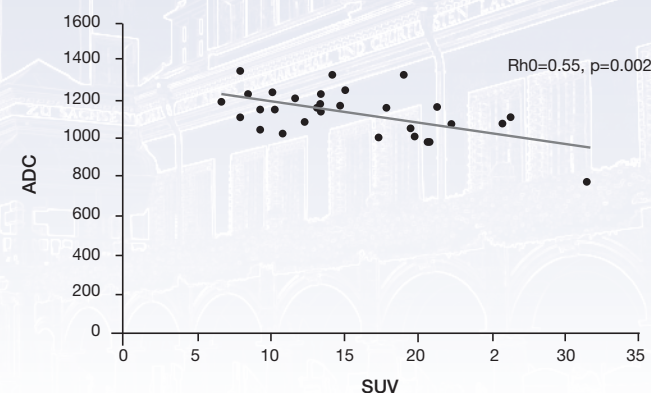
Co-Authors: Bonello L, Petralia G, Giannitto G, Raimondi S, Travaini S, Summers P, Di Filipp R, Bellomi M

OBJECTIVES: To prospectively assess the correlation between the apparent diffusion coefficient (ADC) of squamous cell carcinoma (SCC) of the oral cavity and oropharynx obtained with Diffusion Weighted Magnetic Resonance Imaging (DW-MRI) and maximal Standardized Uptake Value (SUVmax) obtained with FDG-PET/CT.

MATERIALS AND METHODS: 30 patients with untreated histologically proven SCC of the oral cavity and oropharynx underwent conventional (including T2-weighted and T1 pre and post contrast) and DW-MRI (b-values 0, 50, 250, 500 and 900 s/mm²) on a 1.5T MR scanner (Avanto, Siemens, Erlangen, Germany). The ADC was calculated from regions of interest drawn manually on the highest b-value images using the ImageJ (ImageJ, NIH) and fsl (fsl 4, University of Oxford) image processing packages. The same patients underwent staging FDG-PET/CT (Discovery, GE Medical Systems Waukesha, WI); FDG uptake of the tumor was measured by SUVmax.

RESULTS: 30 patients (22 male, 8 female, mean age 53.9 years, range 26–76 years) with 24 tumours of the oral cavity and 6 tumours of the oropharynx were suitable for ADC and SUVmax calculation. Mean tumour size was 36 ± 15 mm. The mean ADC value was 1129.7 ± 121.4 × 10⁻⁶ mm²/s, while the mean SUVmax was 15.4 ± 6.2. A statistically significant inverse correlation (Rho=0.55, p=0.002) was observed between ADC and SUVmax (Figure 1).

CONCLUSIONS: We found that diffusivity of water molecules (ADC) and metabolism (SUVmax) in SCC of the oral cavity and oropharynx are inversely correlated; tumours exhibiting increased metabolism showed impeded diffusion which could indicate increased cellularity. Further studies on larger cohorts are encouraged to confirm this preliminary evidence on tumour biology.



11.40 – 11.50 am

Diffusion-weighted MRI and FDG PET/CT in head and neck squamous cell carcinoma: is there any correlation between ADC and SUV values?

Arthur Varoquaux (short oral presentation)

Geneva University Hospital, Department of Radiology,
Geneva, Switzerland

Co-Authors: Rager O, Kohler R, Masterson K, Ratib O, Becker M

OBJECTIVES: The purpose of this study was to assess the correlation between apparent diffusion coefficient (ADC) values and standardized uptake values (SUV) in patients with biopsy-proven primary squamous cell carcinoma of the head and neck (HNSCC).

MATERIALS AND METHODS: Retrospective analysis of a consecutive series of 33 patients with 34 biopsy-proven primary HNSCC (11 females and 22 males, mean age=55 years) who have undergone MRI at 1.5 T and contrast enhanced FDG PET CT prior to biopsy or surgery. Axial diffusion weighted EPI sequences (DWI) were obtained using b-values of 0 mm²/s and 1000 mm²/s. Calculation of ADC maps was done automatically. The ADC and the SUV tumor values were measured with regions of interest (ROIs) matched for shape, surface and position by two experienced readers, who were blinded to the histological and clinical data. Statistical analysis

was done using Spearman s rank correlation analysis, Bland Altman and intraclass correlation coefficients (ICC).

RESULTS: ICC showed almost perfect reproducibility (>0.96) for the ADC_{mean}, ADC_{min}, SUV_{max} and SUV_{mean} for intra-observer and inter-observer agreement. ADC_{mean} values in primary HNSCC were 1.03 ± 0.29 x10⁻³mm²/sec and SUV_{mean} values were 10.66 ± 3.72. We observed no significant correlation between ADC_{mean} values and SUV_{mean} or SUV_{max} measurements in primary HNSCC (r[-0.105; -0.09]; p[0.382; 0.941]).

CONCLUSIONS: Our data suggest that in primary HNSCC there is no correlation between FDG uptake and ADC values. Further studies are necessary to investigate the possible complementary role of DWI and FDGPET/CT in HNSCC.

11.50 – 12.00 am

Can diffusion weighted imaging differentiate recurrent disease from reactive nodes in patients with treated head and neck squamous cell carcinoma?

Cristina Dudau (short oral presentation)

University College London Hospitals, Radiology,
London, United Kingdom

Co-Authors: Halligan S, Bell N, Adjey Gyamfi Y, Beale T, Morley S, Punwani S

OBJECTIVES: Modern chemo and radiotherapy treatment (CRT) is able to eradicate nodal disease, even in advanced stages of squamous cell carcinoma of the head and neck. However,

conventional morphologic MR imaging cannot currently distinguish between benign post treatment residual masses following CRT [REF]. PET-CT when negative is a good indicator of a

benign mass, but when positive has a specificity of 50%. We report a series of patients with CRT treated head and neck squamous cell carcinoma (SCC) that underwent multi-b-value diffusion weighted imaging (DWI) during the course of routine post-treatment follow-up to ascertain whether DWI was able to differentiate reactive nodal masses from residual disease.

MATERIALS AND METHODS: The institutional picture archiving and communications (PACS) database was searched for all patients with CRT treated head and neck SCC that underwent assessment for a residual nodal mass with MRI between 2011 and 2012. In total 16 patients were eligible for study inclusion. Each patient had a single residual nodal neck mass. Eight patient residual masses were classified as disease and eight as reactive based on a reference standard of fine needle aspiration and clinical follow-up. DWI was performed using a Short Tau Inversion Recovery Spin Echo Echo Planar Imaging sequence with 6-b values (0, 50, 100, 300, 600 and 1000 s⁻¹mm²). For each patient the diffusion weighted images were analysed to extract the signal intensity of the node on the slice containing the maximum cross sectional diameter for each b-value image. Apparent diffusion coefficient was calculated using a least

squares fit for all b-values (ADC_{6b}); b₀₋₅₀₋₁₀₀ (ADC_{fast}); and b₃₀₀₋₆₀₀₋₁₀₀₀ (ADC_{slow}). Mean values for each parameter were compared between benign and disease nodal groups using a Students t-test.

RESULTS: There was no significant difference between reactive and disease nodal mass mean ADC_{6b} (1.21±0.59 [SD] vs. 1.21±0.33 [SD] x10⁻³mm²s⁻¹, p=0.98) or ADC_{fast} (2.68±1.18 [SD] vs. 2.35±1.27 [SD] x10⁻³mm²s⁻¹, p=0.60). Mean ADC_{slow} was 0.67±0.35 x10⁻³mm²s⁻¹ for reactive nodes and 0.98±0.29 x10⁻³mm²s⁻¹ for disease with the difference approaching statistical significance (p=0.07).

CONCLUSIONS: ADC values calculated with low-b values alone (b₀₋₅₀₋₁₀₀) or using a mixture of low and high (b₀₋₅₀₋₁₀₀₋₃₀₀₋₆₀₀₋₁₀₀₀) b-values are unable to differentiate residual disease from reactive nodes. However ADC calculated using high b-values alone (b₃₀₀₋₆₀₀₋₁₀₀₀) demonstrates a tendency towards a larger value in diseased nodal masses compared with reactive lymph nodes post CRT of head and neck patients treated for SCC. Recruitment into the study continues and full results will be presented.

12.00 – 12.10 am

Dual metric differentiation of non-tumorous parotid gland diseases using high-resolution dynamic contrast-enhanced and diffusion weighted MRI

Jasmin D. Busch (short oral presentation)

University Medical Center Hamburg-Eppendorf, Department of Diagnostic and Interventional Radiology,
Hamburg, Germany

Co-Authors: Treszl A, Bier J, Muenscher A, Adam G, Habermann C

OBJECTIVES: To determine the value of combining dynamic contrast-enhanced (DCE) and diffusion weighted (DWI) MRI for the differentiation of non-tumorous diseases of parotid glands.

MATERIALS AND METHODS: 143 consecutive patients with clinically and sonographically proven non-tumorous diseases of the parotid glands were prospectively examined with a DCE sequence using a 1.5 T unit. A single transverse

4mm thick slice with FOV of 200x188mm² was measured with a dynamic gradient echo sequence (TR/TE=15/4.4 msec) with 2.9s/image. A dose of 0.1mmol/kg Gd-DTPA was injected with 2.5ccm/s. Following parameters were evaluated: bolus arrival time (BAT), tumor blood flow (TBF), tumor blood volume (TBV), volume transfer constant (Ktrans), and exchange rate constant (Kep). Additionally, a DW EPI sequence (TR/TE=1,500/77 msec) was performed. The b factors used were 0, 500 and 1000 sec/mm². Analyses were performed with an in-house developed semi-automatic software tool. For comparison of perfusion parameters and ADC (apparent diffusion coefficient), paired two-tailed Student's t-test with Bonferroni correction for multiple testing was used.

RESULTS: In all 143 patients a parotid gland disease was histologically (n=72) or clinically (n=71) confirmed (Sjögren syndrome: n=56, sialadenoses: n=39, sialadenitis: n=48). Based on PBF discrimination between sialadenitis and Sjögren syndrome was possible (p=0.02). PBV differentiated not only sialadenitis and Sjögren syndrome (p<0.001) but also sialadenitis and sialadenoses (p=0.002). A differentiation between Sjögren syndrome and sialadenose based on PBV (p=0.619) was not possible. Ktrans and Kep offered no discriminative potential. Using ADC differentiations between Sjögren syndrome and sialadenose (p=0.0008) as well as sialadenitis and sialadenose (p<0.001) are possible.

CONCLUSIONS: The combination of DCE MRI and DWI has the potential to differentiate the most common non-tumorous diseases of parotid glands. An invasive seems to be obsolete.

12.10 – 12.20 pm

Non-invasive differentiation of primary parotid gland tumors: does the combination of high-resolution dynamic contrast-enhanced MRI and diffusion-weighted imaging improve diagnostics?

Christian R. Habermann (short oral presentation)

University Medical Center Hamburg-Eppendorf, Department of Diagnostic and Interventional Radiology, Hamburg, Germany

Co-Authors: Treszl A, Bier J, Muenscher A, Adam G, Busch JD

OBJECTIVES: To determine the value of combining dynamic contrast-enhanced (DCE) MRI with diffusion-weighted MRI (DWI) in differentiating primary parotid gland tumors.

MATERIALS AND METHODS: 112 consecutive patients with a suspected tumor of the parotid gland were prospectively examined with a DCE sequence using a 1.5 T unit. A single transverse 4mm thick slice with FOV of 200x188mm² was measured with a dynamic gradient echo sequence (TR/TE=15/4.4, $\alpha=50^\circ$, matrix 256x192) with 2.9s/image. A

dose of 0.1mmol/kg Gd-DTPA was injected with 2.5ccm/s in the antecubital vein followed by saline. Analyses were performed with an in-house developed semi-automatic software tool. The following parameters were evaluated: bolus arrival time (BAT), tumor blood flow (TBF), tumor blood volume (TBV), volume transfer constant (Ktrans), and the exchange rate constant (Kep). Histological diagnosis was obtained in every patient. For comparison of perfusion parameters, paired two-tailed Student t-test with Bonferroni correction for multiple testing was used.

RESULTS: In all 112 patients a primary parotid gland tumor was histologically confirmed (48 pleomorphic adenomas, 44 Warthin tumors, 5 basal cell adenomas, and 15 carcinomas). Based on ADC, pleomorphic adenomas were discriminated from carcinomas (p=0.03), from Warthin tumors (p=0.003), and basal cell adenomas. Warthin tumors were not distinguishable by ADC from carcinomas (p=0.997). TBF and TBV of basal cell adenomas differed significantly from all other entities (p<0.001 to 0.006). Additionally, TBF distinguished carci-

nomas significantly from pleomorphic adenomas (p=0.008), but not from Warthin tumors (p=0.365). Whereas, TBV offers a significant distinction between carcinomas and Warthin tumors (p=0.01). Ktrans and Kep offered no discriminative potential.

CONCLUSIONS: Combination of DCE- and DW MRI improves the discriminative potential of MRI for differentiation of primary parotid gland tumors.

Short oral presentations: Varia

14.09.2012, 14.30 – 15.30 pm

Chairs: Heidi Beate Eggesbø, Oslo (Norway) / Holger Gress, Ostfildern (Germany)

14.30 – 14.40 pm

Algorithm of radiologic examination of patients with diseases of lacrimal pathways

Ekaterina Privalova (short oral presentation)

Moscow State University of Medicine and Dentistry, Radiology Department, Moscow, Russia

Co-Authors: Vasiliev A, Davydov D

OBJECTIVES: To develop an algorithm of radiologic examination of patients with diseases of lacrimal pathways.

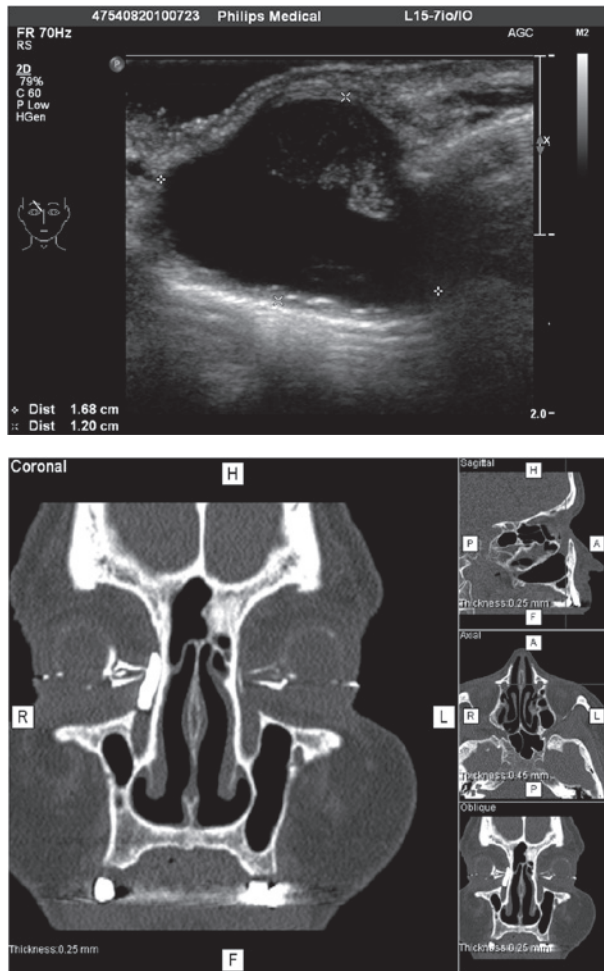
MATERIALS AND METHODS: 69 people at the age of 19 to 75 years with different diseases of lacrimal pathways were examined. 25 patients were performed multislice computed tomography with contrast enhancement. We used nonionic low-osmolarity contrast agents. 8 patients were carried out MSCT without contrast enhancement. 25 patients were examined with high resolution ultrasonography, we used sensor line-scanning with frequency 7–15 MHz. Group of the patients with silicon intubation in lachrymal pathways was analyzed separately. 7

people were carried out with CBCT with contrast enhancement and 4 patients without contrast enhancement.

RESULTS: As the result of MSCT with contrast enhancement, we found chronic dacryocystitis of inflammatory genesis (14 cases), chronic posttraumatic dacryocystitis (6 observation), formation of lachrymal sac (1 patient), the absence of pathological changes (4 people). As MSCT without contrast enhancement data was analyzed it was not possible to estimate changes in lachrymal pathways. As the result of CBCT with contrast enhancement, we diagnosed chronic dacryocystitis of inflammatory genesis (2 cases), chronic posttraumatic dacryocystitis (2 observa-

tion), the absence of pathological changes As (3 people). As high resolution ultrasonography data was analyzed it we had identified chronic dacryocystitis of inflammatory genesis (5 cases), chronic posttraumatic dacryocystitis (5 observations), formation of lachrymal sac (1 patient), and the absence of pathological changes (3 people). The patients with intubation of lachrymal pathways was carried out under the control of high resolution ultrasonography.

CONCLUSIONS: High resolution ultrasonography should be considered as a method of the first stage for patients with lachrymal pathways diseases. In the second stage of the diagnostic search, it is advisable to make MSCT with contrast enhancement in presence of osteotraumatic deformation of midface and changes in soft tissues. CBCT with contrast enhancement should be applied to patients without attendant changes. MSCT and CBCT without contrast enhancement were uninformative in the diagnosis of lachrymal pathways diseases. Figure.



14.40 – 14.50 pm

Craniosynostosis and “Black Bone” MRI: An alternative to CT

Karen A Eley (short oral presentation)

University of Oxford, Nuffield Department of Surgical Sciences, Oxford, United Kingdom

Co-Authors: Watt-Smith SR, Sheerin F, Golding SJ

OBJECTIVES: The diagnosis of craniosynostosis is routinely confirmed on CT imaging with three-dimensional reconstruction. The risks associated with ionising radiation are of greatest concern in young patients with benign conditions, and particularly where repeated imaging is required throughout childhood. A non-ionising alternative that provides the same level of accuracy and 3D reconstructive capabilities may potentially change the methods with which we image children with craniosynostosis in the future. We have previously reported the potential of Black Bone MRI in the identification of the normal patent cranial suture and in 3D reconstruction. The aim of this study was to investigate the potential of “Black Bone” MRI in craniosynostosis.

MATERIALS AND METHODS: Following ethical approval, “Black Bone” MRI was obtained in 9 children with a clinical diagnosis of craniosynostosis at the time of CT scanning (whilst under general anaesthesia). “Black Bone” imaging was completed in a further 3 children with craniosynostosis who were old enough to negate the need for general anaesthesia.

RESULTS: Findings on “Black Bone” MRI were consistent with those on CT imaging and clinical findings. The Black Bone sequence accurately distinguishing the normal patent suture from the prematurely fused. This was further enhanced with the creation of three-dimensionally reconstructed images.

CONCLUSIONS: “Black Bone” MRI appears to offer a reliable method of imaging children with craniosynostosis, with comparable results to CT.

14.50 – 15.00 pm

Multimodality imaging in adolescent patients with advanced stage nasopharyngeal carcinoma, a single centre experience

Cristina Dudau (short oral presentation)

University College London Hospitals, Radiology, London, United Kingdom

Co-Authors: Stoneham S, Shankar A, Bomanji J, Adjey Gyamfi Y, Beale T

OBJECTIVES: Nasopharyngeal carcinoma (NPC) is a rare disease in children and adolescents with over 80% presenting with advanced loco-regional disease. There are currently no imaging guidelines or protocols for MR and PET/CT fol-

low up for detecting disease recurrence in this patient group. We report a series of 8 adolescent patients treated in our institution and discuss the disease response evaluation with both MRI and FDG PET.

MATERIALS AND METHODS: A retrospective review of 8 consecutive adolescent patients diagnosed with NPC who were treated at University College London Hospital between 2003 and 2011 with the paediatric chemo radiotherapy approach (cisplatin-5 fluorouracil based chemotherapy, lower dose radiotherapy of 45Gy and maintenance interferon). All patients had pre and post treatment MRI scans and 7/8 had FDG PET as part of the diagnostic staging and early response evaluation after 3 cycles of chemotherapy, followed by regular interval MRI.

RESULTS: Eight patients (median age 14.1 years) were identified. M: F ratio was 1:1. Seven patients presented with stage IV and one with stage II disease by MRI staging criteria. 7/8 patients underwent initial staging FDG PET. In 6/7 patients this correlated with the staging MRI, whilst in one patient the FDG PET diagnosed distant metastases. One patient did not undergo PET imaging. MRI post 3 cycles of chemotherapy showed complete response by RECIST criteria in 2 patients and partial response in 6 patients, of whom 2 relapsed. The FDG PET showed complete or good metabolic response in 4 patients and partial response in 3, 2 of which

relapsed. Post treatment follow up imaging by MRI was performed at 3 to 6 months interval, for an average period of 2 years, followed by yearly scans. Of the relapses: one patient (distant metastases at diagnosis) progressed during maintenance interferon and died and the other patient had a local relapse 6 months after completion of treatment but was salvaged with laser surgery and nasopharyngeal brachytherapy.

CONCLUSIONS: Initial staging with combined MRI and FDG PET (or PET MR) is recommended, as the MRI defines the local tumor extent whilst FDG PET detects distant metastasis. Early response evaluation at 3 cycles post chemotherapy can be done with MRI only, as our results show good correlation between MRI and FDG PET in assessing initial response to treatment. This would result in significant dose reduction in this young population. Follow up with clinical examination and MRI at regular intervals (4 monthly for the first year, 6 monthly for the second year and yearly scans for up to 5 years) is suggested. FDG PET is helpful in follow up for those patients where the MRI findings are equivocal and can not clearly differentiate post treatment change from residual/recurrent disease.

15.00 – 15.10 pm

CT angiography of the external carotid artery branches in the neck: sufficient resolution to plan microvascular flap reconstruction procedures?

Romain Kohler (short oral presentation)

Geneva University Hospital, Radiology,
Geneva, Switzerland

Co-Authors: Masterson K, Schaepkens van Riepmst J, Terzic A, Dulguerov P, Becker M

OBJECTIVES: Head and neck tumor patients often require extensive reconstructive procedures with microvascular free flaps. The purpose of this study was to evaluate the performance of multislice computed tomography angiography (MSCTA) for vascular mapping of host vessels prior to microvascular flap reconstruction procedures in the head and neck.

MATERIALS AND METHODS: MSCTA was carried out before surgery in 30 patients (22 males, 8 females, mean age 60 years) scheduled for microvascular reconstruction with free flaps (21 antebrachial, 7 fibular, 1 latissimus dorsi, 1 anterolateral thigh). A 64-slice spiral computed tomography (CT) was performed with MPR, MIP

and 3-dimensional VR reconstructions. MSCTA images were analyzed retrospectively by two readers, who were blinded to intraoperative findings. The diagnostic MSCTA quality, vessel diameter, patency, arteriosclerotic changes, stenoses and occlusions of the relevant host vessels (superior thyroid (STA), facial (FA) and lingual arteries (LA)) were assessed. Results were compared with intraoperative findings.

RESULTS: No adverse reactions or complications were seen. With the exception of 2 MSCTA, all remaining examinations were of good or excellent quality. Of the 180 assessed vessels, 148

(82.2 %) were normal, 20 (11.1 %) were occluded and 7 (3.9 %) were stenotic. Seven (3.9 %) showed calcified atheromatous plaques. Based on MSCTA, all normal, stenotic and occluded vessels were correctly identified despite their small diameter (mean diameters for, FA, LA and STA were 1.94, 1.64 and 1.47 mm, respectively).

CONCLUSIONS: Our data indicate that MSCTA provides sufficient anatomic detail for the correct assessment of the critical vasculature of the recipient. Microvascular reconstruction procedures may thus be planned by means of MSCTA.

15.10 – 15.20 pm

Origin and course of the extracranial Vertebral Artery - CTA findings and embryologic considerations

Nikola Dür (short oral presentation)

Klinikum Duisburg Sana Kliniken, Department of Radiology and Neuroradiology,
Duisburg, Germany

Co-Authors: Meila D, Tysiac M, Theisen O, Brassel F, Berenstein A

OBJECTIVES: The aim of this study was to show the different origins and courses of the extracranial VA on CTA with special emphasis on embryological considerations. The duplicated VA is an anomaly that has been assumed to predispose for dissection and to be associated with aneurysms. We report its frequency and clinical significance.

MATERIALS AND METHODS: We retrospectively reviewed CTA of 539 patients by using a contrast-enhanced CTA protocol of the VA on CT.

RESULTS: 94.2% of left VA originated from left subclavian artery and entered the transverse foramen at C6 in nearly all cases. 6.3% of left VA (m=4%, f=10%) originated from the aortic arch and entered the transverse foramen either at C4, C5 or C7 but never at C6. One case of an aberrant retroesophageal right VA originated from the aortic arch distal to the left subclavian artery and

entered at C7 (0.19%). All other right VA originated from the right subclavian artery (99.8%) and entered between C4 and C6. We diagnosed 4 cases of duplicated VA (0.74%) with a female predominance (1.9%) without any signs of dissection on CTA. Two cases with VA duplication had intracranial arterial aneurysms.

CONCLUSIONS: The VA is a longitudinal anastomosis of segmental metameric arteries. The level of entrance into the transverse foramen indicates which metameric artery or arteries persist. Duplication corresponds to persistence of two segmental arteries and is a rare phenomenon. VA duplication might be associated with vascular lesions.

15.20 – 15.30 pm

Rektorzik's Plexus – evaluation with contrast enhanced flat panel computed tomography and 3-DSA

Goetz Benndorf (short oral presentation)

Baylor College of Medicine, Radiology,
Houston, Texas, USA

OBJECTIVES: The internal carotid artery venous plexus, (ICAVP) has been first described by REKTORZIK in 1858 as pars intracanalium sinus caroticus, was observed as inferior petroocapital vein by TROLARD, or as sinus venous caroticus after HAIKE, and descends from the inferior cavernous sinus (CS) enclosing the carotid artery more or less completely at the lower part of the carotid canal. This plexus converges to form one or more trunks, which opens finally into the internal jugular vein (IJV), resembles the architecture of the CS, consisting of numerous small vascular spaces in children that confluent to larger lacunes. Due to its complex structure, small lumen and its postero-lateral orientation, the ICAVP is obscured between other efferent veins of the CS, and is barely visible on routine angiograms. It has been largely neglected in recent anatomical descriptions and major textbooks. The purpose of this study was to evaluate the topographic anatomy of the ICAVP plexus and its relationships to adjacent veins with high-resolution cross sectional vascular imaging using contrast-enhanced Flat Panel Computed Tomography (FP-CT, DynaCT) and 3-D DSA).

MATERIALS AND METHODS: In five patients undergoing petrosal sinus sampling, 3-DSA of the IPS/IJV junction was performed using a C-arm mounted flat detector system (Axiom Artis dBA, Siemens Medical Solution) and the following parameters: 10 sec, 2.5 cc/sec, total of 28ml (300mg Iodine). Dual volumes were obtained by separate reconstructions of mask and filling runs and subsequent fusion using a dedicated commercially available workstation (Leonardo Siemens Medical Solution). Contrast-enhanced

FP-CTs were performed using the following parameters: 20sec rotations, 0.4° increment, 219° total angle, 1240x960 detector matrix, 543 projections, bone sharp kernel, 512x512 reconstruction matrix, 20% dilution (300mg Iodine), 2cc/sec, total of 40 ml. Image post-processing was performed using maximum intensity projections (MIPs) and volume renderings (VRTs).

RESULTS: After emerging from the CS, Rektorzik's plexus initially appears more like a continuous venous structure, lining the osseous petrous canal and covering the wall of the carotid artery with a very thin inner lumen. Following the course of the ICA, the plexus travels more laterally than the other efferent veins and seemed to transform into a network of small veins, appearing more like a plexus. In this material, this plexus-like structure ended somewhere in the carotid canal of the petrous pyramid and was not directly connected with the IPS, but gave rise to a very small curved vein that courses medially to reach the IPS/IJV junction. The IPCV arises between Rektorzik's plexus and the inferior petrosal sinus and courses almost in parallel to the IPS, posterolaterally and caudally towards the IPS/IJV junction.

CONCLUSIONS: Rektorzik's plexus appears to be a constant venous outlet of the CS, emerging between the emissary vein of the foramen ovale and the IPCV, and creating a consistent anatomical arrangement of four efferent veins arising from the lateral and lateroposterior CS: 1) Foramen ovale plexus 2) Internal carotid artery venous plexus (ICAVP) 3) Inferior petroclival vein (IPCIV) 4) Inferior petrosal sinus (IPS).

Short oral presentations: Temporal bone

14.09.2012, 14.30 – 15.30 pm

Chairs: Timothy Beale, London (United Kingdom) / Marc Keberle, Paderborn (Germany)

14.30 – 14.40 pm

Are there substantial differences in spatial resolution of subtle temporal bone structures on CBCT and MDCT?

M. Katharina Pein (short oral presentation)

University Hospital Halle (Saale), Department of Otorhinolaryngology, Head- and Neck Surgery, Halle, Germany

Co-Authors: Plontke S, Kösling S

OBJECTIVES: Today Cone Beam CT (CBCT) became a standard diagnostic procedure in dentistry, oral-maxillofacial surgery and otorhinolaryngology. Especially in temporal bone imaging, industry courted CBCT as the better imaging technique with lower radiation, higher accuracy and a much better 3d-performance compared to Computed Tomography (CT). Currently available data, however, are still contradictory. The purpose of this study was to compare the spatial resolution in vivo of subtle, non-pathological temporal bone structures on CBCT and Multi-detector CT (MDCT).

MATERIALS AND METHODS: For comparison of spatial resolution, temporal bone PACS recordings of 38 patients were randomly selected, 23 of them were imaged by MDCT (Somatom Sensation 64, Siemens, Erlangen, Germany) and 15 by CBCT (3D Accuitomo 170, J. Morita MFG. Corp., Kyoto, Japan). All patients enrolled into this study had normal findings in temporal bone anatomy, absence of previous surgery or other abnormalities. The image series were blindly evaluated by 3 trained observers. Using a 5-point scale, ten subtle structures of the temporal bone were evaluated (tendon of tensor tympani muscle, tendon of the stapedius muscle, incudostapedial joint, incudomalleal joint, crurae and head of the stapes, tympanic

membrane, osseus spiral lamina, chorda tympani and modiolus). Optimized scanning protocols were used in both techniques. Statistical analysis included Mann-Whitney U-test and Kendall's coefficient of concordance. The study was approved by the local independent ethics committee.

RESULTS: Subtle middle ear structures were better shown on CBCT. In contrast, osseus spiral lamina and modiolus tended to be better distinguishable by MDCT. Significant differences between MDCT and CBCT could be shown for the tendon of the stapedius muscle and the crurae of the stapes, which were significantly better visible on CBCT images ($p = 0.003$ and $p = 0.033$, respectively). The osseous spiral lamina showed significantly better representation on MDCT ($p=0.001$). The inter-observer variability was 0.83 (Kendall's W). Intra-observer variability was negligible.

CONCLUSIONS: Adequate imaging results could be obtained by both CT techniques. In the diagnostic setting, differences are not as large as several studies suggest. Overall, both CBCT and MDCT appear of equivalent clinical value with respect to image quality, if optimized protocols are chosen.

14.40 – 14.50 pm

The use of cone beam CT (CBCT) to determine intracochlear electrode positioning in human temporal bones

Timothy Beale (short oral presentation)

The Royal Free Hampstead NHS Trust, Radiology, London, United Kingdom

Co-Authors: Siddiqui J, Saeed Sh, Selvadurai D, Murray B, Biggs N, Risi F

OBJECTIVES: To assess whether CBCT can accurately assess both the scalar positioning and depth of insertion of electrodes in cochlear implants.

MATERIALS AND METHODS: There are 2 current methods for post-operative radiological assessment of cochlear implant positioning. Plain radiography (reverse Stenvers) which although a low radiation dose technique provides limited detail and CT scanning a high radiation dose technique, but with metallic artefact from the implant resulting in a lack of scalar differentiation. There is increasing evidence that scalar positioning and accurate knowledge of electrode insertion depth affect the final functional outcome. CBCT has a lower radiation dose and higher resolution than CT and does not suffer from metallic artefact. Eight human cadaveric temporal bones from the USA underwent cochlear implantation (CI) and post implant CBCT in London (UK). Two different implants and two different surgical approaches (round window and cochleostomy) were used. The post CI CBCT images were examined by a surgeon (SS) and radiologist (TB) blind both to the type of implant used and surgical approach. Each individual electrode was assessed as to whether it was in the scala tympani (ST) or scala vestibuli (SV) and the number of electrodes within the cochlea noted. The implanted temporal bones were prepared and sectioned in Sydney (Australia) and the histological sections examined independently by three histopathologists.

RESULTS: There was 100% concordance in the histopathological and CBCT assessment with regards to scalar positioning and insertion depth by the radiologist (TB). In two temporal bones the reviewing surgeon (SS) thought incorrectly that the electrodes 16-22 in the mid to distal turn of the cochlea were in the scala vestibuli.

CONCLUSIONS: CBCT is a lower dose technique than CT and provides the requisite detail in the majority of instances but further work is required to assess the distal cochlea. These preliminary results are encouraging and we are commencing a prospective randomized study of round window versus cochleostomy insertion using CBCT to assess CI positioning. **Figures 1 a & b**

Fig.1a: CBCT section through mid and distal turn of the cochlea.

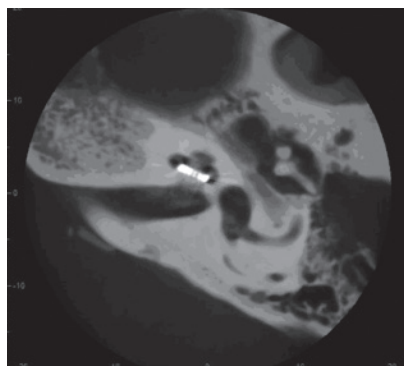
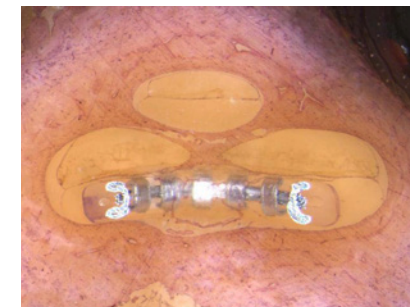


Fig.1b: Equivalent histopathological section. Both images demonstrating CI within scala tympani of middle turn.



14.50 – 15.00 pm

CT-based length assessments of cochlear implant (CI) electrodes in human temporal bone specimens, accuracy evaluation

Andreas Pomschar (short oral presentation)

Ludwig-Maximilians-University Hospital Munich, Institute for Clinical Radiology, Munich, Germany

Co-Authors: D'Anastasi M, Kisser U, Reiser M, Hempel JM, Mueller JM, Ertl-Wagner B

OBJECTIVES: To investigate the feasibility and accuracy of length measurements of the cochlear implant (CI) electrode by high-resolution computed tomography (HR-CT) using CI electrodes of a predefined length in human temporal bone specimens.

MATERIALS AND METHODS: Eight human temporal bone specimens were surgically prepared analogous to a regular CI surgery for the study. The round window was opened and the cochleae were then injected with a physiologic saline solution to avoid air bubbles, which could interfere with CT scanning. Dummy-electrodes by MED-EL with two markers in a predefined distance of 20 mm were inserted and fixated in the round window. Two temporal bones at a time were inserted into both sides of a plastic head phantom and HR-CT imaging was performed with a dual source CT (Somatom FLASH, Siemens). The data were reconstructed with a slice thickness of 0.4 mm, an increment of 0.1 mm in a maximum-intensity-projection technique (MIP).

For data analysis OsiriX (version 4.1, 64-bit) was applied using a 3D-curved MPR technique. Readings were performed by 3 M.D.s of differing experience (Reader 1: otolaryngology resident, Reader 2: junior radiology resident, Reader 3: head and neck staff radiologist). Mean values and standard deviation for time and measured length were calculated.

RESULTS: The mean measurement error from 20 mm over all specimens and readers was 0.8 mm \pm 0.9 (reader 1 to 3: 1.1 mm \pm 1.2 ; 0.7 mm \pm 0.8; 0.7 mm \pm 0.7 respectively). The time needed to measure one electrode was similar for all readers with an average of 6.20 min \pm 3.30 min. Electrode markers were reliably identified by all readers in all specimen.

CONCLUSIONS: Our results show that CT based measurement of cochlear implant length is highly accurate and can be done in a limited time. This may aid in the post-operative assessment of electrode positioning.

15.00 – 15.10 pm

Quality control after cochlear implant surgery using Cone Beam CT

M. Katharina Pein (short oral presentation)

University Hospital Halle (Saale), Department of Otorhinolaryngology, Head- and Neck Surgery, Halle, Germany

Co-Authors: Plontke S, Kösling S

OBJECTIVES: For the radiological description of the intra-cochlear position of electrode arrays after cochlear implant surgery several parameters have been published. The purpose of this study was to analyze the position of electrode arrays using different radiological parameters with respect to a critical re-evaluation of own surgical techniques and results.

MATERIALS AND METHODS: Temporal bones of 36 patients with inserted cochlear implants were imaged by CBCT. The position and insertion depth of electrode arrays were assessed based on: 1.) measurement of rotation angle θ and distance p between last electrode and top of the modiolus as described by Verbist et al.(2010), 2.) visual assignment of electrode position in relation to scala tympani or vestibuli on different multi-planar reconstructions, 3.) visual assessment whether there is a kinking or reversal of the electrode. Image analysis was performed with iDixel® v.1.5.0 (J. Morita MFG Corp.). The study was approved by the local independent ethics committee.

RESULTS: With regard to analysis of insertion depth two different types of electrode arrays have to be distinguished – shorter (e.g. CochlearTM) and longer electrodes (e.g. Med-EITM). Mean rotation angle θ was $409.3^\circ \pm 129.8^\circ$ for shorter arrays, and p distance averaged 1.8 ± 0.7 mm. The θ mean for longer arrays was $642.4^\circ \pm 81.9^\circ$, and p distance averaged 1.3 ± 0.3 mm. Primary (mis-)insertions into scala vestibuli was seen in eight cases. In two patients

an array changeover from scala tympani to scala vestibuli was observed. One electrode showed a very slight kinking at the distal end, while another one showed significant kinking. An electrode reversal was seen in two cases. Retrospective evaluation of the surgical technique revealed clearly more primary electrode dislocations into scala vestibuli when the cochleostomy approach was used compared to a round window insertion, where no primary incorrect electrode placement could be detected.

CONCLUSIONS: CBCT is a well applicable method for post-operative control of electrode array position. Commonly known differences between the various available electrode arrays have to be considered. Particularly CBCT is useful for the surgeon to provide quality control, improvement of surgical techniques and a useful support in the decision considering revision surgery. None of the patients from this study underwent revision surgery. In general, revision surgery is only done in cases of distinct misinsertions like reversal, not in cases of scale dislocations. Even the patient with the strongest kinking developed sufficient hearing capabilities and is satisfied. Data obtained in this study changed our surgical approach whenever it is possible round window insertion is preferred.

15.10 – 15.20 pm

Surgical relevance of the persistent petrosquamosal sinus (PSS)

Anja Giesemann (short oral presentation)

Medizinische Hochschule Hannover, Institut für Diagnostische und Interventionelle Neuroradiologie, Hannover, Germany

Co-Authors: Lyutenski S, Lanfermann H, Lenarz T, Götz F

OBJECTIVES: The persistent petrosquamosal Sinus (PSS) is a rare anatomical variant of the cerebral venous drainage in the temporal bone. In 80% of the cases with complete aplasia of the semicircular canals (SCCs) a PSS can be found. These children are often candidates for a cochlea implant (CI). Using the method of posterior tympanotomy the PSS is at risk.

MATERIALS AND METHODS: The temporal bone CTs of all patients with complete aplasia of the semicircular canals were retrospective evaluated by two neuroradiologists. In addition all surgical reports of cochlea implantations on a temporal bone with a PSS were acquired from the patients health record by an otolaryngologist.

RESULTS: 31 patients with complete aplasia of the SCCs were evaluated. In 25 patients a uni- or bilateral PSS was found. A cochlea implantation was performed on 8 temporal bones with a PSS. The surgical reports documented accidental opening of the PSS or the inhibition of surgical exposure by the structure of the PSS.

CONCLUSIONS: Thorough evaluation of temporal bone CTs prior to cochlea Implantation is essential. The PSS presents a risk for cochlear implant surgery that can be detected by the neuroradiologist in advance.

15.20 – 15.30 pm

Prevalence of Chiari I malformation and cerebellar ectopia in patients with Sensorial Hearing Loss

Alpay Haktanır (short oral presentation)

Afyon Kocatepe University, Radiology, Afyonkarahisar, Turkey

Co-Authors: Yücedağ F, Ayçiçek A, Kaçar E, Ulu S, Gültekin MA

OBJECTIVES: Displaced cerebellar tonsils may cause otological disturbances by means of brainstem and/or lower cranial nerve compression. In the literature, a few studies and a number of case reports presented an association between sensorial hearing loss and Chiari 1 malformation. Still, the real reason of such a connection remains speculative. To the best of our knowledge, ectopia of cerebellar tonsils along with Chiari 1 malformation in sensorial hearing

loss has not been studied previously. We aimed to examine the prevalence of cerebellar tonsil ectopia and Chiari 1 malformation in sensorial hearing loss and discuss a probable correlation between them.

MATERIALS AND METHODS: Magnetic resonance imaging (MRI) records of 166 subjects with sensorial hearing loss, 79 men (47.6%) and 87 women (52.4%) (aged between 8 and 85;

mean, 50,03±17,12); and 50 controls, 21 men (%) and 29 women (%) (aged between 8 and 80; mean, 46,88±17,83) were included in this retrospective study. Audiometric and demographic information of patients were obtained from the hospital information system. Presence of hearing loss was accepted when hearing threshold was higher than 20 dB at all frequencies. On coronal T1 weighted images having 3-mm thickness, center of bilateral lower end of occipital condyles were established for the cerebellar tonsillar ectopia measurements. A tonsils descent more than 2 mm was assumed as cerebellar ectopia and a descent equal or more than 5 mm was assumed as Chiari 1 malformation. A tonsil descent group was also formed by summation of both groups for statistical analysis. Transverse diameters of bilateral intracranial vertebral arteries and transverse sinuses were also measured for any possible correlation.

RESULTS: The prevalence of Chiari 1, ectopia, and tonsil descent in sensorial hearing loss and controls were 7,2% (n=12) and 0,5% (n=1);

13,3% (n=22) and 0,5% (n=1); and 20,5% (n=34) and 1% (n=2), respectively. A significant difference of frequencies of all three parameters was detected between patients and controls. In comparison of cerebellar ectopia and Chiari 1 groups, sensorial hearing loss did not show any significant difference. The left lateral sinus diameter showed positive correlation with tonsil descent. There was no significant correlation for the diameters of other vessels. A powerful correlation was detected between sensorial hearing loss and age. Also, right and vertebral artery diameters showed positive correlations with age.

CONCLUSIONS: Chiari 1 malformation and a small amount descent of cerebellar tonsils known as cerebellar ectopia show an association with sensorial hearing loss. Compression of brain stem and/or stretching of the sixth nerve may be a reason. On the other hand, embryologic and pathophysiologic changes causing cerebellar tonsil descent may also result in sensorial hearing loss. This seems to be as a topic of interest for high resolution MRI studies.

Systematic approach for compartment based image interpretation

14.09.2012, 16.00 – 17.30 pm

Chairs: Alexandra Borges, Lisbon (Portugal) / Sylva Bartel-Friedrich, Halle (Germany)

16.00 – 16.30 pm

Suprahyoid neck

Frédérique Dubrulle (Invited presentation)

Centre Hospitalier Régional Universitaire de Lille, Imagerie, Médecine nucléaire et Explorations fonctionnelles, Lille, France

Co-Authors: Sufana A

SUMMARY: The deep suprahyoid neck spaces, divided into anatomical compartments, remain poorly known and of difficult reputation amongst radiologists. Nevertheless the anatomical knowledge of these compartments and their contents

allows to localize exactly a lesion and to evoke a diagnostic checklist. Some of these suprahyoid compartments are real columns allowing the extension of the pathologies to the corresponding infrahyoid space even into the mediastinum.

These compartments communicate easily as well with the intracranial middle fossa by means of the perineural foraminal extensions. This type of extension will always have to be looked for.

TAKE-HOME-POINTS: From the anatomy, based on the new international terminology, we shall learn to localize a lesion into a compartment and thanks to this localization, we shall analyze the extensions and the potential diagnostic checklist to be evoked according to the characteristics of the lesion. We shall also approach the transspatial and multispatial suprahyoid pathologies.

16.30 – 17.00 pm

Infrahyoid neck

Nicole Freling (Invited presentation)

Academisch Medisch Centrum / Universiteit van Amsterdam, Polikliniek Radiologie, Amsterdam, The Netherlands

SUMMARY: Anatomy: The deep neck consists of three main compartments: the visceral-centrally located, the vascular around the carotid artery and jugular vein, and the para- or perivertebral compartment posteriorly (= posterior cervical space). The visceral compartment contains the larynx, the trachea, the thyroid, the parathyroid glands and fat and muscles. The vascular space contains the carotid artery and jugular vein and the lower cranial nerves. The perivertebral space or posterior cervical space contains bone, muscles and peripheral nerves. The deep cervical fascia surrounds these spaces. It has a superficial layer, a middle and a deep layer. These play an important role in the spread of deep neck abscesses. **Pathology:** What pathology can be expected in these different spaces? Along the remnant of the thyro-glossal duct a midline cyst may arise. Benign and malignant laryngeal lesions are located within the visceral space. Thyroid disease and parathyroid adenomas are also found here. And inflammatory changes may occur, which may compress the trachea. More laterally, between the vascular and the visceral space, the lateral neck cyst can be found as well enlarged lymph nodes. Pathology arising in the vascular space is related to vessel- or nerve-related abnormalities. In the

posterior cervical space posttraumatic lesions of the bone and malignant disease may be found. The neck is host to a large variety of benign and malignant diseases ranging from simple cysts to acute inflammation with complications to highly malignant sarcomas and imaging plays an important role to assess the nature and the extension of disease. Patient history and clinical presentation will decide which imaging modality is best suited to resolve the diagnostic dilemma. **Imaging:** Ultrasound is recommended to differentiate between a solid and a cystic lesion, and FNA can be added in selected cases to obtain a diagnosis. In acute illnesses with anticipated complications of the airways or vessels, such as a deep neck abscess, CECT is required to assess the extension of the abscess in the deep spaces of the neck and to demonstrate mediastinal or pleural complications or thrombophlebitis. MRI is indicated to assess non-inflammatory, subacute or chronic diseases, such as vascular malformations, branchial cleft cysts, benign and malignant soft tissue tumours, brachial plexus pathology and neurologic diseases. Vascular malformations are easily depicted with MRI using T2 sequences in different image planes. Persistent fistulas of the branchial system also can be depicted by MRI running from the ante-

rior border of the sternocleidomastoid muscle to the lateral pharyngeal wall. Assessing the origin of a soft tissue tumour has major implications for surgery. Staging a malignant soft tissue tumour must comprise the skull base and upper mediastinum including local extension, pathologic neck nodes and perineural spread. Follow-up during chemotherapy and postoperative monitoring of malignant disease is an important in-

dication for (MR) imaging, the more so in young patients, diminishing ionizing radiation.

TAKE-HOME-POINTS: The infrahyoid neck can be divided in different compartments or spaces. The main reason to do so is to locate a lesion and to reduce the potential list of differential diagnoses.

17.00 – 17.10 pm

Retropharyngeal calcific tendonitis of the longus colli muscle: a case report

Theodosia Kontaki (short oral presentation)

“Mamatseio” General Hospital, Radiology, Kozani, Greece

Co-Authors: Grigoriadis G, Tziola M, Markou A, Kougias L, Pozoukidis C

OBJECTIVES: Retropharyngeal calcific tendonitis is an inflammatory process of the superior oblique tendon of the longus colli muscle, a neck flexor in the upper cervical spine, caused by deposition of calcium hydroxyapatite crystals. Our report describes a case of retropharyngeal calcific tendonitis diagnosed with MDCT and MRI.

MATERIALS AND METHODS: An otherwise healthy 31-year-old man presented with a 4-day history of left-sided neck pain, exacerbated by movement, pharyngalgia and odynophagia. The patient's temperature was 37.7 °C, white blood cell count was 13,400/μL (NEU 69%) and CRP was 2.7 mg/dL.

RESULTS: Contrast-enhanced CT of the neck (with sagittal reconstructed images) demonstrated fluid collection in the retropharyngeal space without wall enhancement and amorphous calcification anterior to C1–C2. MRI examination of the neck also showed a lenticular shaped prevertebral fluid collection from C1 to C5, as well as inflammation of the left longus colli muscle

and decrease in the anteroposterior diameter of the oropharynx left to the midline. Based on the characteristic imaging findings and the patient's clinical symptoms, he was diagnosed with retropharyngeal calcific tendonitis and successfully was managed with non-steroidal anti-inflammatory medication for 2 weeks.

Repeat CT scan performed 9 days after the initial, demonstrated significant decrease in the prevertebral fluid collection and also reduction in calcification size at the C1–C2 level.

CONCLUSIONS: Retropharyngeal calcific tendonitis is a cause of neck pain that can mimic infection. Recognition of this entity is critical in order to avoid misdiagnosis and inappropriate treatment with antibiotics and possible “abscess” drainage.

In the proper clinical setting, the presence of prevertebral fluid collection along with amorphous calcification anterior to C1–C2, is nearly pathognomonic of this entity.

17.10 – 17.20 pm

Role of Ultrasonography in characterising benign and malignant thyroid nodules

Ayman Elsayed (short oral presentation)

Diana Princess Of Wales Hospital, Northern Lincolnshire and Goole NHS foundation Trust, Radiology Department, North East Lincolnshire, United Kingdom

Co-Authors: Awad M, Abdulquader H

OBJECTIVES: The aim of our study is to evaluate the role of Ultrasonography (US) in predicting benign and malignant thyroid nodules by correlating US findings with US-guided Fine Needle Aspiration Biopsy (FNAB) and post operative pathology results.

MATERIALS AND METHODS: In this study we looked retrospectively at four hundred and eight US and US-guided FNAB reports done for three hundred and forty consecutive patients; referred to the radiology department for evaluation of thyroid lumps in a five-year period. We reviewed the US features including colour Doppler of the thyroid nodules and correlated them with US guided FNAB results and post operative histol-

ogy. All US scans and US guided FNAB were performed by the same consultant radiologist and the FNAB were reported by two consultant cyto-pathologists.

RESULTS: US characteristics including size, shape, contour, echogenicity, micro- and macro-calcifications and vascularity were evaluated for every nodule sampled and correlated with benign and malignant pathology. Results were studied statistically.

CONCLUSIONS: Our study suggests US characteristics of benign and malignant thyroid nodules with review of the literature.

17.20 – 17.30 pm

Ectopic parathyroid adenomas localized by dual-energy computed tomography

Beatrix Kovacs (short oral presentation)

University Hospital, Linköping, County Council of Östergötland, Department of Radiology, Linköping, Sweden

Co-Authors: Persson A, Gimm O, Wallin G

OBJECTIVES: Ultrasonography, nuclear imaging, computer tomography, magnetic resonance imaging and angiography are used to localize ectopic parathyroid adenomas (PA). Their sensitivity and specificity in detecting the adenoma have been investigated in several studies. Very little has been written about the ability of dual-energy CT (DECT) in localizing the ectopic adenomas.

MATERIALS AND METHODS: DECT can acquire two data sets simultaneously showing different attenuation levels and allowing quantification of iodine uptake in the soft tissues. DECT has been used extensively in our department in post mortem CT and cardiac imaging. Now we investigate its ability to localize ectopic PA and mapping the blood supply of the lesion. We present two cases where DECT was invaluable

in finding the ectopic adenoma. The examinations were performed on SIEMENS Somatom Definition Flash machine in native, arterial and venous phase.

RESULTS: The 61 year old woman underwent bilateral cervical exploration with removal of the suspected enlarged lower right gland. However, the PTH and s-calcium levels remained elevated. Methionine PET showed a right-sided intrathyroidal nodule but it proved to be a thyroid lesion. The PTH peak was located in the left lower jugular vein, which is not a typical location for a PA, and conventional imaging could not detect any lesion in that region. DECT identified a small contrast uptake ventrally of the vein. The lesion was proved to be the missing adenoma during the third operation and patient is now symptom free. The 43 year old woman s hyperparathyroidism was accidentally discovered. Cardiolite SPECT showed a suspected ectopic adenoma in the upper mediastinum. Despite the fact that the traditional CT showed a very highly suspi-

cious adenoma in the upper mediastinum, the patient underwent a DECT to prove the origin of the lesion and determine the exact location (thymus remnants or outside of it), as the operation technique (thoracotomy or not) was dependent on this information. DECT convincingly located the adenoma outside the thymic remnants. The lesion in the aorto-pulmonary window was successfully removed. The PTH and s-calcium values normalized and most likely the patient is cured.

CONCLUSIONS: According to our knowledge this is the second report on DECT localizing ectopic PA. A study evaluating the clinical impact of DECT in localizing ectopic PA is now ongoing.

Special techniques – state in 2012

14.09.2012, 16.00 – 17.30 pm

Chairs: Julie Olliff, Birmingham (United Kingdom) / Agnieszka Trojanovska, Lublin (Poland)

16.00 – 16.30 pm

Fibre tracking - can it help with head and neck problems?

Minerva Becker (Invited presentation)

Université de Genève / Faculté de Médecine, HUG/ Dpt Radiologie, Serv. Radiodiagnostic, Geneva, Switzerland

16.30 – 17.00 pm

Imaging in computer-assisted head and neck surgery

Florian Dammann (Invited presentation)

Klinik am Eichert, Institut für Radiologie mit Nuklearmedizin, Göppingen, Germany

17.00 – 17.10 pm

Improved in vivo visualisation and evaluation of endolymphatic hydrops using high-field MRI in Menier's disease and correlation with audiovestibular function

Wilhelm Flatz (short oral presentation)

Ludwig-Maximilians-Universität München Campus Großhadern, Institut für Klinische Radiologie, Munich, Germany

Co-Authors: Guerkov R, Dietrich O, Reiser M, Ertl-Wagner B

OBJECTIVES: To improve detection and evaluation of endolymphatic hydrops in Meniere's disease in vivo using MRI and to determine whether the degree of endolymphatic hydrops as it is detected in vivo in patients with definite Meniere s disease correlates with audiovestibular functions.

MATERIALS AND METHODS: 37 patients suffering from clinical symptoms of Meniere's disease according to AAO-HNS criteria were examined in a prospective study. Diluted gadolinium was administered intratympanically 24 hours prior to the MR-scan. MRI was performed using a 3 T-scanner using a dedicated 8-channel surface-coil and a head-coil acquiring a 3D-FLAIR sequence, a 3D-IR TSE sequence and a high-resolution True-FISP dual excitation sequence (CISS). Correlation with clinical symptoms and audiovestibular function testing was performed using audiometric hearing tests, caloric stimulation, electrocochleography (ECochG) and vestibularevoked myogenic potentials (VEMP).

RESULTS: There was a significant correlation between the degree of hydrops, on the one hand, and the averaged hearing level at 0.25–1 and 0.5–3 kHz and the vestibular evoked myogenic potential interaural amplitude ratio, on the other hand. A trend towards a correlation was noticed

between the hydrops and the caloric response, no correlation was noticed between the hydrops and the SP/AP ratio. The degree of endolymphatic hydrops correlates with a progressive loss of auditory and sacculus function in patients with Meniere's disease.

CONCLUSIONS: The degree of endolymphatic hydrops in patients with definite Meniere s disease, as it is detected by in vivo MRI imaging, correlates with a loss of audiovestibular function. This underlines the usefulness of this technique in the evaluation of Meniere's disease.

17.10 – 17.20 pm

Comparison of true real-time MR imaging with radial k-space sampling to videofluoroscopy in the follow up evaluation of velopharyngeal dysfunction or insufficiency treated by surgery

Maya Christina Larson (short oral presentation)

Clinic of the Goethe University Frankfurt, Department of diagnostic and interventional Radiology, Frankfurt, Germany

Co-Authors: Kerl MJ, Bauer RW, Zhang Sh, Hammerstingl R, Vogl TJ, Mack MG

OBJECTIVES: Velopharyngeal dysfunction or velopharyngeal insufficiency can have many causes and results in difficulties in speaking and swallowing. Often patients are treated by surgery. After surgery the resulting improved closure of the velopharyngeal port during speaking and swallowing is the maneuver of interest which is usually monitored by videofluoroscopy. The aim of our study was to show that a rapid MRI protocol with equal temporal resolution (27Hz) to videofluoroscopy examinations is as accurate as videofluoroscopy, without exposure to X-rays and without necessity of contrast media application.

MATERIALS AND METHODS: With the approval of our institutional review board 25 patients underwent 3.0 T MR real-time imaging and videofluoroscopy examinations. Our approach concerning the MRI scan protocol was to use a fast low-angle shot (FLASH) gradient-echo sequence with radial k-space sampling and sliding-window reconstruction (5 subframes) for achieving an image update rate of 27 Hz (27 frames per second). Sagittal views with 8 mm slabs were obtained during speech with a TE of 1.97 ms, a TR of 3.95 ms, a flip angle of 20°, and a matrix size of 128 pixels. The image quality was assessed by two independent radiologists; special focus was on the soft palate and the velopharyngeal valve. Additionally the closure of the velopharyngeal port during speaking was compared in both diagnostic methods.

RESULTS: The obtained real-time MR cinematics were equal to the videofluoroscopic images to evaluate the closure of the velopharyngeal port during speech to assess the postoperative results. In case of presence of a gap between soft palate and the posterior pharyngeal wall no significant difference in comparison of both methods could be calculated. Both radiologists rated the overall image quality in consensus as diagnostic.

CONCLUSIONS: Realtime MRI based on radial FLASH sequences is to consider equal to fluoroscopic imaging in the evaluation of the closure of the velopharyngeal port during postoperative follow up exams without exposure to X-rays. Furthermore it is a repeatable examination without the necessity of contrast media application. Clinical use of realtime MRI to evaluate the severity of velopharyngeal dysfunction or insufficiency is possible and can be considered as a good alternative to videofluoroscopy.

17.20 – 17.30 pm

Detecting cholesteatoma on HASTE (nonechoplanar) diffusion-weighted MRI: the value of quantitative assessment using ADC values

Ravi Lingam (short oral presentation)

North West London Hospitals NHS Trust, Departments of Radiology and ENT Surgery, London, United Kingdom

Co-Authors: Boyd E, Khatri P, Hughes J, Singh A

OBJECTIVES: To determine if ADC (Apparent Diffusion Coefficient) values can differentiate between residual/recurrent cholesteatoma and non-cholesteatomatous tissue (granulation tissue and fibrosis) in the post operative middle ear cleft on HASTE non echoplanar diffusion weighted MRI. (DWI) and aid in the detection of cholesteatoma

MATERIALS AND METHODS: HASTE DWI images of 30 cases of post-operative cholesteatoma prior to re-look surgery were retrospectively reviewed for the presence of cholesteatoma by 2 radiologists. DWI images were acquired with a b-factor of 0 and 1000 s/mm² and a slice thickness of 2mm. A diagnosis of cholesteatoma was made qualitatively with high signal relative to cerebral gray matter on b1000 images and low signal on ADC map, with a confidence level (1=no cholesteatoma, 2=probable non-cholesteatoma, 3=possible cholesteatoma, 4=probable cholesteatoma, 5=definite cholesteatoma). The ADC value of the abnormal middle ear soft tissue (ROI) was also measured giving a median of 3 values. The final diagnosis of the abnormal middle ear cleft soft tissue was established by surgery with histological confirmation.

RESULTS: 3 cases of cholesteatoma (less than 3mm on surgery) were excluded from the analysis as they were not seen on DWI (false negative cases). The remaining 13 cases of cholesteatoma and 14 cases of non-cholesteatomatous tissue (granulation tissue or fibrosis) were included

in the analysis. The ADC value of cholesteatoma (median 717 (442–1032) x 10⁻⁶mm²/s) was significantly lower than that of non-cholesteatomatous tissue (median 1930 (1438 – 2331) x 10⁻⁶mm²/s) (p<0.001). Receiver operating characteristic (ROC) curve analysis shows perfect predictive powers (AUC=1) of ADC values in detecting cholesteatoma. There is good interobserver agreement with an intra-class correlation coefficient of 0.98. Our analysis shows that an ADC value of 1200 x 10⁻⁶mm²/s can completely distinguish the two entities and help improve the confidence level in detection of cholesteatoma by qualitative means (in 2 of 13 cholesteatoma cases).

CONCLUSIONS: The ADC value of cholesteatoma on HASTE DWI is significantly lower than that of non-cholesteatomatous tissue (granulation tissue and fibrosis) and this difference can aid in the detection of post-operative middle ear cholesteatoma. This is work in progress recruiting more cases into the study.

Special focus – vascular malformations and tumours

15.09.2012, 08.30 – 10.00 am

Chairs: Martin G. Mack, Munich (Germany) / Jochen A. Werner, Marburg (Germany)

08.30 – 09.00 am

From the clinical point of view

Jochen A. Werner (Invited presentation)

Universitätsklinikum Gießen und Marburg GmbH, Klinik für Hals-, Nasen- und Ohrenheilkunde, Marburg, Germany

SUMMARY: The field of vascular anomalies is rapidly growing and the current established classification system is established by the International Society for the Study of Vascular Anomalies (ISSVA). This differentiates strictly between vascular malformations (further between truncular and extratruncular, and between low- and high-flow) and vascular tumors (with hemangiomas being the most common representatives of the latter ones). Accurate nomenclature should be respected in all involved disciplines. There are nonetheless several aspects that show how special and difficult it is to diagnose treat vascular diseases. Treatment is multimodal and in most cases individualized. Close interdisciplinary cooperation is essential to warranty patient care on a high level, and this fact is especially valid for collaboration between the radiologist, and the surgeon, preferably in a specialized center. Individual procedures must be discussed in vascular anomalies boards, as it is usual practice in the field of oncology. We are witnessing a significant progress in basic and clinical research, which brought up new insights to the pathogenesis and new therapeutic strategies for managing vascular anomalies of the head and neck in the recent years. Thus, it is necessary to intensify ongoing efforts in clinical and experimental re-

search on vascular malformations and hemangiomas of the head and neck.

TAKE-HOME-POINTS:

- ISSVA Classification
- Multimodal management
- Modern therapeutic approaches
- Interdisciplinary cooperation
- Vascular Anomaly Board in specialized centers
- Recent clinical and scientific developments in the field of vascular anomalies

09.00 – 09.30 am

From the radiological point of view

Ulrike Ernemann (Invited presentation)

Eberhard Karls Universität Tübingen / Universitätsklinikum Tübingen, Diagnostische und Interventionelle Neuroradiologie, Tübingen, Germany

SUMMARY: The treatment of patients with extended vascular anomalies requires an interdisciplinary diagnostic and therapeutic concept based on a straightforward classification of vascular lesions. In this talk the diagnostic algorithm of vascular lesions according to the International Society for the Study of Vascular Anomalies (ISSVA) is presented. Vascular lesions are classified into haemangiomas as proliferating endothelial tumors on the one hand and congenital vascular malformations on the other. As a valuable adjunct to the clinical examination diagnostic imaging contributes to clarify the specific differential diagnosis of a vascular lesion and is targeted at the structural and functional informations required for treatment planning. In haemangiomas diagnostic MRI is rarely required for deep-seated lesions; the specific MRI criteria will

be highlighted. In vascular malformations MRI supplemented by MRA is the method of choice to delineate the extension of a lesion and to differentiate between low flow (venous, lymphatic or capillary) or high flow vascular lesions. Only in high flow vascular malformations diagnostic angiography is required for interdisciplinary treatment planning.

TAKE-HOME-POINTS: Classification of vascular anomalies into haemangiomas as endothelial tumors and congenital vascular malformations. MRI characteristics of haemangiomas and of low flow (venous, lymphatic or capillary) and high flow vascular malformations. Indication for conventional angiography in high flow vascular malformations.

09.30 – 10.00 am

Interventional possibilities

Ulrike Ernemann (Invited presentation)

Eberhard Karls Universität Tübingen / Universitätsklinikum Tübingen, Diagnostische und Interventionelle Neuroradiologie, Tübingen, Germany

SUMMARY: Interventional therapy plays an important role in the treatment concept for vascular malformations. For all lesions not accessible by the transarterial route pecutaneous sclerotherapy is the treatment of choice and is therefore applied for low flow (venous or lymphatic) vascular malformations. The aim of the treatment is a step by step reduction of the lesion volume and thus alleviation of clinical symptoms such as swelling, pain or airway obstruction. Sclerotherapy comprises transcutaneous or transoral

puncture of the lesion, aspiration of its content, fluoroscopic visualization of the punctured compartment and then injection of the sclerosing agent which is mostly ethanol for venous malformations and OK-432 (picibanil) for lymphatic malformations. Tipps, tricks and potential pitfalls of the procedures will be highlighted during the talk. In high-flow vascular malformations transarterial embolization aiming at a reduction of the nidus of the malformation is indicated in an interdisciplinary treatment plan which usually

involves preoperative embolization followed by surgical removal of the nidus.

TAKE-HOME-POINTS: Interventional therapy of vascular malformations involves: Percutaneous

sclerotherapy for low flow (venous or lymphatic) malformations with different sclerosing agents; Transarterial embolization of high-flow vascular malformations in an interdisciplinary treatment concept.

Pitfalls and challenges

15.09.2012, 10.30 – 12.00 am

Chairs: Roberto Maroldi, Brescia (Italy) / Minerva Becker, Geneva (Switzerland)

10.30 – 11.00 am

Pseudolesions

Can Karaman (Invited presentation)

Adnan Menderes Üniversitesi, Radyoloji Anabilim Dalı
Aydin, Turkey

SUMMARY: Radiologists mostly prefer to use the comparative technique while evaluating radiological images, especially when the anatomy is identical for both sides. Comparative analysis mostly works if the anatomic details are not complex or right resembles left. However the complex anatomy and relatively high incidence of individual variations in head and neck region may hinder this way of interpretation. Variable pneumatization of paranasal sinuses and temporal bone may cause difficulty. Extensive pneumatization of sphenoid sinus or asymmetrically aerated petrous apices may be sources of pseudolesions especially when they are complicated, i.e. sporadic sinusitis of the sphenoid sinus. Pneumatization of the petrous apex can be observed in 1/3 of patients. Only when asymmetric it may cause a diagnostic dilemma, in particular on magnetic resonance imaging. In this case aerated and there for signal free apex looks completely different from the opposite side with the usual fatty marrow signal, and the common can be mistaken for a mass lesion. Vascular system, especially venous structures may be an

other source for pseudolesions. Asymmetrically enlarged or dominant internal jugular vein, prominent external jugular veins, or venous plexuses at any location in the neck that are not identical on either sides may be misinterpreted as mass of any origin including lymph nodes or vascular malformations. The most common bewildering structure is an enlarged lymph node. This misinterpretation can have a variety of causes; variable anatomy and size, asymmetry, and variable degrees of contrast enhancement at CT. In this case following the structure on adjacent images mostly enables the correct interpretation. Veins may also become problematic on MR imaging due to entry slice phenomenon, in-plane flow, and flow turbulence effects and can have variable enhancement. Normal anatomical structures such as facial nerve may enhance and can be mistaken to be pathologic on MRI. It is well known that the anterior tympanic portion of the facial nerve may be enhanced to a mild or moderate degree due to the presence of a rich peri-venous plexus surrounding the nerve in the fallopian canal. It has been shown that

the tympanic segment with or without proximal vertical segment may be enhanced as well. Technical issues can be considered as a group that may cause pseudolesions. Images of the patients who were not positioned on the imaging table properly may become problematic while evaluating tiny structures. In that occasion fine sutures of skull base may be misinterpreted as fractures especially in trauma patients. While evaluating these fine structures one should always keep in mind that the conspicuity of sutures mostly depend on their size, imaging parameters and patient's age. PET and PET-CT carry their own risks for pitfalls. Normal structures such as parotid and submandibular glands, and lymphoid tissue of the adenoids and Waldeyer ring may confound interpretation and result in false-positive findings at PET-CT. Similarly, normal FDG uptake in muscles that are contracting or tensed during the uptake phase (eg, in anxious or talkative patients) may lead to false-positive findings. The situation may become much more complicated when functional disturbances such as vocal cord paralysis occur that hinder comparative analysis. Similarly atrophy and unilateral absence of a structure may be misread as a mass on the contra-lateral side. For example, a normal submandibular gland may be called as mass in congenital absence of contra-lateral side.

Because of the complex anatomy and relatively high incidence of individual variations head and neck imaging demands much more attention, and careful analysis. The appropriate imaging technique and detailed knowledge of anatomy is essential to recognize pseudolesions and keep away from pitfalls.

FURTHER READINGS: 1. Al-Noury K, Lotfy A. Normal and pathological findings for the facial nerve on magnetic resonance imaging. *Clin Radiol* 2011; 66:701-707. 2. Escott EJ, Branstetter

BF. It's Not a Cervical Lymph Node, It's a Vein: CT and MR Imaging Findings in the Veins of the Head and Neck. *Radiographics* 2006; 26:1501-1516. 3. Fukui MB, Blodgett TM, Snyderman CH, et al. Combined PET-CT in the Head and Neck Part 2. Diagnostic Uses and Pitfalls of Oncologic Imaging. *Radiographics* 2005; 25:913-930. 4. Hansberger RH, et al. Diagnostic imaging: Head and neck. 2nd ed. Amrys Co. 2010. 5. Koesling S, Kunkel P, Schul T. Vascular anomalies, sutures and small canals of the temporal bone on axial CT. *Eur J Radiol* 2005; 54:335-343. 6. Schmalfluss IM, Camp M. Skull base: pseudolesion or true lesion? *Eur Radiol* 2008; 18:1232-1243. 7. Swartz JD, Harnsberger HR. Trauma. In: Swartz JD, Harnsberger, editors. *Imaging of the temporal Bone*. 3rd ed. New York Stuttgart: Thieme; 1998. p. 318-44.

11.00 – 11.30 am

Difficult cases

Julie Olliff (Invited presentation)

University Hospital Birmingham, Radiologie,
Birmingham, United Kingdom

SUMMARY: The correct interpretation of imaging of the head and neck depends on obtaining the optimum scan, good communication between the clinician and the radiologist, in depth knowledge of anatomy, disease processes and their imaging appearance and detailed knowledge of post treatment changes. This talk will cover: Technique related problems which lead to a scan being difficult or misinterpreted How benign disease can mimic malignancy Post treatment changes which can make a scan difficult to interpret The ideal scan will be tailored to answer the clinical question. CT scans should be performed with IV contrast. The patient should not swallow during the scan and should breathe

gently during the acquisition of images. The choice of MR sequence and imaging plane is important. Intravenous gadolinium is necessary particularly if there is potential peri-neural spread of disease. Artefacts from flow and metal clips etc need to be recognised and minimised. Some benign diseases can mimic malignancy and correlation with good clinical information and histology is important.

Post treatment changes (biopsy, radiotherapy and surgery) often increase the complexity of appearances and may lead to misinterpretation. Post biopsy changes can lead to over-staging of malignancy.

11.30 – 12.00 pm

Incidental findings - how to handle them?

Timothy Beale (Invited presentation)

The Royal Free Hampstead NHS Trust, Radiology,
London, United Kingdom

Interactive image interpretation session with TED

15.09.2012, 12.00 – 12.50 pm

12.00 – 12.50 pm

Neck

Davide Farina (Invited presentation)

Azienda Ospedaliera Spedali Civili, Radiologie,
Brescia, Italy

ESHNR Refresher Course – 1st part

15.09.2012, 14.00 – 16.00 pm

Chairs: Can Karaman, Aydın (Turkey) / Christian Czerny, Vienna (Austria)

14.00 – 14.30 pm

Thyroid and parathyroid glands

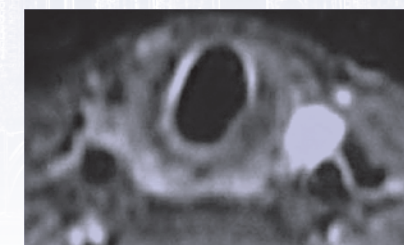
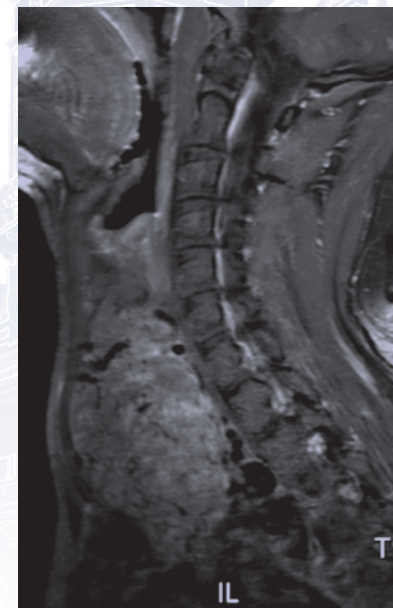
Christian Czerny (Invited presentation)

Medizinische Universität Wien/Universitätsklinik für Radiodiagnostik, Neuroradiologie und Muskulo-skeletalen Radiologie, Vienna, Austria

SUMMARY: The thyroid can be affected by many pathologies. The most common pathologies are inflammations and tumorous lesions. Inflammatory pathologies can be separated into autoimmune diseases and acquired viral or bacterial inflammatory processes. Tumorous lesions can be separated into benign and malignant pathologies. The most common pathology of the parathyroid glands is the hyperparathyroidism. The hyperparathyroidism can be caused either by an adenoma or more rarely by multiple adenomas

or by a hyperplasia of one or more glands. Very rarely can a carcinoma of a parathyroid gland be the cause for hyperparathyroidism. The imaging modalities to investigate the pathologies of the thyroid and parathyroid glands are ultrasonography, computed tomography, magnetic resonance imaging, scintigraphy, and PET or PET-CT, PET-MRI. These imaging modalities can detect and differentiate the various pathologies and are used for pretreatment and posttreatment imaging. The different imaging modalities show the pathologies in a different way and are also used complementary. The radiologist should be familiar with the different imaging techniques, the different imaging characteristics, and the complementary use to establish the most correct diagnosis of the pathology which is looked for.

TAKE-HOME-POINTS: The different imaging modalities, their use, their imaging characteristics, and the interpretation of them will be shown and explained in the refresher course.



14.30 – 15.00 pm

Nasopharynx: benign and malignant lesions

Roberto Maroldi (Invited presentation)

University of Brescia, Dipartimento di Specialità Chirurgiche, Scienze Radiologiche e Medico Forensi, Brescia, Italy

15.00 – 15.30 pm

Hypopharynx and larynx

Minerva Becker (Invited presentation)

Université de Genève/Faculté de Médecine, HUG/Dpt Radiologie, Serv. Radiodiagnostic, Geneva, Switzerland

15.30 – 16.00 pm

Salivary glands

Nicole Freling (Invited presentation)

Academisch Medisch Centrum / Universiteit van Amsterdam, Polikliniek Radiologie, Amsterdam, The Netherlands

SUMMARY: The major salivary glands consist of three paired organs: the parotid, the submandibular and the sublingual glands. Minor salivary glands are found within the mucosa of the upper aero-digestive tract, but not seen when normal. The most common cause of salivary gland swelling is sialadenitis. Acute sialadenitis can be due to viral (mumps) or bacterial infection, or as a consequence of obstructive calculous disease. Autoimmune diseases as M.Sjogren, or granulomatous disease (sarcoidosis, tuberculosis) also can cause diffuse swelling of the salivary glands, most often of the parotid gland. After radiation treatment radiation sialadenitis may occur, in the end leading to complete atrophy of the glands, which is the cause of xerostomia. Due to the greater viscosity of the saliva of the submandibular glands and the steep bend of its duct in the floor of the mouth, calculi are seen more often in the submandibular duct (80%) compared to the parotid duct (20%). Ultrasound is often the first modality to evaluate a patient with a submandibular swelling to differentiate salivary from non-salivary pathology (e.g. lymph

nodes). Dilated ducts can be depicted, and small calculi up to 3mm can be demonstrated. For evaluation of ductal anatomy, prior to (endoscopic) treatment, MR-sialography is the method of choice. Strongly T2 weighted sequences with thin slices with reconstructions in all desired planes. Dilatation, strictures and the cause of obstruction can be predicted in almost all patients (Becker, Kalinovsky). CT can be reserved for questionable results and a strong clinical suspicion for stones; 80% contain calcium. Salivary gland tumours are rare, making up about 3% of all head and neck tumours. About 60–75% of all tumours occur in the parotid gland, about 15% arise in the submandibular glands and rarely the sublingual glands are the origin of a tumour. Around 70–80% of parotid tumours are benign, 50% of submandibular gland tumours are malignant and tumours of the sublingual glands are considered malignant until proven otherwise. Tumours of the minor salivary glands are malignant in about 40% of cases. Parotid surgery means surgery of the facial nerve, and damaging the facial nerve is a risk, the risk being greater when

total parotidectomy must be performed compared to superficial parotidectomy. The facial nerve normally is not seen on routine imaging and it remains difficult to predict the course of the facial nerve medial or lateral in relation the tumour in some patients. Imaging is important:

- » to locate the mass (within the parotid / submandibular gland or not)
- » to differentiate solitary from multiple lesions
- » to detect clinically unnoticed bilateral disease
- » to depict invasion of adjacent compartments
- » to demonstrate abnormal perineural enhancement of the cranial nerves
- » to depict enlarged neck nodes
- » to demonstrate distant metastases Perineural spread is a radiological diagnosis;

most patients are asymptomatic. Not to overlook the sometimes subtle pathologic enhancement is important for treatment strategy, but also for planning postoperative radiation fields. Perineural spread which occurs during treatment may

be due to inflammatory changes neuritis without focal thickening and persist for years. In a number of patients, imaging can not differentiate between benign and malignant nature of a solitary lesion, and biopsy is mandatory. However, because in the adult patients the treatment of choice of a solitary well-defined tumour is parotidectomy, and cytology may be confusing, some surgeons proceed directly to parotidectomy. Histology will direct postoperative additional treatment (radiotherapy). In patients, in whom malignant lymphoma is suspected, fine needle aspiration biopsy may precede surgery. Salivary gland tumours in children are rare. A biopsy is mandatory to differentiate epithelial from non-epithelial tumours (sarcoma, lymphoma), because treatment is different (surgery vs chemotherapy / radiation therapy).

In this refresher course examples of different clinical presentations and imaging findings will be presented.

ESHNR Refresher Course – 2nd part

15.09.2012, 16.30 – 18.30 pm

Chairs: Bodo Kress, Frankfurt am Main (Germany) / Thi Dao Nguyen, Halle (Germany)

16.30 – 17.00 pm

Orbit and Globe

Wibke Müller-Forell (Invited presentation)

Universitätsmedizin Mainz, Institut für Neuroradiologie, Mainz, Germany

SUMMARY: Only a small number of the large variety of orbital diseases demand imaging with Computed Tomography (CT) and Magnetic Resonance Imaging (MRI) but are essential in order to define the lesion itself and / or influence therapeutic decisions. The different techniques and examination protocol should be adapted

with regard to the specific and individual clinical findings and questions of the individual patient. The identification of the pathology with respect to the different orbital compartments (globe, intra- extraconal space and optic nerve) is not only mandatory but most helpfully in order to answer the specific questions as sufficient as possible.

CT is the method of choice in traumatic cases, not only due to prompt availability, but also because of excellent high resolution. Both methods may be indicated in cases of orbital inflammation, especially in Graves disease, the most frequent cause of proptosis in adults. Differential diagnosis of idiopathic orbital inflammation represents a challenge for both, CT and MRI. Apart from the common signs of benign or malignant growth,

tumors and other space occupying lesions in the depth of the orbital cone should be preferably examined with MRI, although erosions of the bony walls are best defined with CT.

TAKE-HOME-POINTS: The aim of this course is to present a structured protocol for preparing and performing diagnostic imaging in orbital pathology.

17.00 – 17.30 pm

Trauma in the head and neck

Berit M. Verbist (Invited presentation)

Leiden University Medical Center, Dept of Radiology, C2S, Leiden, The Netherlands

SUMMARY: Blunt and/or penetrating trauma to the face and/or neck may lead to severe and complex injury to the bony structures and soft tissues. With thorough anatomical knowledge, however, fracture patterns can be recognized and potential complications become predictable based on related anatomic relationships. Naso-orbital-ethmoid, orbitozygomatic/zygomatico-maxillary-complex and maxillary fractures will be reviewed. Possible life-threatening complications and delayed complications will be discussed. Laryngotracheal injury most commonly results from compression of the larynx/

trachea between the cervical spine and a force applied from anterior. Fractures of the laryngeal cartilages and associated soft tissue injuries will be illustrated.

TAKE-HOME-POINTS: The audience will be shown how to:

- report injuries in a comprehensive way
- identify acute complications putting the patient at risk for functional losses or even death
- anticipate delayed complications based on injured structures.

17.30 – 18.00 pm

Temporomandibular joint

Bodo Kress (Invited presentation)

Krankenhaus Nordwest GmbH, Zentralinstitut für Radiologie und Neuroradiologie, Frankfurt am Main, Germany

SUMMARY: Internal derangement is very common especially in young women. To diagnose this entity you've to use proper equipment and MR protocol and you've to have a common understanding of underlying pathologies. Sys-

tematic of internal derangement is very simple but very often misunderstood by radiologists.

TAKE-HOME-POINTS: Therefore this refresher course has following objectives: 1) To clarify anatomy of the temporomandibular joint (TMJ) 2) To give advice of minimal standard of equip-

ment which should be used 3) To recommend a proper protocol 4) To describe pathological findings 5) To provide a handout

18.00 – 18.30 pm

Lymph nodes in the neck

Alexandra Borges (Invited presentation)

Instituto Português de Oncologia Francisco Gentil Centro de Lisboa, Departamento Radioterapia e Imagem / Radiologia, Lisbon, Portugal

SUMMARY: In head and neck oncology, lymph node involvement results essentially from 3 major groups of malignancies: Epithelial neoplasms, squamous cell cancer being the most common, thyroid gland tumors and lymphoma. A wide gamut of imaging modalities can be used to depict cervical lymph node metastases: US, Doppler US, CT (with CT perfusion), MRI (including DWI, PWI, MRS and the use of different contrast media), PET, PET-CT and more recently PET-MR. Some of these modalities may also be used to guide fine needle aspiration cytology or biopsy of suspicious lymph nodes allowing for a cytopathological or histological diagnosis. Improvement in cytopathologic technique, including immunohistochemical analysis and cytogenetics, increased the detection rate and the accuracy of lymph node characterization. Lymph node metastases have a dramatic impact in patient's management and prognosis. Regarding squamous cell cancer, by far the most frequent malignancy in the head and neck region, the presence of a single metastatic lymph node decreases the 5 year survival rate in 50% which is further reduced when bilateral involvement, nodal necrosis or extracapsular spread are present. In these circumstances the role of imaging in lymph node staging and, in particular, discriminating the N0 from the N1 neck can never be too overemphasized. In the past decades imaging has moved from purely anatomic to provide additional physiologic and

metabolic information overcoming the obvious limitations of lymph node size criteria. This additional information is being progressively incorporated in cancer staging systems and in oncologic management guidelines. However, in spite of all these advancements, FNAB is still, among the minimally invasive modalities, the most accurate in lymph node characterization.

TAKE-HOME-POINTS:

- » Detection of metastatic lymph nodes is one of the most important roles of imaging in head and neck cancer staging.
- » Imaging criteria for metastatic lymph node depiction should be exclusively applied to patients with cancer.
- » A combination of anatomic, physiologic and metabolic criteria taken together helped improve the accuracy of imaging in depicting lymph node metastasis.
- » Image guided FNAB remains the technique with the highest accuracy although a 17% false negative rate is still to be expected even in referral centers.

POSTER

Educational Poster

P01	Imaging of different vibroplasty couplers attached to a floating mass transducer of vibrant soundbridge on MDCT and CBCT in a cadaveric model. Nguyen TD et al (Halle, DE)
P02	A snapshot of imaging in mixed hearing loss. Mundada P et al (Singapore, SG)
P03	Imaging considerations in patients with anotia-microtia. Loney E et al (Bradford, UK)
P04	Thyroid eye disease – What do we need to tell the clinicians. Suresh Babu S et al (Leicester, UK)
P05	Infectious and inflammatory orbital lesions – A pictorial review. Suresh Babu S et al (Leicester, UK)
P06	Eyes popped! proptosis: MRI and CT features of common causes. Hart M et al (Oxford, UK)
P07	Foreign head and neck bodies on CT. Sebastian A et al (Halle, DE)
P08	Diffusion negative lesion does not indicate that that is not an abscess. Kress B et al (Frankfurt a. Main, DE)
P09	Long-term sequelae of maxillofacial injuries. Radiologic features. Castaldi A et al (Genova, IT)
P10	A Systematic approach to reporting panoramic radiographs. Viner S et al (Bradford, UK)
P11	Newly emerging methods for periodontal diagnosis. Dumitrescu AL et al (Bucharest, RO)
P12	Fibrous dysplasia in the head and neck: clinical presentation, radiological variety, differential diagnosis and therapeutic options. de Win M et al (Amsterdam, NL)
P13	Stage by stage pictorial review of tongue and floor of mouth malignancies. Abdur-Rahman M et al (London, UK)
P14	CT evaluation of cystic lesions of submandibular space and their masquerades: A systematic approach. Mundada P et al (Singapore, SG)
P15	The Great pretender - Extracranial head and neck lymphoma. Loney E et al (Bradford, UK)
P16	Carotidynia: a multimodality evaluation of 34 cases. Costa YB et al (São Paulo, BR)
P17	The bony pseudomass and calcifications in the neck. Singh F et al (Stockport, UK)
P18	Human papillomavirus (HPV) and head and neck carcinomas: pictorial essay and literature review. Gomes R et al (São Paulo, BR)
P19	IgG4-related disease presenting as head and neck lesions: Pictorial essay and literature review. Gebrim E et al (São Paulo, BR)
P20	Diagnostic adequacy of ultrasound guided fine needle aspiration cytology in the investigation of neck lumps: A comparative audit of three institutions between March 2007 – March 2008 and March 2011 – March 2012. Adjei - Gyamfi Y et al (London, UK)
P21	Thyroiditis and its appearances on US and Nuclear imaging. Cook JL et al (Swindon, UK)
P22	Expected CT and MRI findings after laryngectomy – Pictorial essay and literature review. Gebrim E et al (São Paulo, BR)

Scientific Poster

Studies

P23	Skull base osteomyelitis mimicking nasopharyngeal carcinoma: imaging features at initial presentation. Goh J et al (Singapore, SG)
P24	Comparison of cone beam and multi-detector computed tomography in the visualisation of PORPs and TORPs - a cadaveric study. Nguyen TD et al (Halle, DE)
P25	Radiologic assessment of temporomandibular joint in patients with malocclusion. Perova N et al (Moscow, RU)
P26	The role of imaging techniques for diagnosis and monitoring of response to therapy of primary lymphoma of the orbit. Grzesiakowska U et al (Warsaw, PL)
P27	Quality comparison of digital x-ray devices with 3D-visualization capability in imaging of paranasal sinuses and temporal bone. Knörger M et al (Halle, DE)
P28	The radiology of mechanical combined injuries of facial skull and orbit structures. Lezhnev D et al (Moscow, RU)
P29	The application of phase AIF for pharmacokinetic analyses in the maxillofacial region. Chikui T et al (Fukuoka, JP)
P30	The application of a pharmacokinetic analysis to maxillofacial tumors. Kitamoto E et al (Fukuoka, JP)
P31	Osteomyelitis in the maxillofacial region in case of immunodeficiency state. Zorina E et al (Moscow, RU)
P32	Position of the impacted third molar in relation to the mandibular canal. CBCT patterns. Lo Casto A et al (Palermo, IT)
P33	The comparison of radiological methods in the diagnostics of the radiation osteonecrosis in skull and cervical spine. Kurlaeva Y et al (Moscow, RU)
P34	Imaging features of extranodal lymphoma originating in the head and neck. Avril L et al (Geneva, CH)
P35	Diagnosis and management of mass-like lesions of the tongue. Kawazu T et al (Fukuoka, JP)
P36	MRI of nasopharyngeal adenoid hypertrophy – is DWI helpful for the characterization as a benign entity? Surov A et al (Halle, DE)
P37	Cone-beam computer tomography in styloid syndrome diagnosis (Eagle syndrom). Solonskaya N et al (Moscow, RU)
P38	Tumor Response Assessments of oral cancer to pre-operative chemoradiotherapy (CRT) with permeability and diffusion MRI. Chikui T et al (Fukuoka, JP)
P39	US-guided fine-needle aspiration of thyroid nodules – “Brainstorm” on polemic issues! Fernandes L et al (Lisbon, PT)
P40	Digital dynamic sialography in diagnosis of sialolithiasis. Lezhnev D et al (Moscow, RU)
P41	Swelling of the parotid gland with cystoid pattern on ultrasound: a spectrum of diseases. Kunze C et al (Halle, DE)

P42	Diagnostic performance of ultrasound guided fine needle aspiration cytology in the assessment of major salivary gland masses: a retrospective analysis. Kohler R et al (Geneva, CH)
P43	Non-invasive differentiation of primary parotid gland tumors: Does high-resolution dynamic contrast-enhanced MRI offer a solution? Busch J et al (Hamburg, DE)
P44	Non-invasive differentiation of non-tumorous parotid gland diseases using high-resolution dynamic contrast-enhanced MRI. Habermann CR et al (Hamburg, DE)

Cases

P45	Reparative granuloma post-stapedectomy in patients with otosclerosis: Distinctive and unusual imaging appearances. Siddiqui J et al (London, UK)
P46	Cholesteatoma: A rare differential diagnosis of intracranial masses. Niestroj S et al (Hamburg, DE)
P47	Osteolysis of the skull base mimicking M. Gorham-Stout – A case report. Gramsch C et al (Essen, DE)
P48	Chondrosarcoma of the base of skull. Starvic T et al (Belgrade, RS)
P49	Lipoblastoma of the nasal cavity. Klintström E et al (Linköping, SE)
P50	Clear cell odontogenic carcinoma with multiple lung metastases and late recurrence. Klintström E et al (Linköping, SE)
P51	Orbital abscess as a result of acute frontal sinusitis and ethmoiditis. Kontaki T et al (Kozani, GR)
P52	Rapidly evolving large extracranial vertebral artery pseudoaneurysm in Behcet's disease. Sibir R et al (Houston, Texas, US)
P53	Prevertebral tendinitis. Schramm D et al (Halle, DE)
P54	Spontaneous idiopathic cervical surgical emphysema and pneumomediastinum: a unique case? Siddiqui J et al (London, UK)

EDUCATIONAL POSTER

P1 Imaging of different vibroplasty couplers attached to a floating mass transducer of vibrant soundbridge on MDCT and CBCT in a cadaveric model

Thi Dao Nguyen (educational poster)

Universitätsklinikum Halle (Saale), Universitätsklinik und Poliklinik für Diagnostische Radiologie, Halle (Saale), Germany

Co-Authors: Mlynski R, Plontke S, Kösling S

SUMMARY: Vibrant sound bridge (VSB) has been successfully approved as an active middle ear implant in the treatment of sensorineural and mixed hearing loss. VSB consists of two components: an external Audio Processor (AP), and an implanted Vibrating Ossicular Prosthesis (VORP). AP contains a microphone, a digital signal processor and a battery. VORP consists of a receiver/stimulator, a conductor link and the transducer [Floating Mass Transducer (FMT)]. The patient wears the AP on the head. The receiver is implanted in a drilled depression on the skull surface of the temporal bone. The conductor link runs through a mastoidectomy cavity and the facial recess into the middle ear. Conventionally, FMT is attached to the incus or placed at the round window. Now, there are couplers available, which offer additional options for attaching FMT to various middle ear structures in order to adapt them to different conditions and anatomical situations of the middle ear. Radiological evaluation of the position of FMT and the attached coupler is up-coming for quality control. Both, Cone Beam CT (CBCT) and Multi-Detector CT (MDCT), are appropriate methods for post-operative imaging to evaluate the exact position of FMT. The detection of a malposition or an early complication requires knowledge of the normal post-operative image after implanta-

tion of FMT and different couplers. In cooperation with the Department of Otorhinolaryngology of the University of Halle VSBs with various attachments were correctly implanted in formalin fixed human heads and afterwards imaged using MDCT and CBCT. The purpose for this paper is to demonstrate the normal appearance of FMT and available couplers on CBCT and MDCT. Additionally, limits of the two methods and their differences are presented.

TAKE HOME POINTS: Normal appearance of VSB and various couplers on CBCT and MDCT. CBCT and MDCT permit a precise post-operative localization of FMT. CBCT has advantages due to lower radiation dose, lower metal artefacts and better spatial resolution.

P2 A snapshot of imaging in mixed hearing loss

Pravin Mundada (educational poster)

Changi General Hospital, Depart of Radiology,
Singapore, Singapore

Co-Authors: Tan TY

SUMMARY: Patients are often referred to the diagnostic imaging department with a clinical diagnosis of mixed hearing loss. It is imperative for a radiologist to be aware of various conditions which may lead to mixed hearing loss. The purpose of this exhibit is to acquaint the readers with the spectrum of imaging findings and various common and uncommon conditions which are associated with MHL. There is no published literature found compiling all the causes and imaging evaluation of MHL under one heading as our educational exhibit does. MHL is a combination of conductive hearing loss (CHL) and sensorineural hearing loss (SNHL) which is diagnosed on audiography by the presence of elevated bone and air conduction thresholds, with the latter being more elevated than the former. The pathology involves external and/or middle ear and also the inner ear and/or auditory nerve. Imaging in MHL is performed with CT by acquiring 0.4–0.6 mm slices with minimal overlap and multiplanar reconstruction. Additional evaluation may be done with contrast enhanced CT and/or

MRI in some cases. The MRI protocol includes whole brain T2W and /or FLAIR, thin slice heavily T2- weighted sequences (FIESTA) and contrast enhanced T1WFS in coronal and axial planes. Various bone dysplasia cause MHL, commonest of which is otospongiosis. Other dysplasia which cause MHL include osteogenesis imperfecta type 1, Camurati-Engelmann disease and Paget's disease. Congenital causes of MHL include large vestibular aqueduct syndrome (LVAS) and X-linked progressive deafness. Idiopathic fixation of malleus head is also causes MHL. Acquired causes of MHL include cholesteatoma, post traumatic fractures and facial nerve schwannomas. Few of the MHL cases may not reveal any imaging abnormality.

TAKE HOME POINTS: Mixed hearing loss (MHL) has a profound effect on the quality of life of affected individuals. Imaging plays a crucial role in determining the underlying cause and also in determining the choice of treatment.

P3 Imaging considerations in patients with anotia-microtia

Elizabeth Loney (educational poster)

Bradford Teaching Hospitals NHS Foundation Trust, Radiology,
Bradford West Yorkshire, United Kingdom

Co-Authors: Viner S, Strachan D, Raine C

SUMMARY: Anotia-Microtia is a congenital abnormality characterized by non/under-development of the pinna. This may be unilateral or bilateral and occurs in approximately 1 per 8–10,000 births. Multiple classification systems have been proposed based on the severity of

the deformity/surgery it will require to correct it. The most commonly used of these will be presented. Affected patients often have a degree of conductive hearing loss due to associated external ear canal atresia / stenosis. Up to 40% of cases are syndromic. There are two priorities

from an imaging perspective: firstly thorough evaluation of the temporal bone and secondly a broader over-view considering other body areas associated with developmental aural abnormalities. Whilst the degree of malformation of the pinna is amenable to direct inspection, temporal bone imaging with high resolution CT is necessary to assess underlying structures. The extent of stenosis/ atresia and its position in relation to the tympanic membrane is noted. The degree of associated mastoid hypoplasia is important. The size of the middle ear and the presence, continuity and appearance of the ossicular chain is assessed. The course of the facial nerve must be described due to a higher risk of anomalous course in this patient group. Surgery addresses both cosmetic and functional issues. This may involve the attachment of a false pinna or bone anchored hearing aid, requiring assessment of local bone stock and adjacent vascular structures. Not all patients will benefit from reconstruction of the external canal as outcomes can be excellent with modern assisted hearing devices. These points will be addressed with examples of normal anatomy and abnormalities in patients we have imaged. Looking at the broader picture, there are many

congenital / genetic associations with anotia-microtia. The pinna derives from the 1st and 2nd branchial arches therefore those conditions that involve these arches will have an increased risk of aural problems, including hemifacial microsomia, Treacher Collins and Goldenhar Syndromes. Microtia is also seen in patients with coexistent renal, GI, cardiac and skeletal anomalies and these other anatomical areas may require imaging. Chromosomal abnormalities occur in 6-16% of anotia-microtia, including trisomies and deletion complexes. The most common syndromes will be described, along with some pictorial examples.

TAKE HOME POINTS: Anotia-microtia is not uncommon in Head and Neck Radiology and it is important to describe a number of key factors that will affect both hearing and cosmetic outcomes when reporting CT scans of the region. The poorly developed pinna may also be the tip of the iceberg in patients with syndromic conditions, particularly those affecting 1st and 2nd branchial arch structures. It is necessary to consider such associations when imaging these patients. Both areas will be addressed in this presentation.

P4 Thyroid Eye Disease – What do we need to tell the clinicians

Sarawathy SureshBabu (educational poster)

University Hospitals of Leicester NHS Trust, Department of Radiology & Ophthalmology,
Leicester, United Kingdom

Co-Authors: Sampath R, Burns J, Vaidhyath R

PURPOSE: To present imaging features of thyroid eye disease and highlight issues those are relevant to the clinicians.

CONTENT ORGANISATION:

1. Introduction
2. Proptosis – Definition & Cause
3. Clinical presentation of Thyroid eye disease
4. Radiological features of Thyroid eye disease

- a. Imaging modality of choice – CT vs. MRI
- b. Imaging spectrum
 - i. Extra ocular muscle involvement – single vs. multiple
 - ii. Orbital fat
 - iii. Optic nerve compression and stretch
 - iv. Assessment of activity
 - v. Post surgery appearance
 - vi. Status of the structures around the orbit
- 5. Other causes for extra ocular muscle enlargement
 - a. Idiopathic orbital inflammation
 - b. Myositis
 - c. Lymphoma
 - d. Metastasis
 - e. Carotid – cavernous fistula

CONCLUSIONS:

- » Diagnosis of cause of proptosis on imaging
- » Extra ocular muscle vs. orbital fat involvement in the orbit
- » Assessment of optic nerve compression secondary to thyroid eye disease
- » Post surgical spectrum

TAKE-HOME-POINTS:

- » Imaging is useful to determine the cause of proptosis
- » The assessment of optic nerve compression is critical in the management of patients with thyroid eye disease
- » Imaging is also useful to assess perioptic soft tissue structures and in the post surgical management

P5 Infectious and inflammatory orbital lesions – A pictorial review

Sarawathy Suresh Babu (educational poster)

University Hospitals of Leicester NHS Trust, Department of Radiology & Ophthalmology, Leicester, United Kingdom

Co-Authors: Vaidhyanath R

PURPOSE: To present clinical and imaging spectrum of infective and inflammatory disease involving the orbit

CONTENT ORGANISATION:

- 1. Introduction
- 2. Clinical presentation of orbital infection & inflammation
- 3. Imaging modality of choice – CT vs. MRI
- 4. Radiological features of following infective & inflammatory disease will be presented.
 - a. Orbital cellulitis
 - b. Sub periosteal / Orbital abscess
 - c. Thrombophlebitis of ophthalmic veins

- d. Idiopathic Orbital Inflammation
- e. Necrotising fasciitis
- f. Post traumatic
- g. Sarcoidosis
- h. Sjogren syndrome
- i. Wegener's Granulomatosis
- j. Lacrimal gland / sac inflammation
- k. Cysticercosis

TAKE-HOME-POINTS:

- » Imaging helps in diagnosis possible cause and extent of infection / inflammation.
- » CT is the initial modality of choice and should include post contrast imaging and adequate assessment of paranasal sinuses & bones
- » MRI is essential to exclude potentially life-threatening complications like cavernous sinus thrombosis.

P6 Eyes Popped! Proptosis: MRI and CT features of common causes

Mary Hart (educational poster)

Oxford University Hospitals NHS Trust, Radiology, Oxford, United Kingdom

Co-Authors: Woo E

SUMMARY: Proptosis is one of the more common signs in ophthalmology. It is relatively easy to identify clinically. However, the aetiology and differential diagnosis for this sign is wide. Imaging is excellent in localising and demonstrating underlying pathology in relation to the eye. Like in most fields of radiology, CT and MRI are complimentary in these cases. Either or both modalities together allow diagnosis to be achieved for most pathology without invasive procedures around the orbit. This poster illustrates the MRI and CT features of common pathology presenting as proptosis in patients. Emphasis will be placed on typical and characteristic imaging features for each abnormality. orbital lymphoproliferative lesions

- » lacrimal gland benign mixed tumour
- » metastases
- » optic nerve sheath meningioma
- » thyroid ophthalmopathy
- » orbital idiopathic inflammatory pseudotumour
- » orbital subperiosteal abscess
- » orbital cavernous haemangioma
- » orbital venous varix
- » orbital neurofibromatosis

TAKE HOME POINTS:

- » Imaging features of proptosis
- » Characteristic MRI and CT features of common causes of proptosis

P7 Foreign head and neck bodies on CT

Anja Sebastian (educational poster)

Martin-Luther-Universität Halle/Wittenberg, Universitätsklinik und Poliklinik für Diagnostische Radiologie, Halle, Germany

Co-Authors: Meltendorf C, Herzog M, Kösling S

SUMMARY: Foreign head and neck bodies may occur as isolated injury, combined with other traumatic lesions (especially fractures after accidents) or as a complication of therapeutic intervention. Most indications for imaging are the search of ingested and orbital foreign bodies followed by the search for metallic foreign bodies before MRI in vague anamnesis. Whereas X-ray fluoroscopy is the leading imaging modality for the first indication, CT plays the major role for the second. CT is considered to be most sensitive in the detection of foreign bodies. The fast scanning time allows imaging with no or minimal motion artifacts. Apart from the detection or exclusion of a foreign body, exact localization and relationship to critical neighboring structures are very important for the planning of treatment. The type of material influences possible complications. Foreign bodies of wood may cause severe inflammatory reactions reaching from a cellulitis to an abscess or a phlegmon. They have to be removed in each case. Inorganic foreign bodies are inert and can stay in the body if removal would damage critical structures. On CT most

foreign bodies are hyperdense, but it is not possible to estimate the exact type of the material by measuring of Hounsfield units. The size of a foreign body has also a great influence on the measured density. Wood can cause some problems in the detection. Its density depends on the type of wood and dryness. Typically, dry wood shows low Hounsfield units up to minus 600. To differentiate it from air, it is important to use appropriate window settings. Fresh wood or wood which stayed for some times in the body has a higher density similar to soft tissue. With selected cases we demonstrate the broad spectrum of foreign bodies in the head and neck region and summarize the results of the literature.

TAKE HOME POINTS: CT is most sensitive in detection, exclusion and exact localization of foreign bodies. The density of the foreign objects differs, depending on their type and size, but it is not possible to determine the type of material. Wood is, because of its low density values, the most difficult to detect.

P8 Diffusion negative lesion does not indicate that that is not an abscess

Bodo Kress (educational poster)

Krankenhaus Nordwest GmbH, Zentralinstitut für Radiologie und Neuroradiologie, Frankfurt am Main, Germany

Co-Authors: Ravindranathan N

SUMMARY: Objective: To present 3 cases of abscesses in the head and neck. **Methods:** Three patients will be presented with huge mass lesions in the head and neck, without clinical evidence for abscess symptoms. Two cases were

presented with suspicion on tumor, one case has been an incidental finding. The MR protocol included beside axial diffusion weighted images and ADC, T2 and T1 before and after contrast administration. Result: One case showed

a diffusionrestricted lesion in the left temporal muscles, the MR diagnosis therefore has been abscess which has been proven by surgical drainage. The second case presented as a huge midfacial lesion, which did not show any diffusionrestriction and has been reviewed as tumor. This lesion has been proven as an abscess by surgical operation. The third case showed a diffusionrestricted lesion inside the maxillary sinus which has been proven as an empyema.

CONCLUSION: Non diffusionrestricted lesion does not mean that this is not an abscess, although these lesions are huge and have no clinical symptoms of an abscess.

P9 Long-term sequelae of maxillofacial injuries. Radiologic features

Antonio Castaldi (educational poster)

E.O. Ospedali Galliera, Diagnostic and Interventional Neuroradiology, Genova, Italy

Co-Authors: Parodi S, Pensa M, Nuzzi NP

SUMMARY: Maxillofacial (MF) injury is a frequent component of major trauma (reported incidence: 15-34%). A large percentage of patients experiencing MF trauma may develop chronic functional sequelae. Epidemiologic data on incidence and entity of late post-traumatic disabilities are largely variable, depending both on the different evaluation criteria and on the paucity of follow-up analysis of the factors predicting the functional outcome (mechanism, trauma entity, social status, psychological impact, etc.). Therefore, a systematic correlation between the MF traumatic lesions and the spectrum of long-term effects is objectively hard to achieve. A part of the aesthetic and psychological consequences following serious MF injury, there is a significant number of late functional limitations such as visual problems, alterations of smell, impaired mastication, difficulty with breathing,

and epiphora. Cranial nerve deficits and sinus problems can also occur. Patients sustaining MF trauma require careful management and thorough assessment to reduce the risk of misdiagnosis. Imaging plays a decisive role in the diagnostic work-up, to establishing the early diagnosis and to orientate further treatments. Computed tomography (CT) is widely considered the best diagnostic tool in the evaluation of traumatic lesions, providing excellent detail of fracture lines and bone fragments orientation and providing multiplanar and three-dimensional reformations. Imaging findings are often subtle, potentially overlooked. Undetected lesions if not properly managed can result in future functional limitations. Therefore, knowledge of traumatic injury patterns is important for accurate image interpretation and adequate clinical planning.

TAKE HOME POINTS:

1. To provide a pictorial review of unusual MF trauma late sequelae with a systematic approach:
 - a. vascular (dissections, pseudoaneurysms, arteriovenous fistulae, venous thrombosis)
 - b. ophthalmic (diplopia, enophthalmos, global damage)
 - c. nasolacrimal (ductal stenosis/occlusion with epiphora, chronic dacriocystitis)

- d. cranial nerve (anosmia, impaired sensitivity of trigeminal or facial nerve, traumatic neuromas)
- e. sinuses (mucocele)
- f. dural tear (rinorrhea, otorrhea)
- g. temporomandibular (malocclusion/impaired mastication)

2. To emphasize the importance of imaging in both initial assessment and follow-up examination of MF injury 3
3. To highlight the need for specific expertise to identify and properly evaluate imaging features. A missed/late diagnosis can lead to inadequate or delayed treatment with residual functional losses.

P10 A systematic approach to reporting panoramic radiographs

Stuart Viner (educational poster)

Bradford Teaching Hospitals NHS Foundation Trust, Radiology,
Bradford West Yorkshire, United Kingdom

Co-Authors: Loney E, McCaul L

SUMMARY: Historically dental radiology is often overlooked as part of Clinical Radiology training. The majority of panoramic radiographs are interpreted in many Institutions, including our own, by Maxillofacial and Dental colleagues. It often seems ironic that we, as Head and Neck Radiologists, are only sent those cases that these practitioners find difficult to report on for a second opinion! Although this investigation may be considered low tech and is mainly used in Dental Practice, images can demonstrate a wide variety of relevant dental pathology that will influence treatment decisions such as the presence of caries and infection. Whilst as a group we are good at reporting the more unusual findings of cystic change, trauma and tumours it is often the basics that are overlooked. Dental anatomy, nomenclature and common normal variants will be reviewed. How to describe dental roots, their orientation and patterns of third molar eruption

are described. Commonly encountered dental restorations and how to report on caries, periodontal and periapical disease will be covered. The aim of this presentation is therefore to not to review mandibular cysts, tumour and trauma that are often covered in poster presentations, but to demonstrate a systematic approach to producing a meaningful and helpful OPT report by non-dentally qualified Head and Neck Radiologists.

TAKE HOME POINTS: Although the reporting of panoramic radiographs is not common practise in clinical radiology it is important that Head and Neck Radiologists in particular have a systematic approach to panoramic radiographs. By understanding dental anatomy and nomenclature one will produce OPT reports worth reading, and important pathology will not be overlooked.

P11 Newly emerging methods for periodontal diagnosis

Alexandrina L. Dumitrescu (educational poster)

Dental Private Clinic
Bucharest, Romania

Co-Authors: Zetu L, Teslaru S, Haba D

SUMMARY: Periodontitis is an inflammatory disease of bacterial origin that results in the progressive destruction of the tissues that support the teeth, specifically the gingiva, periodontal ligament, and alveolar bone. Although there have been significant advances in the understanding of the cause and pathogenesis of periodontal disease over the past 40 years, the traditional methods by which clinicians diagnose periodontal disease have remained virtually unchanged. The diagnosis of periodontal disease relies almost exclusively on clinical parameters and traditional dental radiography. Current diagnostic methodologies do not enable us to accurately predict which periodontal sites, teeth, or individuals are susceptible to further periodontal breakdown. Given the limitations of current diagnostic tools, researchers are working to develop techniques that address some of these inadequacies. New approaches and technologies that are being developed to improve the diagnosis of periodontal disease are here presented: Digital Subtraction Radiography (DSR) and Analysis of alveolar bone structure Fractal Analysis. Others newly emerging methods for periodontal diag-

nosis presented here are: 1. Cone-beam Computed tomography (CBCT) 2. Optical coherence tomography (OCT) 3. Tuned aperture computed tomography (TACT) 4. Magnetic resonance imaging (MRI) 5. In vivo monitoring and screening of periodontitis by near infrared (NIR) spectroscopy 6. Non-invasive diagnosis of periodontitis by acoustic microscopy.

TAKE HOME POINTS: Recent technologies used in dentistry, including the field of periodontology, are not limited to 2-dimensional (2-D) systems. The problem inherent to 2-D systems is that 3-dimensional (3-D) anatomy is collapsed into 2-D space, resulting in the superimposition of structures that potentially obscure features of interest and decrease diagnostic sensitivity. The results of these new technologies provide a new understanding of the periodontal disease, the possibility to characterize the type and healing process of periodontal inflammation, as after the therapy the decrease of inflammation in periodontal tissues and the improvement in clinical parameters.

P12 Fibrous dysplasia in the head and neck: clinical presentation, radiological variety, differential diagnosis and therapeutic options

Maartje ML de Win (educational poster)

Academic Medical Center, Radiology,
Amsterdam, The Netherlands

Co-Authors: Deurloo EE, Freling NJ

SUMMARY: Fibrous dysplasia is a rare condition characterized by replacement of normal bone by fibro-osseous connective tissue. Young adults

are most frequently affected. One of the preferential localisations is the bone of the craniofacial complex. The skull and facial bones are

involved in 10-25% of patients with monostotic fibrous dysplasia and in up to 50% of patients with polyostotic fibrous dysplasia. It has a broad variation in clinical presentation - from asymptomatic or mild cosmetic deformity to blindness in case of optic nerve compression. The diagnosis is made by a combination of clinical, radiological, and sometimes pathological findings. However, it is not always possible or safe to get histological confirmation and potential harmful biopsies should be avoided for this benign disease. To draw a correct (differential) diagnosis is important because it has consequences for therapy and follow-up regimen. Therefore, it is desirable that radiologists have knowledge about clinical manifestations, radiological features and most important differential diagnosis of craniofacial fibrous dysplasia. In this educational poster we will illustrate the imaging features of fibrous dysplasia and look-alikes on CT and MRI and address the most important differential diagnostic considerations. Besides the well known typical ground glass appearance on CT (fig 1) – seen in about 55% of the cases – we will show examples of less characteristic patterns. On MRI (fig 2), fibrous dysplasia often lacks the distinc-

tive features seen on CT and a potential diagnostic pitfall is to misdiagnose fibrous dysplasia for a malignant tumor. We will show patterns and signal intensities of fibrous dysplasia and look-alikes on MRI. We will discuss the differential diagnoses and indicate when additional CT is advisable. Briefly, we will address potential therapeutic options and/or follow-up strategy.

TAKE HOME POINTS: Craniofacial fibrous dysplasia has a broad variation in features on CT and MRI.

It may mimic other benign or malignant conditions of the craniofacial bones.

Knowledge of the various imaging characteristics of craniofacial fibrous dysplasia is important to distinguish this benign condition from look-a-likes and to draw a correct (differential) diagnosis.

Fibrous dysplasia is more difficult to recognize on MRI and additional CT might help to make the correct diagnosis.

Figure 1. CT

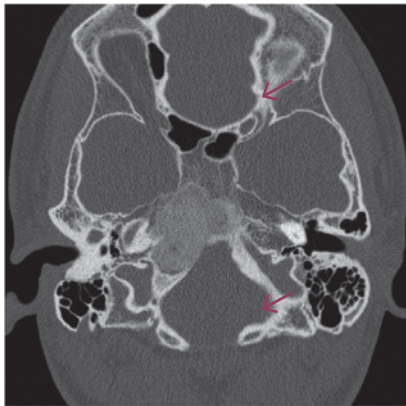


Fig 1: typical ground glass appearance of fibrous dysplasia on CT.

Figure 2. MRI



Fig 2: T2 MRI: non-specific presentation of fibrous dysplasia, difficult to distinguish from other benign or even malignant conditions.

P13 Stage by stage pictorial review of tongue and floor of mouth malignancies

Muhammad Abdur-Rahman (educational poster)

Barts and The London School of Medicine and Dentistry, Queen Mary, University of London, School of Medicine and Dentistry, London, United Kingdom

Co-Authors: Singh F, Qureshi S

SUMMARY: Malignancies in the oral cavity particularly the tongue and floor of mouth can pose great management difficulties. The majority (nearly 90%) present at a fairly late stage particularly at Stage III-IV. This can result in difficulties with curative management and require multimodality treatments involving a multidisciplinary approach. We draw on the extensive experience of the South Manchester Head and Neck Can-

cer Multidisciplinary Team and present a stage by stage pictorial review of the aforementioned malignancies. This will be in the background of an anatomical context with degrees of increasing degrees of dissemination.

TAKE HOME POINTS: To be able to summarise and stage malignancies of the tongue and floor of mouth.

P14 CT evaluation of cystic lesions of submandibular space and their masquerades: A systematic approach

Pravin Mundada (educational poster)

Changi General Hospital, Department of Radiology, Singapore, Singapore

Co-Authors: Tan TY

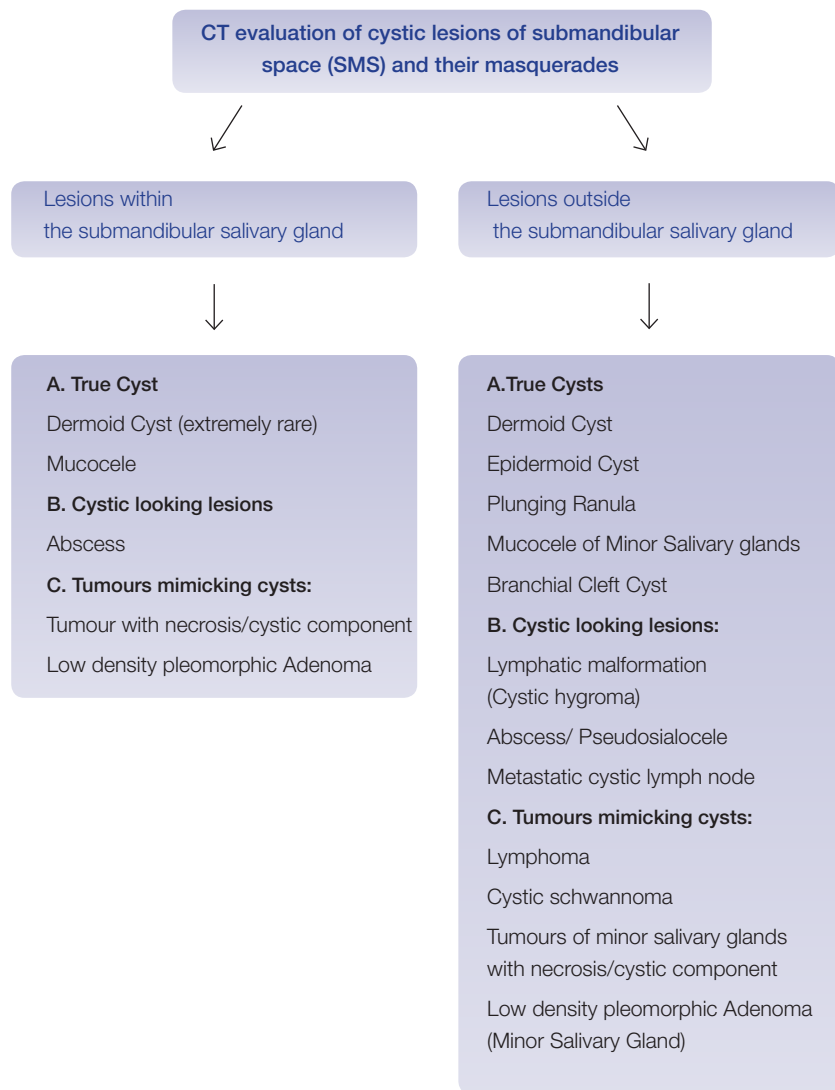
SUMMARY: Imaging with CT plays a vital role in the evaluation of the cystic masses of submandibular space (SMS). A wide range of common and uncommon pathologies can present as a cystic lesion of the SMS. A few low attenuation solid lesions mimic cystic lesions of the SMS. Characterization of these lesions is vital as they include benign as well as few malignant pathologies. It is often difficult to differentiate these lesions from each other as there is significant overlap in their imaging features. It is also important to differentiate these lesions from those in the sublingual space as the surgical approach to lesions may differ. The objective of this article is to define and identify various cystic lesions of the SMS, identify the pathologies which may

masquerade as cystic lesions of the SMS and to develop an algorithm based on the imaging features of these lesions which can help in deriving a diagnosis in most of the instances or narrow the list of differentials. While developing this algorithm, the various imaging parameters we have considered are: anatomical context / extent of the lesion, density of the lesion, presence or absence of a wall, characteristics of the wall, presence of a solid component and also the complexity of the lesion. Application of various tell-tale signs on imaging like tail sign, claw sign, separation sign, anterior facial vein sign and demonstration of extension in adjacent spaces are also helpful in distinguishing one lesion from another.

TAKE HOME POINTS:

1. Various benign and malignant pathologies may present as cystic lesions of SMS or masquerade as cystic lesions of SMS. There is significant overlap in the imaging features of these cystic lesions.

2. A systematic evaluation of the anatomical context of the lesion and its various CT imaging features can help in arriving at a diagnosis in most of instances or can help in narrowing the differentials.



P15 The great pretender - extracranial head and neck lymphoma

Elizabeth Loney (educational poster)

Bradford Teaching Hospitals NHS Foundation Trust, Radiology, Bradford West Yorkshire, United Kingdom

Co-Authors: Mohammed A, Viner S

SUMMARY: Lymphoma is the commonest non-epithelial malignancy of the Head and Neck. It encompasses a large group of conditions under the broad headings Hodgkins and Non-Hodgkins lymphoma (NHL). Hodgkins disease is more frequent in a younger age-group and often presents as painless cervical nodal enlargement. Primary extranodal disease is rare. NHL is a disease mainly of the middle-aged and elderly. It can be divided into nodal, extranodal (lymphatic) and extranodal (extralymphatic) groups. Nodal disease of the head and neck is common, with cervical lymphadenopathy being the presenting complaint in 15% of patients. Extranodal (lymphatic) NHL refers to disease found in Waldeyers ring, most commonly the palatine tonsils. Extranodal (extralymphatic) disease is a mixed entity with multiple manifestations, hence the title of this poster The Great Pretender. Lymphoma of the Head and Neck may be part of disseminated disease, or the sole site, when it poses a greater diagnostic challenge. Lymphoma as part of the differential diagnosis may be overlooked in unusual sites until histology points in its direction. Lymphoma may be imaged using multiple modalities. Ultrasound, CT and MR features of nodal disease will be demonstrated. Extranodal (lymphatic) disease in Waldeyers ring is often mistaken for the commoner condition, Squamous Cell Carcinoma. Features that may help distinguish the two will be demonstrated. Extranodal (extralymphatic) disease has many guises. We will show examples including orbital, thyroid, sinus, salivary, laryngeal and neural involvement. Some of these are rare but important differentials. Whenever an infiltrating mass

is noted in these areas, lymphoma should be considered, even if there are no suspicious local nodes. All however share certain characteristics with other more common conditions and in considering lymphoma one should also think pseudotumour, eosinophilic granuloma and Wegeners disease. We aim to highlight what (if any) clues can be gleaned from imaging to narrow the differential. PET-CT is an important modality for staging disease and monitoring response to treatment but will not be covered in depth. If a diagnosis of lymphoma is confirmed it is important to look elsewhere for other disease sites. In our clinical practice we have seen many examples of such cases and will present a pictorial review, grouping images into anatomical areas. In each case key similarities and differences from top differential diagnoses will be covered.

TAKE HOME POINTS: Lymphoma is commonly encountered in our day-to-day practice, and can be a straightforward diagnosis to make. However, it is also a great mimic of other conditions, often more common than itself in extranodal locations. We aim to increase awareness of its manifestations and provide an overview of this extremely important disease that can often be treated non-surgically with excellent results.

P16 Carotidynia: a multimodality evaluation of 34 cases

Yves Bohrer Costa (educational poster)

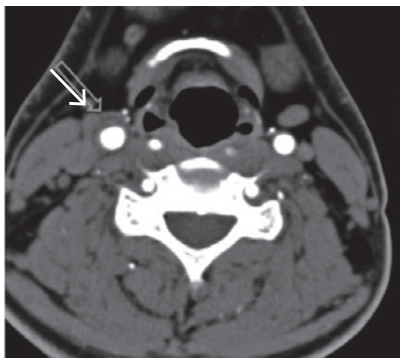
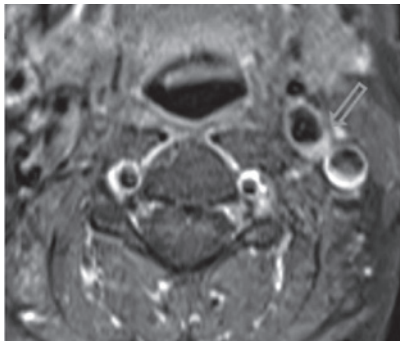
Hospital Israelita Albert Einstein, Diagnostic Image, São Paulo, Brazil

Co-Authors: Camara L, Soares C, Garcia M, Daniel M, Gomes R, Funari M

SUMMARY: The term carotidynia was first used in 1927 by Dr. Temple Fay to describe patients with atypical migraine. In the last two decades this subject has been very controversial, including being removed from The International Classification Of Headache Disorders, published in 2004. Recently, with the development of new technologies and better quality images, some authors have reaffirmed the importance of this entity on the context of neck pain and headache. We retrospectively evaluated patients with images features compatible with carotidynia which were attended at our institution from 2009 to 2012. We performed epidemiological data and

imaging features analysis. Most of those patients were evaluated by more than one image method. We included patients 36 with images features compatible with this entity. We used as exclusion criteria: recent radiotherapy or neck surgery, patients with severe carotid stenosis. Two patients were excluded by these criteria. We obtained similar distribution between genders, between 31–67 years old. The carotid bulb was the site most frequently affected in the vast majority of patients. The presence of an abnormal enhancing tissue surrounding carotid bulb was seen in all cases. MRI showed to be the most sensitive method, especially on post-contrast T1 weighted images. We also observed a great correlation between the clinical complain and the affected site.

TAKE HOME POINTS: Carotid bulb is the most frequently site affected by carotidynia. There was a great correlation between the clinical complain and the affected site. MRI was the most sensitive method, especially on post-contrast T1 weighted images.



P17 The bony pseudomass and calcifications in the neck

Fiona Singh (educational poster)

Stepping Hill Hospital, Radiology, Stockport, United Kingdom

Co-Authors: Felton M, Ramamurthy L, Kay N, Choudhri A

SUMMARY: Physicians may refer patients for imaging for a clinically suspected neck mass, or to elucidate the cause of pain or other symptoms. Where no soft tissue mass is demonstrated on imaging, normal or anomalous bony structures, benign bone pathology, or soft tissue calcifications can be the underlying cause. However, this often may not be appreciated by the reporting radiologist, who may overlook them by concentrating just on soft tissue structures, or dismiss them as irrelevant and not comment on them. We will illustrate a variety of bony pseudomasses and calcific structures in the neck, including cervical ribs, mastoid/C1 pseudoarticulation, prominent cervical osteophytes, transverse

processes, osteitis clavicle, osteochondroma and calcified stylohyoid process; and describe the various symptoms or signs that may be associated with them.

TAKE HOME POINTS:

1. Be aware of the spectrum of normal, anomalous or benign bony or calcific structures and the symptoms they may cause.
2. Always interrogate all available CT images on bone window settings regardless of clinical indications.
3. Know the value of ultrasound in further evaluation.

P18 Human papillomavirus (HPV) and head and neck carcinomas: pictorial essay and literature review

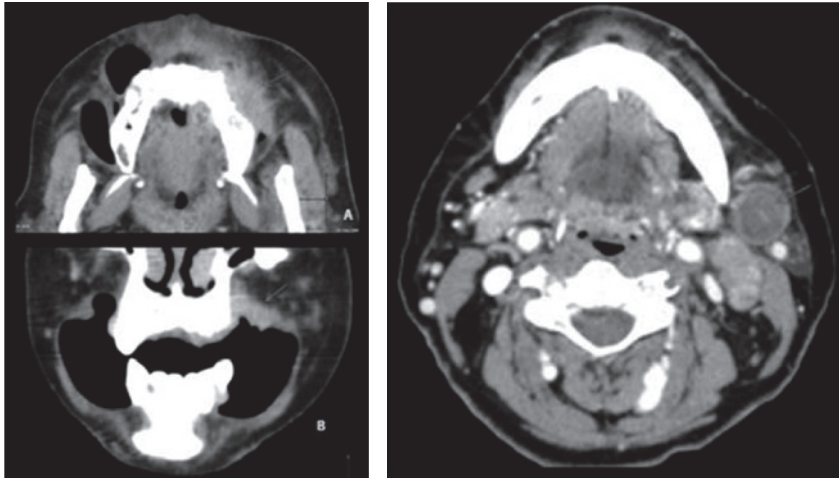
Regina Gomes (educational poster)

nRad – HCFMUSP, Departamento de Radiologia da Faculdade de Medicina da Universidade de São Paulo, São Paulo, Brazil

Co-Authors: Sarpi M, Gebrim E, Martins E, Murakoshi R, Hirata F

SUMMARY: It is well established that the most important risk factors for head and neck cancer are tobacco and alcohol use, and squamous cell carcinoma represents the predominant lesion in frequency. It is the 5th leading cause of cancer by incidence and the 6th leading cause of cancer mortality in the world. The incidence of head and neck squamous cell carcinoma (HNSCC) has been gradually increasing in the world, and in the USA it has reached a plateau despite CDC data regarding smoking and tobacco use that shows slight decline of this practice. Recently a viral etiology has been attributed to a subset

of head and neck cancers HPV infection that is likely to be sexually acquired. It may be asymptomatic or related to laryngeal papillomatosis, usually correlated with subtypes 6 and 11. Several publications studying HPV DNA detection in HNSCC has shown significant association between these conditions. Results from a systematic meta-analysis conducted by Kreimer et al. in 2005 demonstrated a HPV prevalence of 35.6% in oropharyngeal cancers, 23.5% in oral cancers and 24.0% in laryngeal cancer (among 5046 cases of squamous cell cancers). The dominant subtype is HPV 16 present in 86.7%



of oropharyngeal lesions, followed in prevalence by HPV 18. The association HNSCC HPV usually occurs in younger patients. Accumulating evidence suggests it is an important prognostic factor patients with HPV positive tumors seems to have better response rates after induction chemotherapy and after chemoradiation treatment compared to patients with HPV negative tumors, and it is possibly related to improved survival rates and decreased risk of progression. Several treatment options are being developed. Approximately 30 to 40% of patients present with early stage disease. It is important for the radiologist to acknowledge the oral cavity, pharynx and larynx anatomy, as well as the most common routes of spread, providing adequate classification regarding tumor extension and lymphnode spread. Lesions most commonly occur in the tonsils and tongue. Imaging features of the primary tumor are nonspecific, but

the presence of cystic cervical nodal metastasis represents a specific finding in this clinical context. Cases selected from our digital archive will exemplify these imaging findings. Based on a recent literature review this pictorial essay will enrich radiologists knowledge regarding head and neck squamous cell carcinomas associated with HPV infection.

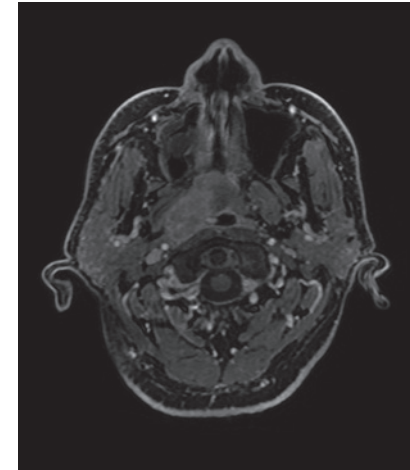
TAKE HOME POINTS: Acknowledge the importance and epidemiological data on HNSCC and its recent association with HPV oral infection. Recognize the presence of cystic metastasis as a specific imaging feature in this clinical context. To review anatomy and most common routes of spread for these tumors by selected cases, emphasizing the radiologist role in providing accurate information for adequate staging of the patients.

P19 IgG4-related disease presenting as head and neck lesions: pictorial essay and literature review.

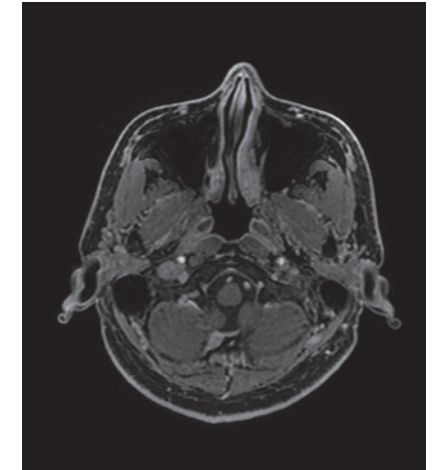
Eloisa Gebrim (educational poster)

nRad – HCFMUSP, Departamento de Radiologia da Faculdade de Medicina da Universidade de São Paulo, São Paulo, Brazil

Co-Authors: Sarpi M, Gomes R, Murakoshi R, Cevasco F, Daniel M



SUMMARY: IgG4-related disease has been recently recognized as an inflammatory and systemic condition. It is characterized by pseudotumoral lesions, particular histopathological findings and, often but not always, elevated serum IgG4 concentrations. It was first described in patients with autoimmune pancreatitis, and recently it has been understood that manifestations in diverse organs are linked by the same histopathological characteristics and expression of IgG4 molecule. By that, previously recognized conditions including several head and neck lesions are now acknowledged as manifestations of IgG4-related disease: inflammatory pseudotumors, Küttner's tumor, Mikulicz's syndrome, Riedel's thyroiditis, among others. As some patients have disease confined to a single organ for many years, usually expressed as a tumefactive lesion, it is important to recognize this condition in the differential diagnosis for head and neck tumors. Usually imaging features are nonspecific and do not permit distinction between IgG4-related disease and cancer. However, when clinical and histopathological data directs the diagnosis to an inflammatory pseudotumor and IgG4-related disease is considered or confirmed, imaging follow up demonstrates the response to clinical treatment with glucocorticoids with a significant reduction in



tumor volume. Cases selected from our Imaging Center digital archive will exemplify the variety of manifestations in different head and neck structures, and demonstrate clinical response by imaging follow up in some of them. Based on a recent literature review this pictorial essay will enrich radiologists knowledge regarding this newly recognized clinical condition, aggregating this differential diagnosis in interpretation of head and neck tumors, contributing to adequate clinical management of the patients.

TAKE HOME POINTS: Recent literature review about IgG4-related disease, emphasizing head and neck manifestations. Selected cases highlighting and exemplifying possible imaging features and follow up findings. To enrich radiologists knowledge regarding this newly recognized clinical condition. To aggregate this differential diagnosis in interpretation of head and neck tumors, leading to adequate clinical management of the patients.

P20 Diagnostic adequacy of ultrasound guided fine needle aspiration cytology in the investigation of neck lumps: a comparative audit of three institutions between 03/2007– 03/2008 and 03/2011– 03/2012

Yvette Adjei-Gyamfi (educational poster)

University College Hospital, Radiology,
London, United Kingdom

SUMMARY: Ultrasound-guided fine needle aspiration (FNA) forms the basis of the primary investigation of head and neck lumps, most commonly of the thyroid, salivary glands or lymph nodes and has a sensitivity of 80 – 98% making it the initial imaging modality of choice. A major factor in achieving good results is the interpretation, communication and reporting of the cytological findings.

The guidelines of the Papanicolaou Society of Cytopathology for the FNA procedure recommend that the cytologist interpreting the FNA should have a sound knowledge of surgical pathology and demonstrable competence in cytopathology, whilst aspirators who persistently produce a high rate of inadequate aspirates (>15%) should be identified and given remedial training, thus deeming an adequate aspirate rate of ≥85% as standard.

This retrospective audit was based on the results of FNAs performed by one head and neck radiologist at three London hospitals (A, B and C) from March 2011 to March 2012 under ultrasound guidance using identical technique. The cases were classified by patient demographics, FNA site, and the conclusion of the cytological report (Inadequate/Benign/Suspicious/Malignant/Inflammatory).

The results were compared with an identical audit performed by the same radiologist between March 2007 and March 2008.

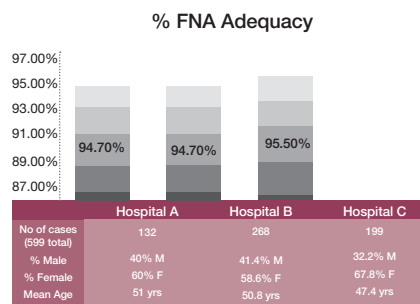


Figure 1a: Table & chart demonstrating similar comparative adequacy rates at hospitals A-C from March 2011 to March 2012.

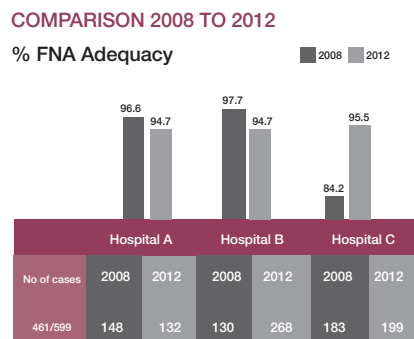


Figure 1b: Table & chart demonstrating comparative adequacy rates at hospitals A-C March 2007 to March 2008 and March 2011 to March 2012.

Between March 2007 and March 2008 the adequacy rate of FNA specimens obtained at one hospital (C) was 84.2% and significantly lower than results from the other two despite identical technique, US machine, operator and a similar case mix. During this period however the specimens at hospital C were randomly assigned to one of six general cytologists. Conversely, specimens were interpreted by only two specialist head & neck cytologists at hospital A and three specialist head & neck and one general cytologist at hospital B.

Based on these findings, the cytology services were reorganised at hospital C. Two cytologists with an interest in head & neck (and only 2 general cytologists) were assigned to analyse the head and neck specimens.

The current audit highlights a significant increase in the adequacy rates at hospital C to 95.5% following implementation of these changes.

TAKE-HOME-POINTS: We demonstrate in this retrospective audit the importance of the radiologists and cytologists working together as a team, with regular review of inadequate specimens and cytological techniques. The specimens should be reported by cytologists with subspeciality interest in head and neck pathology in order to improve adequacy rates. Regular audit will ensure maintenance of a good standard of practice.

P21 Thyroiditis and its appearances on US and Nuclear imaging

John-Luke Cook (educational poster)

Great Western Hospital, Radiology,
Swindon / Wiltshire, United Kingdom

Co-Authors: Lyen S

SUMMARY: Thyroiditis is a common condition, particularly in women, and its appearances on Ultrasound are specific with few mimics. The condition affects all ages and both sexes and diagnosis by Ultrasound is possible before clinical presentation, with considerable benefit for the patient, by raising the possibility of hyper or hypo thyroidism. The ultrasound appearances can be misinterpreted or ignored if not recognized. These ultrasound findings will be described and illustrated. All cases presented have been confirmed by histology.

TAKE HOME POINTS: Consider the possibility of thyroiditis when performing ultrasound of the neck or thyroid. Acquaint yourself with its appearances and mimics. Do not misinterpret or ignore the findings.

P22 Expected CT and MRI findings after laryngectomy – pictorial essay and literature review

Eloisa Gebrim (educational poster)

InRad - HCFMUSP, Departamento de Radiologia da Faculdade de Medicina da Universidade de São Paulo, São Paulo, Brazil

Co-Authors: Sarpi M, Garcia M, Gomes R, Cevasco F, Rodrigues F, Zuppani H

SUMMARY: The current treatment for laryngeal carcinoma includes surgery, radiation therapy, chemotherapy or a combination of various modalities. Both radiation therapy and surgery alter the normal anatomic structures thereby making interpretation of post treatment imaging challenging. Several surgical techniques have been developed to treat laryngeal carcinoma, aiming to remove even advanced carcinomas and, at the same time, to preserve physiological functions (respiratory, phonatory, sphincteric) whenever possible. These techniques can be basically described as partial laryngectomy (conservative) or total laryngectomy (radical). Examples of conservative excision are cordectomy, vertical partial laryngectomy, horizontal supraglottic laryngectomy, supracricoid laryngectomy with cricohyoidopexy or cricohyoidoepiglottopexy and near total laryngectomy. The decision about which surgery should be performed depends on the location and extent of the tumor, institutional experience and the patient's preferences. Applications of imaging follow up include characterization of postoperative changes, and surveillance to complications and recurrence of the disease. Although MRI may be used, CT is the preferred modality for these evaluations. Post-surgical follow up with CT or MRI gain its great importance when a recurrent tumor is suspected, to confirm the presence of the lesion and to determine its extent; this is important information to determine the possibility of salvage therapy. Familiarization with the expected imaging changes following surgical treatment allows proper evaluation of imaging studies and

can prevent misinterpretation of post surgical changes as recurrent disease. To achieve an accurate interpretation, radiologists must know surgical techniques and understand how they affect imaging results. Cases selected from our digital archive exemplify the variety of possible findings, highlighting and consolidating the radiologist role in proper interpretation leading to adequate clinical management of the patients.

TAKE HOME POINTS: To describe surgical techniques used for the treatment of laryngeal cancer. To recognize anatomic changes associated with each type of laryngeal surgery. To differentiate anatomic changes from persistent or recurrent disease in the postsurgical follow up with MRI and CT scan. Highlighting and consolidating the radiologist role in proper interpretation of the imaging findings, leading to adequate clinical management of the patients.

SCIENTIFIC POSTER STUDIES

P23 Skull base osteomyelitis mimicking nasopharyngeal carcinoma: imaging features at initial presentation

Julian Goh (Study)

Tan Tock Seng Hospital, Diagnostic Radiology, Singapore, Singapore

Co-Authors: Loke S, Karandikar A, Ho C, Lim W, Lim T

OBJECTIVES: Skull base osteomyelitis (SBOM), a late complication of malignant otitis externa (MOE), involves both the skull base and adjacent soft tissue spaces. The diffuse skull base and soft tissue involvement may be mistaken at initial imaging for nasopharyngeal carcinoma (NPC). We attempt to identify imaging features which may differentiate between these two conditions.

MATERIALS AND METHODS: Patients with SBOM as a complication of MOE seen at imaging were identified in a retrospective review of CT and/or MRI examinations from 2009 to 2012. Features suggesting these conditions were documented, including a) lack of a nasopharyngeal mass; b) direct involvement of lateral structures e.g. parotid

gland, TMJ; c) abscess formation; d) soft tissue enhancement without architectural distortion. was made, where available.

RESULTS: 19 patients were identified. 18 MR and 16 CT examinations were performed. All showed relative architectural preservation and lack of a nasopharyngeal mass. 17 patients showed lateral structure involvement, while abscesses were seen in 11. The most common causative organism was *Pseudomonas aeruginosa*.

CONCLUSIONS: Although SBOM and MOE may mimic NPC at initial presentation, careful image evaluation and clinical correlation should alert the reader to this inflammatory condition.

P24 Comparison of cone beam and multi-detector computed tomography in the visualisation of PORPs and TORPs - a cadaveric study

Thi Dao Nguyen (Study)

Universitätsklinikum Halle (Saale), Universitätsklinik und Poliklinik für Diagnostische Radiologie, Halle (Saale), Germany

Co-Authors: Mlynski R, Plontke S, Kösling S

OBJECTIVES: With further development middle ear prostheses become smaller and more subtle resulting in a poorer recognisability on imaging compared to previously used prostheses. The purpose for this study was to assess the ac-

curacy and reliability of Cone Beam CT (CBCT) compared with Multi-Detector CT (MDCT) in visualizing the correct position and displacement of new subtle middle ear prostheses.

MATERIALS AND METHODS: Several partial and total ossicular replacement prostheses (PORPs and TORPs) were implanted in formalin fixed human heads, partly in correct position, partly with displacement. Each intended position was photo-documented and imaged using MDCT and CBCT. Afterwards the specimen underwent surgical evaluation to ensure the maintained position. The images were stored anonymously on a workstation and evaluated by a radiologist specialized in head and neck radiology.

RESULTS: Both methods, CBCT and MDCT, enable precise visualization of middle ear anatomy and structures as well as the ossicular replacement prostheses. Although MDCT was affected

by more metallic artefacts than CBCT, displacement could be clearly detected in both methods. Although CBCT showed lesser metal artefacts and a better spatial resolution, the exact type of the prosthesis could not always be differentiated in either of the two techniques due to their similarity in form and size.

CONCLUSIONS: MDCT and CBCT are comparable in detecting correctly positioned or displaced newer subtle PORPs and TORPs. CBCT has advantages due to lower radiation dose, lower metal artefacts and better spatial resolution. Both methods have limits in their ability to discriminate similar types of prostheses.

P25 Radiologic assessment of temporomandibular joint in patients with malocclusion

Nataliya Perova (Study)

Clinic of Moscow State University of Medicine and Dentistry, Depart of Radiology, Moscow, Russia

OBJECTIVES: To investigate the possibilities of radiological methods in patients with TMJ disorders.

MATERIALS AND METHODS: A total of 100 patients with an average age of 37 years (range 20-55 years), with signs and symptoms of temporomandibular joint dysfunction were referred for imaging in the diagnostic radiology department. These patients were evaluated by transcranial view radiography, TMJ tomography, cone-beam computer tomography (CBCT), multislice computer tomography (MSCT), magnetic resonance (MR).

RESULTS: The majority of patients have malocclusion combined with TMJ disorders. In some cases dysfunctions were detected during and after orthodontic and prosthodontic treatment.

These patients should be taken the high informative radiological methods as CBCT, MSCT and MR. The advantages of these methods are the wide range of diagnostic possibilities, they support to show an early signs of bone pathology in both joints, both internal derangements and degenerative joint diseases, measure the disc displacement, muscles, ligaments and functional disorders. CBCT, MSCT, MR should be included in diagnosis before the orthodontic planning for primary examination of TMJ function, bone and disc structure. Transcranial view radiography and TMJ tomography yield to CBCT, MSCT, MR in diagnostic efficiency.

CONCLUSIONS: CBCT, MSCT and MR imaging ideally complement each other for the thorough examination of the structure of TMJ and replaced conventional techniques in diagnosing TMJ pain syndrome.

P26 The role of imaging techniques for diagnosis and monitoring of response to therapy of Primary Lymphoma of the orbit

Urszula Grzesiakowska (Study)

Maria Skłodowska-Curie Memorial Oncology Center of Warsaw, Department of Radiology and Diagnostic imaging, Warsaw, Poland

Co-Authors: Jezierski A, Olszewski M, Dziuk E, Wysocka PC

OBJECTIVES: The aim of the study is to describe the clinical symptoms and radiological signs of Primary Lymphoma of the orbit, as well as defining the role of imaging techniques and monitoring therapy in these cases.

MATERIALS AND METHODS: In our study 15 cases of Primary Lymphoma of the orbit were diagnosed by CT or/and MR imaging before treatment and follow-up by these methods after the therapy.

RESULTS: 14/15 cases the Lymphoma infiltration were localized in one orbit. Only one patient had both orbits involved. There was 12/15 cases with extraconal localization. 3/15 cases were more advanced and had extra- and intraconal

involvement. CT exams showed similar density of the lymphoma infiltration to intraocular muscles, with enhancement after i.v contrast administration. In MRI T1 and T2 weighted sequences the lymphoma lesion was hypo- or isointense in compare to the signal intensity of the muscles. In 9/15 cases there was complete response after Radiotherapy, 6/15 showed partial response with residual masses after the treatment.

CONCLUSIONS:

1. Both-CT and MRI are equal in the diagnosis and post-therapy evaluation of Primary Lymphoma of the orbit.
2. The clinical symptoms and radiological features are suggestive for Malignant Lymphoma, however histological confirmation is necessary.

P27 Quality comparison of digital x-ray devices with 3D-visualization capability in imaging of paranasal sinuses and temporal bone

Manfred Knörger (Study)

Martin-Luther-Universität Halle-Wittenberg, Universitätsklinikum, Klinik und Poliklinik für Diagnostische Radiologie, Halle, Germany

Co-Authors: Brandt S, Kösling S

OBJECTIVES: Currently, different digital x-ray devices are used for imaging of paranasal sinuses (PNS) and temporal bone (TB): Multi-Detector CT, Cone Beam CT (CBCT) and for special TB indications also Digital Angiography (DSA) with the capability to provide cross-sectional images. All these devices are available at our department. We compared the dosage and spatial resolution between the three on-site devices to substantiate the choice of device in imaging of PNS and TB.

MATERIALS AND METHODS: All measurements were performed with device-typical protocols for PNS and TB imaging. Alderson head phantom was used for measuring the radiation exposure of the x-ray devices with regard to the standard protocol and a dose-reduced one. Thereby chipstrate dosimeters were used in the regions of the eyes and thyroid gland to obtain organ doses. In a second step the dose index was measured with a puncture measuring chamber

on a CTDI head phantom as well. Additionally, images of a self-made phantom were used to assess high-contrast resolution. Finally, a qualitative analysis of the visibility of small high contrast structures are done by six observers.

RESULTS: The three devices showed markedly variations in the dosage and spatial resolution depending on the protocol and/or modus. In

both points, CBCT was superior to MDCT and DSA using standard protocols whereby the difference was less obvious for the investigation of PNS.

CONCLUSIONS: For high-contrast investigations CBCT is a remarkable option in head and neck radiology.

P28 The radiology of mechanical combined injuries of facial skull and orbit structures

Dimitriy Lezhnev (Study)

Clinic of Moscow State University of Medicine and Dentistry, Depart of Radiology, Moscow, Russia

Co-Authors: Sangaeva L, Kostenko D

OBJECTIVES: The radiology of mechanical combined injuries of facial skull and orbit structures

MATERIALS AND METHODS: Examination data analysis of 70 patients with combined injuries of facial skull and orbit structures established the MSCT's highest diagnostic efficiency in comparison with other radiology methods of radiology. Results: At the stage of radiological examination 70 victims were underwent radiography of skull, multi-slice computed tomography (MSCT), ultrasound (US) of orbits and eyes. The distribution to etiology: traffic collision – 35 accidents (50,0%), mine-explosive wounds - 20 (28,6%), street trauma – 9 (12,9%), day-to-day-life trauma – 6 (8,5 %). Middle age of patients was 34,6 years.

In addition MSCT permitted to radiography to identify: maxillary fracture – 17 victims (23,8%), injuries of medial wall of the orbit – 6 patients (8,4%). Hemosinus was found in 42 cases (58,8%), foreign bodies in 40 cases (56,0%). Besides the method let to expose concomitant changes in brain matter.

The injuries of orbit's structures were made apparent at 59 patients (82,6%): injuries of vitreous humour (hemophtalmia, scares changes) in 49 cases (68,6%), injuries and lens displacement – 4 (5,6 %), injuries of extraocular muscles – 2 (2,8%), posttraumatical changes of optic nerve – 4 (5,6%).

Ultrasound was used for visualization orbit's foreign bodies – 14 patients (19,6%) and retinal detachment in 4 cases (5,6%). Moreover ultrasound was used for dynamics value of hemosinus and for means of control in retinal detachment treatment.

Data analysis showed that in finding traumatical changes of facial skull (tab.1) and foreign bodies (tab.2) the MSCT's diagnostic efficiency exceeded the data of radiology and the data of ultrasound in all parameters.

TAB.1 Comparative informtiveness of radiological methods in detection of traumatical changes of facial skull

Statistic parameters	Radiological methods	
	Radiography (%)	MSCT (%)
Sensitivity (Se)	80,3	93,2
Specificity (Sp)	83,8	96,0
Accuracy (Ac)	85,0	94,6
PVP	89,6	96,0
PVN	81,0	93,3

TAB.2 Comparative informtiveness of radiological methods in detection of foreign bodies

Statistic parameters	Radiological methods		
	Rg (%)	MSCT (%)	US (%)
Se	80,0	99,5	55,0
Sp	95,7	98,6	57,8
Ac	84,3	99,2	68,0
PVP	97,9	98,4	84,6
PVN	64,7	99,5	57,8

CONCLUSIONS: In diagnosis of combined injuries of facial skull and orbit structures the method of choice is MSCT in connection with the best parameters of diagnostical efficiency. Ultrasound examination is necessary used at the patients

with plural trauma of maxillo-facial region and orbit structures with the aim at detection of retinal detachment, hemophtalmia and prevention of development of severe complications connected with these injuries.

P29 The application of phase AIF for pharmacokinetic analyses in the maxillofacial region.

Toru Chikui (Study)

Kyushu University, Department of Oral and Maxillofacial Radiology, Fukuoka Prefecture, Japan

Co-Authors: Kitamoto E, Koga Sh, Simonetti A, Obara M, Yoshiura T, Yoshiura K

OBJECTIVES: The individual arterial input function (AIF) is preferable for accurate pharmacokinetic analyses, even if the estimation of the individual AIF in the neck is challenging. The purpose of

this study is to apply phase information when estimating the AIF for pharmacokinetic analysis.

MATERIALS AND METHODS:Thirteen patients underwent dynamic DCE-MRI. The scan included 3D-T1 FFE sequences with a temporal resolution of 3.5 s. Both magnitude and phase-shift images were reconstructed. the concentration

of contrast medium (CM) in tissue (Ct (t)) was estimated using the magnitude image. The phase image was used to estimate the concentration of CM in artery (Ca (t)).

The average $\Delta\phi$ was converted to Ca(t) using the equation:

$$\Delta\phi = TE \cdot \pi \cdot \gamma \cdot B_0 \cdot \chi m \cdot \Delta Ca \cdot (\cos^2\theta - 1/3)$$

where γ is the proton gyromagnetic ratio, B_0 is the magnitude of the main magnetic field in Tesla, χm is the molar susceptibility of the CM, and θ is the angle of the vessel relative to the main magnetic field. The concentration of CM in plasma (Cp (t)) was defined as; Cp (t) = Ca / (1-Hematocrit).

A single observer, aware of the primary tumor site, placed a ROI on the ipsilateral ICA for the estimation of the AIF. Next, the observer placed it on the contralateral ICA. The peak concentration (Ca_{peak}), the average of the concentration (Ca_{avg}), and the concentration during last 30 phases (Ca_{last 30}) were compared between the ipsilateral and contralateral ICA.

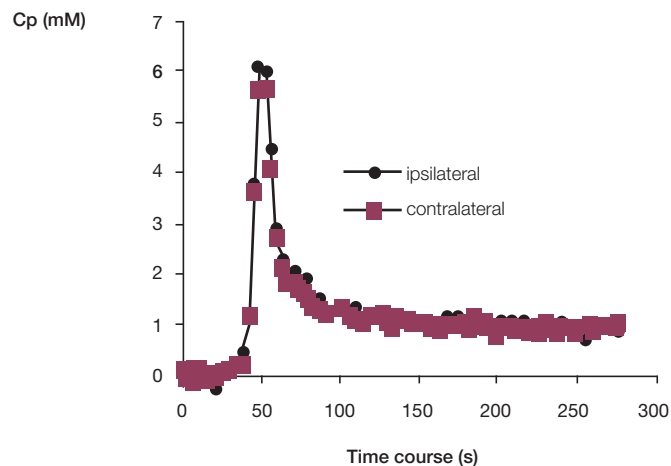
Secondly, the analysis described in the following equation:

$$C_t(t) = K^{trans} \int_0^t C_p(t') \exp \{-K^{trans}(t-t')/v_e\} dt' + v_p C_p(t)$$

was applied to each voxel, where K^{trans} is influx forward volume transfer constant, v_e is fractional volume of EES and v_p is the fractional volume of plasma. Quantitative measurements derived

from the ipsilateral ICA reference curves were compared with similar measurements derived from a contralateral reference.

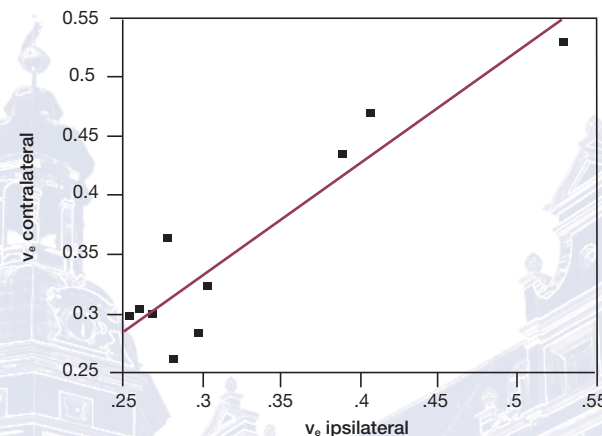
RESULTS: The AIF could be estimated on both sides in 11 out of 13 patients.



The AIF could not be obtained in one patient due to severe body motion. The contralateral AIF was observed to fluctuate in another patient during the equilibrium phase.

Ca_{avg}, (Ca_{last30}, slope=0.97, r=0.49), which may have been affected by the body motion and the lower SN ratio. None of the pharmacokinetic parameters were significantly different, whether the AIF ROI was on the ipsilateral ICA or the contralateral ICA. There was a high correlation in all parameters (K^{trans} , slope=0.94, r=0.79; v_e , slope=0.96, r=0.86; and v_p , slope=0.90, r=0.70).

There was a high correlation between the ipsilateral ICA and the contralateral ICA in both the Ca_{peak} and Ca_{avg} (Ca_{peak}, slope=0.95, r=0.79; and Ca_{avg}, slope=0.97, r=0.65). The Ca_{last 30} had a somewhat lower correlation than either Ca_{peak} or



CONCLUSION: The phase images were thus found to be potentially useful for estimating the AIF and making accurate pharmacokinetic analyses in the maxillofacial region.

P30 The application of a pharmacokinetic analysis to maxillofacial tumors

Erina Kitamoto (Study)

Kyushu University, Department of Oral and Maxillofacial Radiology, Fukuoka Prefecture, Japan

Co-Authors: Chikui T, Kawano Sh, Sugiura T, Obara M, Yoshiura T, Yoshiura K

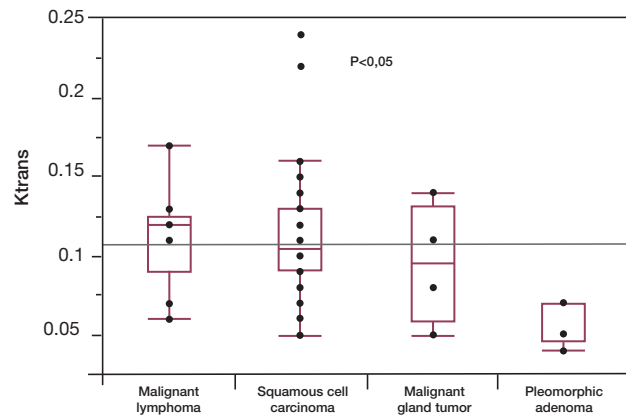
OBJECTIVES: This study was designed to elucidate the characteristics of a primary tumor in the maxillofacial region using pharmacokinetic analyses based on the TK model.

MATERIALS AND METHODS: Dynamic contrast enhanced MRI (DCE-MRI) was performed for 54 patients (35 squamous cell carcinoma, 10 malignant lymphoma, 4 malignant gland tumor,

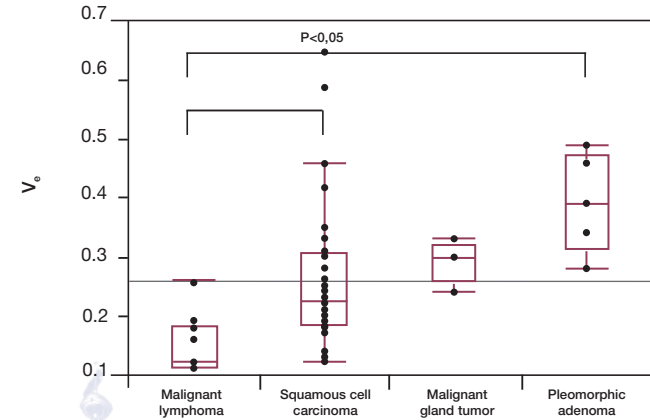
5 pleomorphic adenoma). The location of the tumor included the tongue (n=37), oral floor (n=2), maxilla (n=3), submandibular region (n=6), and others (n=6). The axial DCE scan consisted of a 10 slice, 3D-T₁ fast-field echo sequence. A T₁₀ map was estimated by the dual flip angle method (5° and 15°) and the signal intensity of tissue was converted into the concentration of the contrast medium in tissue. The area under the gadolinium concentration curve (AUGC) was calculated after injection. The data were analyzed using a TK model. The influx forward volume transfer constant into EES from plasma (K_{trans}), fractional volume of the extravascular extracellular space (v_e), and fractional volume of the plasma (v_p) were estimated. This study used a predefined model arterial input function.

The MR image data (Philips PAR/REC format) were transferred to a personal computer from the MRI operating console and processed using a proprietary software program (PRIDE software, Philips Healthcare, Eindhoven, The Netherlands) using the RSI interface data language (IDL). Tukey's HSD test was used to compare the parameters among the four categories.

RESULTS: ML had the lowest AUGC among the four categories and there was a significant difference between ML and SCC (P<0.05). The malignant tumors had a higher K_{trans} than the pleomorphic adenoma, which might reflect the fact that the angiogenesis factors from the malignant tumor caused the higher permeability.



ML had the lowest v_e among the four categories and there was a significant difference between ML and any of the three other categories (P<0.05). The rapid uptake with high washout in time-intensity curve (TIC), commonly shown in ML, was thought to result from the marked low ratio of the EES (v_e).



Both malignant gland tumors and pleomorphic adenoma had a higher v_e, although no significant differences were observed from either ML or SCC. The slow gradual uptake in TIC, which is commonly observed in pleomorphic adenoma, may thus have resulted from the lower permeability and larger interstitium (v_e).

CONCLUSIONS: Both the low v_e in ML and the low K_{trans} in pleomorphic adenoma are characteristic parameters, which could thus represent the nature of the tumors. A pharmacokinetic analysis is therefore considered to be potentially useful for making a differential diagnosis in the maxillofacial region. pictures

P31 Osteomyelitis in the maxillofacial region in case of immunodeficiency state

Irina Zorina (Study)

Moscow State University of Medicine and Dentistry, Radiology Department, Moscow, Russia

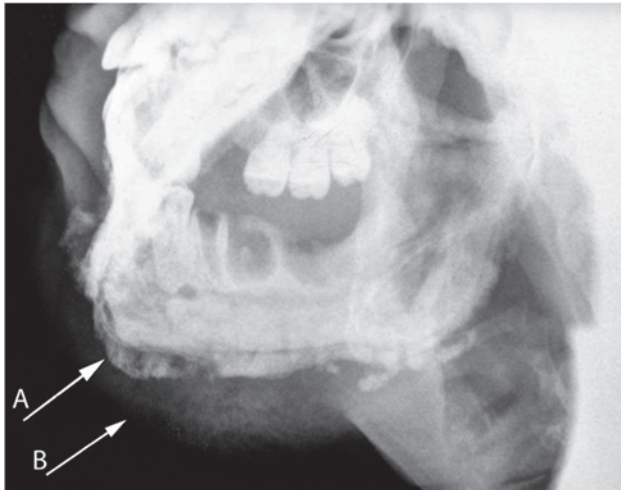
Co-Authors: Egorova E

OBJECTIVES: This was to define semiotics of osteomyelitis (OM) in maxillofacial region (MFR) in case of secondary immunodeficiency.

was made as well as the radiological study of the segment concerned.

MATERIALS AND METHODS: 63 patients aged 19–68 with OM in MFR caused as complication after fractures (68,4%), surgery (9,3%) and others (22,3%) were under study. To research the etiology of the destructive changes in the bones the analysis of general and local status

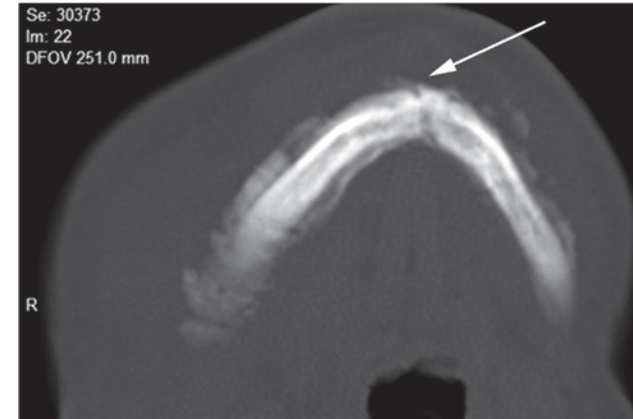
Multislice computer tomography was used to define the character of tissue changes and to access anatomical complicated regions. Blood analysis, immunograms and bacteriologic analysis of the wound tissues were made on the semiautomatic and automatic analyzers.



Pic.1. Lateral target X-ray image of the mandible of the patient Z. 28 years old (opiate addiction - 5 year) made 6 months later after the extraction of 4.5 – 4.7 teeth: A – bone destruction, periostitis; B – edema and infiltration of soft tissues.

RESULTS: Posttraumatic OM of MFR was of typical nature. According to the radiological data no structural bone changes were found out in the acute phase. This phase was characterized by clear clinical manifestations and it was easy enough to make a diagnosis. The effectiveness of radiological methods grew into subacute and chronic phase of OM. A number of factors contributed to the development of atypical forms of OM in 28,8 % of patients: chemical and radiological therapy (in the course of treatment of the tongue and oral cavity), chronic intoxication, alcoholism and drug addiction which lead to immunodeficiency. The pus-necrotic process of these patients localized in the mandible. Inflammation was spread and characterized by fistulas and soft tissue formation. Bone formation prevailed over osteolysis, the jaw looked sclerosed with manifested periosteal thickening.

Differential diagnosis of OM in case of secondary immunodeficiency was carried out on the malignant bone tissues, metastasis and dystrophic changes, and in case after thermal damages. Round cell sarcoma (Ewing) and reticular sarcoma had remission and exacerbation periods, the last one was accompanied by inflammation. Small-focal destruction and periosteal thickening were radiologically defined. Only cytological analysis allowed us to differ round cell sarcoma (Ewing) and reticular sarcoma from OM. Neurotrophic processes in the postponed period after thermic damages (usually in 6–12 months) were manifested in the form of mixed changes of the bone: osteoporosis, osteolysis and osteonecrosis. Necrotic tissue was gradually resorbed and sequestered, there were pathological fractures and fistulas. Clinical radiological picture reminded us of that of OM. The differential diagnosis was carried out on the basis of medical history and laboratory data (with no sign of pus inflammation).



Pic.2. Computer tomogram (the same patient): destructive changes and pathological fracture (arrow) of the mandible, periosteal thickening.

CONCLUSIONS: In immunodeficiency states OM resulted from somatic diseases, chronic intoxication and etc., is atypical. Its differential diagnosis with bone destructive processes resulted from tumor processes, neurotrophic

processes in a number of cases is very complicated and should be based on the results of complex clinical radiological, laboratory and cytological analyses.

P32 Position of the impacted third molar in relation to the mandibular canal – CBCT patterns
Antonio Lo Casto (Study)

DIBIMEF, Università degli Studi di Palermo, Sezione di Scienze radiologiche, Palermo, Italy

Co-Authors: Barreca F, Galbo L, Geraci C, Giordano G, La Tona G

OBJECTIVES: Damage to the inferior alveolar nerve is a serious complication following third molar removal. The overall risk of temporary inferior alveolar nerve injury associated with third molar removal ranges from 0.4-6%, while the risk of permanent injury is less than 1%. The position of the impacted third molar in relation to the mandibular canal is the most important risk factor in the occurrence of inferior alveolar nerve exposure during tooth removal. Thus it is important to assess the position and establish the exact relationship between the impacted third

molar and the mandibular canal preoperatively to reduce the risk of nerve injury. Panoramic radiography is usually the first diagnostic tool to be used for this purpose, however when a close relationship is evidenced, CBCT is a more accurate imaging technique due to 3D acquisition of data for determining the exact relationship between the impacted third molar and the mandibular canal. A description of the different patterns of this relationship for educational purpose is reported.

MATERIALS AND METHODS: Different patterns of the relationship between impacted third molar and the mandibular canal include lingual, buccal, interradiolar or inferior position of the mandibular canal and for each of the mentioned positions interposition of bone or not between the molar root and mandibular canal.

RESULTS: CBCT images provide a reliable depiction of the bucco-lingual relationship between the impacted third molar roots and the mandibular canal. Knowledge of the different CBCT patterns of relationship between an impacted third molar and the mandibular canal is important to be precisely assessed and reported, in order to prevent inferior alveolar nerve damage suggesting the safest surgical approach for tooth removal and for medicolegal purposes.

P33 The comparison of radiological methods in the diagnostics of the radiation osteonecrosis in skull and cervical spine.

Yulia Kurlaeva (Study)

Clinic of Moscow State University of Medicine and Dentistry, Radiology Department, Moscow, Russia

Co-Authors: Zorina I, Egorova E

OBJECTIVES: Assessment of radiological methods in the diagnostics and dynamic control of treatment of the radiation osteonecrosis in skull and cervical spine.

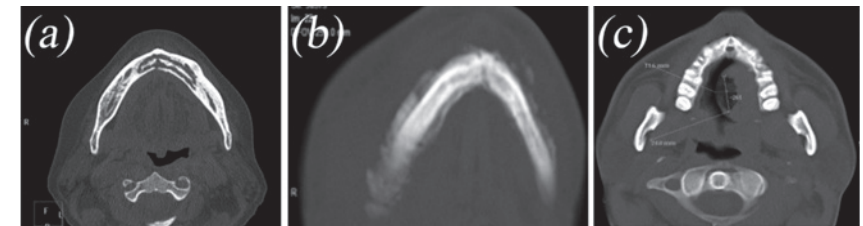
MATERIALS AND METHODS: 34 patients (45–82 years) with the radiation osteonecrosis in skull and cervical spine with radiotherapy of this area in the past history (time-integrated local radiation dosage varies from 60 to 91 mSv) were examined. Orthopantomography (OPG) was applied for all patients, cone beam computed tomography (CBCT) in 70% cases, multispiral computed tomography (MSCT) in 30%, and high resolution ultrasound (US) in 25% cases.

RESULTS: At the first stage of diagnostics OPG was carried out for all patients. This allowed to estimate the prevalence of lesions, topographic anatomical relationships, structural changes in the surrounding bone, the presence and absence of periosteal reaction. In addition it helped to identify possible complications: pathologic fractures and subluxations. In com-

plex diagnostic situations the CBCT, MSCT, and high resolution US were applied to clarify the type of changes. The CBCT identified and characterized small pathologic lesions up to 3 mm in size. The additional advantages it provided were: a) the lack of spatial distortion of images, b) no artifacts from metal structures and filling materials, c) summation effect, d) high reliability assessment of structural changes in bone tissue, e) low radiation exposure of the patient, and f) that the studies were conducted in a comfortable sitting position for a patient. In 11% of CBCT cases the MSCT and high resolution US studies were conducted to clarify pathological changes. The MSCT determined the localization and the dimension of lesions of bones and surrounding soft tissues. The high resolution US method used for reliable visualization of changes in the periosteum and determined the areas of inflammation, scarring, and destructive changes in soft tissue structures which are necessary for evaluation of vascularity of the affected segment of the zone and surrounding tissues.

CONCLUSIONS: The examination of patients has to be complex at all stages. High-tech methods, such as CBCT, should be used first for diagnostics of radiation osteonecrosis. In difficult patho-

logical cases it is necessary to include additional methods, for example, applying MSCT for assessment of bone changes and high resolution US for imaging of soft tissues.



P34 Imaging features of extranodal lymphoma originating in the head and neck

Laurene Avril (Study)

Geneva University Hospital, Radiology, Geneva, Switzerland

Co-Authors: Kohler R, Patsoura S, Masterson K, Rager O, Greloz V, Becker M

OBJECTIVES: Extranodal manifestations of primary head and neck lymphoma (HNL) are rare. Although the definitive diagnosis is made histologically, imaging may help distinguish extranodal HNL from other tumors, especially when biopsy is inconclusive. This educational poster reviews the CT and MRI findings of extranodal HNL with special emphasis on patterns of spread, differential diagnosis and correlation with histology.

MATERIALS AND METHODS: Retrospective analysis of CT, MRI and clinical/surgical data of 54 consecutive patients with extranodal HNL imaged at our institution since 2002. Imaging characteristics (involved sites, appearance on CT and MRI, contrast enhancement, perineural, perivascular and meningeal spread and bony involvement) were analyzed and correlated with clinical symptoms, histology and patient outcome.

RESULTS: Most patients were middle aged or older individuals (mean age 62 years). Characteristic extranodal manifestation sites (n=67) included: pharynx (n=21), orbits (n=12), skin and soft parts (n=9), salivary glands (n=7), sinonasal cavity (n=6), thyroid gland (n=4), mandible (n=3), nerves including brachial plexus (n=3) and skull base (n=2). MRI showed bulky, hypointense masses on T2-weighted sequences, very low ADC values and homogenous enhancement. CT showed hypodense, homogenous masses with minor enhancement. Diffuse bone marrow involvement was seen more often on MRI than on CT. Perineural and perivascular spread was seen in HNL originating close to the skull base.

CONCLUSIONS: Although imaging cannot replace histology, knowledge of the typical manifestations and characteristic imaging features of extranodal HNL is essential for the correct diagnosis, depiction of extent, planning of biopsy, and/or therapy.

P35 Diagnosis and management of mass-like lesions of the tongue

Toshiyuki Kawazu (Study)

Kyushu University Hospital, Dept. of Oral and Maxillofacial Radiology, Fukuoka city, Japan

Co-Authors: Chikui T, Shimizu M, Okamura K, Yoshiura K

OBJECTIVES: Background: Mass-like lesions of the tongue include a variety of lesions, benign or malignant tumors, cysts, benign neoplasms and hypertrophy. In our institute, ultrasonography is the first choice of the imaging procedures for these lesions, because of its non-invasiveness and less expensiveness. After ultrasonographic examination, it is determined whether we need further diagnostic imaging, histopathological inspection or whether we can predict its prognosis. Objective: The aim of this study is to describe the spectrum of tongue masses examined by ultrasonography in our department from January 2007 to December 2011, except squamous cell carcinoma, and to describe their subsequent managements.

MATERIALS AND METHODS: Thirty cases were included in this study. All the cases underwent ultrasonography. The case clinically diagnosed as squamous cell carcinoma was excluded. Ultrasonography was performed on 12MHz(Logiq7, GE Healthcare) or 13MHz (Sequoia512, Mochida Siemens Medical Systems) linear probe. Eighteen of 30 cases underwent

histopathological inspection, and others were clinically diagnosed by long period follow-up (at least one years or more) or other image inspection (CT and/or MRI). A retrospective review was performed for all the cases.

RESULTS: Results are listed below (Table). Thirteen of 30 cases (43.3%) were hemangiomas, and others were cysts (3), Schwannomas (2), fibroma or fibrous tumors (4), granulation tissues (4), Lipoma (1) and malignant tumors (3). Subsequent management, need for further diagnostic imaging, histopathological inspection or prediction of prognosis, was determined based on the ultrasonographic findings; size, margin shape, location, presence or absence of capsule, vascularity, etc. and by the clinical symptoms.

CONCLUSIONS: Twenty-seven (90%) of 30 cases were benign lesion and 12 (44.4%) of them needed no treatment. Ultrasonography was useful to determine subsequent management as well as imaging diagnosis.

Age	Sex	Pathology	US diagnosis	Remarks
5	M		Blandin-Nuhn cyst	Cyst clinically
8	F	Schwannoma	Pyogenic granuloma	
9	F	Fibrous tumor	Fibroma, Neurofibroma	
9	F	Blandin-Nuhn cyst	Mucocele	
12	F	Cavernous hemangioma	Hemangioma	
21	M		Hemangioma	Hemangioma clinically
24	F		No mass	Granulation tissue clinically
41	M	Cavernous hemangioma	Fibroma	
44	F	Intramascular hemangioma	Hemangioma	
45	M	Leiomyosarcoma	Hemangioma	
48	F		Granulation tissue	Granulation tissue clinically
48	M		Hemangioma	Hemangioma clinically
51	F	Lymphoepithelial cyst	No mass	
55	F	Fibrous overgrowth	Granulation tissue	
55	F		Hemangioma	Hemangioma clinically
56	F	Cavernous hemangioma	Hemangioma	
56	M		Hemangioma	Hemangioma clinically
56	M	Cavernous hemangioma	Hematoma Fibrous overgrowth	
57	F		Hemangioma	Hemangioma clinically
58	F	Epitheloid hemangioendothelioma	Inflammation tissue	
62	M	Lipoma	Lipoma	

48	M		Hemangioma	Hemangioma clinically
51	F	Lymphoepithelial cyst	No mass	
55	F	Fibrous overgrowth	Granulation tissue	
55	F		Hemangioma	Hemangioma clinically
56	F	Cavernous hemangioma	Hemangioma	
56	M		Hemangioma	Hemangioma clinically
56	M	Cavernous hemangioma	Hematoma Fibrous overgrowth	
57	F		Hemangioma	Hemangioma clinically
58	F	Epitheloid hemangioendothelioma	Inflammation tissue	
62	M	Lipoma	Lipoma	
63	F	Fibroma	Fibroma	
63	F	Fibrous overgrowth	No mass	
66	M	Schwannoma	Neurogenic or Salivary gland tumor	
71	F		Hemangioma	Hemangioma clinically
73	F	MALT lymphoma	Lymphoma	
74	F		Granulation tissue	Granulation tissue clinically
76	M		Hemangioma	Hemangioma clinically
81	F	Thrombus formation with granulation	Dermoid cyst	
86	M		Hemangioma	Hemangioma clinically
Age	Sex	Pathology	US diagnosis	Remarks
5	M		Blandin-Nuhn cyst	Cyst clinically
8	F	Schwannoma	Pyogenic granuloma	
9	F	Fibrous tumor	Fibroma, Neurofibroma	
9	F	Blandin-Nuhn cyst	Mucocele	
12	F	Cavernous hemangioma	Hemangioma	
21	M		Hemangioma	Hemangioma clinically
24	F		No mass	Granulation tissue clinically
41	M	Cavernous hemangioma	Fibroma	
44	F	Intramascular hemangioma	Hemangioma	
45	M	Leiomyosarcoma	Hemangioma	
48	F		Granulation tissue	Granulation tissue clinically
48	M		Hemangioma	Hemangioma clinically
51	F	Lymphoepithelial cyst	No mass	
55	F	Fibrous overgrowth	Granulation tissue	
55	F		Hemangioma	Hemangioma clinically
56	F	Cavernous hemangioma	Hemangioma	
56	M		Hemangioma	Hemangioma clinically
56	M	Cavernous hemangioma	Hematoma Fibrous overgrowth	
57	F		Hemangioma	Hemangioma clinically
58	F	Epitheloid hemangioendothelioma	Inflammation tissue	
62	M	Lipoma	Lipoma	

63	F	Fibroma	Fibroma	
63	F	Fibrous overgrowth	No mass	
66	M	Schwannoma	Neurogenic or Salivary gland tumor	
71	F		Hemangioma	Hemangioma clinically
73	F	MALT lymphoma	Lymphoma	
74	F		Granulation tissue	Granulation tissue clinically
76	M		Hemangioma	Hemangioma clinically
81	F	Thrombus formation with granulation	Dermoid cyst	
86	M		Hemangioma	Hemangioma clinically

P36 MRI of nasopharyngeal adenoid hypertrophy – is DWI helpful for the characterization as a benign entity?

Alexey Surov (Study)

Martin-Luther-Universität Halle-Wittenberg, Universitätsklinikum, Depart of Radiology, Halle, Germany

Co-Authors: Ryl I, Bartel-Friedrich S, Kösling S

OBJECTIVES: Nasopharyngeal adenoid hypertrophy (NAH) is typical appearance of childhood and then an incidental finding on imaging. Due to involution nasopharyngeal lymphatic tissue usually cannot be found in adults beyond the 30th to 40th years of life. However, cases with persistent NAH do occur. In this age, a differentiation of malignant nasopharyngeal lesions may be difficult. According to literature diffusion-weighted imaging (DWI) could be helpful for the differentiation of malignant and benign lesions. Our aim was to identify and analyse retrospectively NAH on MRI with special attention on DWI.

MATERIALS AND METHODS: In the time period from 2007 to 2011 857 MR investigations of the head were performed in children and adolescents at our institution. MRI was obtained at a 1.5 T MRI device (Magnetom Vision Sonata Upgrade, Siemens, Germany). Beside normal standard sequences (T2-w, T1-w before and after i.v. administration of contrast medium, slice thickness between 3 and 5 mm) EPI-DWI was performed with b values of 0, 500, and 1000 s/

mm²; section thickness of 5 mm with no gap. ADC maps were generated by the implemented software. In cases with NAH the size of the lesion was measured and the appearance on standard sequences was analysed visually (T1-w, T2-w: markedly / slightly hypo-, iso-, hyperintense; T-w with contrast medium: slight, moderate, marked enhancement, presence of enhancing septa). The section with the largest diameter of NAH was selected for ADC calculation. In that image a polygonal region of interest (ROI) as large as possible was drawn without risking partial volume effects. The ADC value was measured on ADC maps as well as calculated after the formula by measuring on b=0 and b=1000 images. NAH below 5 mm in diameter were excluded from the measurements.

RESULTS: NAH was identified in 433 (50.5%) patients. The size of the lesions varied from 5 to 25 mm (median 15 mm). On T2-w images, most NAH were slightly-to-moderate hyperintense (87.9%). On T1-w images, they were isointense (91.4%). After i.v. administration of contrast medium, slight enhancement was seen in 25.2%,

moderate in 12.3%, and marked in 62.5%. Septa could be identified in 90.2% of the cases. Values measured on ADC-maps and calculated values were close together. The estimation was possible in 203 lesions. Values ranged from 0.56 to 1.38 mm²s⁻¹ (mean value 0.80 mm²s⁻¹; median value 0.78 mm²s⁻¹).

CONCLUSIONS: Beside the known MRI appearance NAH showed low ADC values as it is reported of malignancies. To our best knowledge this observation has not been documented until now. It should be known to avoid misinterpretations.

P37 Cone-beam computer tomography in Styloid syndrome diagnosis (Eagle syndrom)

Nataliya Solonskaya (Study)

Moscow State University of Medicine and Dentistry, Radiology Department, Moscow, Russia

Co-Authors: Truten V

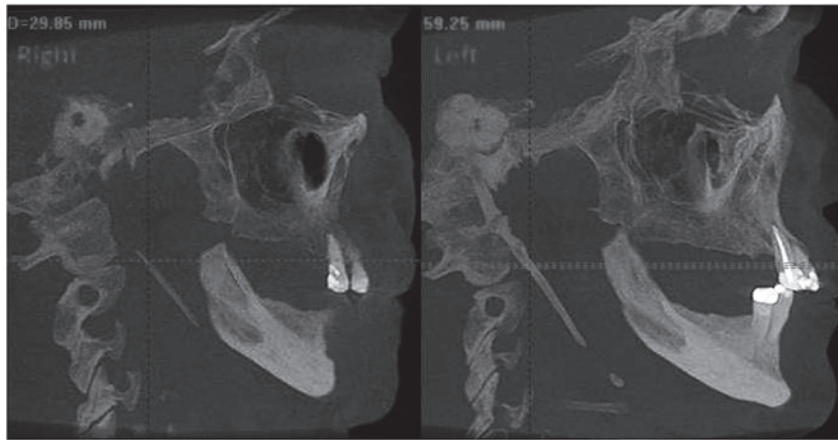
OBJECTIVES: To determine the abilities of cone-beam computer tomography in styloid syndrome diagnostics.

MATERIALS AND METHODS: There were examined a total of 57 patients, range 27–65 years, with pain in parotid region and difficulty with opening mouth. In the first step these patients were evaluated by orthopantomography, where elongated styloid process was reviewed. Cone-beam computer tomography imaging was performed on the tomography, I-CAT, USA on the next step.

RESULTS: Styloid syndrome, or syndrome of elongated process, is characterized by cranio-facial or cervical pain due to an elongated styloid process or calcified stylohyoid ligament. Patients with Eagle s syndrome may present with a sore throat, pain in the ear and surrounding soft tissues. CBCT imaging has several advantages over conventional radiographs. 3D-CBCT is an available imaging tool because of its ability to image the anatomy of styloid process, its fragmentation and calcified stylohyoid ligament. Along with this the angle of process deviation from the temporal bone was measured. The

average length of the process was 63mm (range 34–92mm). 17 patient with process length not high than 34–45mm had miscellaneous calcified stylohyoid ligament. 2 patients with the long process had consolidation with hyoid bone. The average date of process angle deviation from the temporal bone was 39 degrees forward, 21 degrees medial.

CONCLUSIONS: CBCT is a valuable diagnostic imaging tool in patients with Eagle s syndrome that allows clinicians to evaluate the styloid process in spatial geometry, and make accurate length and angle measurements.



ConeBeam – CT-image of a 66-year-old woman

29.8 mm calcification of right stylohyoid ligament

59.2 mm extended and fragmented left styloid process

P38 Tumor Response Assessments of oral cancer to pre-operative chemo-radiotherapy (CRT) with permeability and diffusion MRI

Toru Chikui (Study)

Kyushu University, Department of Oral and Maxillofacial Radiology,
Fukuoka Prefecture, Japan

Co-Authors: Kitamoto E, Kawano Sh, Ohga M, Obara M, Matsuo Y, Yoshiura

OBJECTIVES: To evaluate the utility of both permeability and diffusion MRI for both predicting and monitoring the histopathological response of oral squamous cell carcinoma to CRT.

MATERIALS AND METHODS: This study included 35 patients who underwent dynamic contrast-enhanced MRI (DCE-MRI). The axial DCE scan consisted of a 10 slice, 3D-T₁ fast-field echo sequence. A T₁₀ map was estimated before contrast medium injection by the dual flip angle method (5° and 15°) and the signal intensity of tissue was converted into the concentration of contrast medium in tissue (C_i(t)). The data were analyzed using a TK model. The model described in the following equation was applied to each voxel:

$$C_i(t) = K^{trans} \int_0^t C_p(t') \exp \{-K^{trans}(t-t')/v_e\} dt' + v_p C_p(t)$$

where K^{trans} is influx forward volume transfer constant (into EES(extravascular extracellular space)) from plasma, v_e is fractional volume of EES and v_p is the fractional volume of plasma. A

predefined model arterial input function (AIF) was used for C_p(t), therefore, we did not take individual AIF into account. Axial DW images were also acquired and an ADC map was obtained. The

motion-probing gradient was applied along the right-to-left directions, with b values of 0, 500, 1000, and 1500 s/mm².

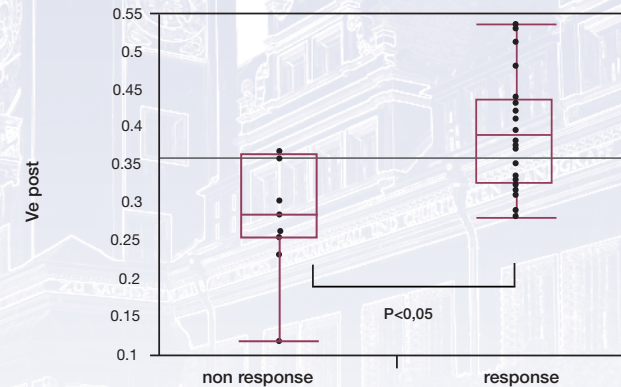
The histological evaluation of the effects of CRT was performed according to Ohboshi and Shimamoto's classification. These criteria grade the tumor response from I to IV. Patients with grades IIb, III and IV are considered to be responders (n=24), while those with grades I and IIa are considered to be non-responders (n=24).

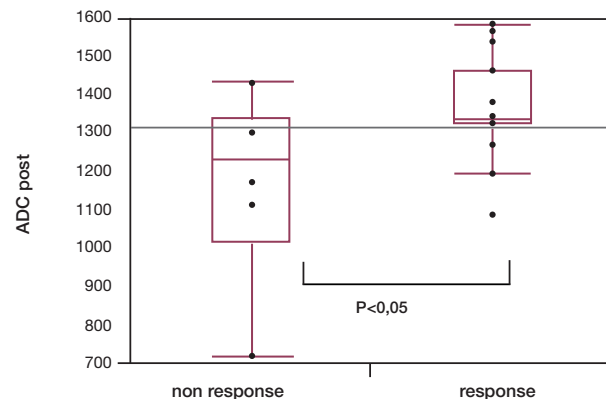
RESULTS: None of the pre-CRT parameters were significantly different between responders and non-responders. The post-CRT v_e of the responders (0.394±0.016) was significantly higher than that of the non-responders (0.288±0.023) (P=0.01). The change in the v_e between the pre and post-CRT of the responders (0.144±0.017) was significantly larger than that of the non-responders (0.046±0.025) (P=0.003).

It was possible to measure ADC in only 21 out of 35 cases (60%), due to severe artifacts. There was no significant difference in the pre-CRT ADC values between responders [(1.08±0.026) ×10⁻³mm²/s] and non-responders [(1.08±0.04) ×10⁻³mm²/s] (P=0.85). The post-CRT ADC of the responders (1.37±0.05)×10⁻³mm²/s was significantly higher than that of the non-responders [(1.17±0.07)×10⁻³mm²/s] (P=0.04)

The increase in both v_e and ADC strongly suggested a good tumor response to CRT, which reflected an increase in the EES secondary to the destruction of the cancer nest.

CONCLUSIONS: The increase in the v_e was indicative of a good tumor response to CRT. ADC was also useful for monitoring the tumor response to CRT; however, the problem of image distortion was sometimes troublesome in the orofacial region. This pharmacokinetic analysis is therefore considered to be potentially useful for monitoring the histopathological response to CRT.





P39 US-guided fine-needle aspiration of thyroid nodules – brainstorm on polemic issues!

Leonor Fernandes (Study)

Santa Maria Hospital, Radiology,
Lisbon, Portugal

Co-Authors: Silva C, M. Almeida M, Távora I

OBJECTIVES: The author proposes to present the personal experience of US-guided fine-needle aspiration of thyroid nodules, with particular interest in the state of the art concerning the updated recommendations, some technical aspects and the outcome results as well as the doubts and usually debated questions on difficult cases.

MATERIALS AND METHODS: From 17 of October 2006 until the present time, around a thousand nodules were punctured on ultrasound guided approach by the first author on the Santa Maria Hospital.

RESULTS: The ultrasound characteristics of the nodules, some technical aspects and the cytological results are reviewed in this personal series, and a critic retrospective analysis is done. Particular emphasis is made on the difficult decision cases and polemic usually debated questions on this matter. A self-criticism is also made, aiming better future results; perhaps giving way to a further prospective study in the years to come.

CONCLUSIONS: Based on a retrospective personal case review, the author concludes that despite the excellent and various recommendations available upon US-guided fine-needle aspiration of thyroid nodules, polemic issues still remains in certain difficult cases on nowadays. Will we ever arrive in the near future to a simple decision chart?

P40 Digital dynamic sialography in diagnosis of sialolithiasis

Dimitriy Lezhnev (Study)

Clinic of Moscow State University of Medicine and Dentistry, Depart of Radiology,
Moscow, Russia

Co-Authors: Sangaeva L, Kostenko D

MATERIALS AND METHODS: Examination data analysis of 125 digital dynamic sialographies of patients with salivary glands pathology established its high diagnostic efficiency. Main cause of the disease is the sialolithiasis.

RESULTS: Symptom similarity of salivary glands diseases complicates the differential diagnosis as result indication several diagnostic methods, even in cases when it is not necessary. Implementation of the highest informative examination permits to reduce diagnostic time and to select adequate treatment method. One of such effective diagnostic methods is digital dynamic sialography (DDSG) in scopic regime. Patients at the age from 18 to 84 were underwent 125 digital dynamic sialographies. These examinations were on apparatus PHILIPS INTEGRIS 3000 with shooting mode - 25 k/s. Contrast medium «Omnipaque-350» 2,0-3,0 ml is injected in the duct through a polyethylene catheter 0,6 or 1,0 mm. Lateral projection is used for visualization major salivary glands. The result is recorded to digital device as video or single-frame photography. The appearance of pain during the contrast enhancement or sufficient grade of filling signaled to the catheter extraction or the beginning of contrast evacuation. Anatomical-topographic variants of concrements displacement, its mobility and amplitude, grade of duct obturation, possibility of contrast enhancing of all duct system and its evacuation are evaluated at the same time. The concrements in ducts of major salivary

glands are detected at 64 patients (51,2%), in 4 cases (3,2 %) the visualization was not informative because of lack of contrast enhancing in duct system. In other 57 cases (45,6%) the reason of inflammation was non-calculous sialadenitis, strictures of ducts and anomalies. These results were used for planning of surgical intervention.

CONCLUSIONS: Examination data analysis of 125 digital dynamic sialographies of patients with salivary glands pathology established its high diagnostic efficiency. Main cause of the disease is the sialolithiasis.

P41 Swelling of the parotid gland with cystoid pattern on ultrasound: a spectrum of diseases

Christian Kunze (Study)

Martin-Luther-Universität Halle-Wittenberg, Universitätsklinikum, Depart of Radiology, Halle, Germany

Co-Authors: Surov A, Müller T, Holzhausen HJ, Spielmann RP

OBJECTIVES: Swelling of the parotid gland is a frequent clinical sign in children and it is associated with several diseases. On ultrasound, they can manifest with different features. Cystoid pattern is rare here. The aim of this study was to describe diseases of the parotid gland associated with a cystoid pattern on ultrasound.

MATERIALS AND METHODS: In the time period from 1999 to 2011 9 patients with uni- or bilateral parotid swelling and cystoid pattern on ultrasound could be identified in our institution. There were 9 patients with a median age of 10 years (range, 2–17 years).

RESULTS: In these patients follow diseases were diagnosed: sarcoidosis (n=1), atypical mycobacteriosis (n=1), Sjögren's syndrome (n=3), idiopathic parotitis (n=3), and atypical lymphogranulomatous phagocytic syndrome (n=1). On ultrasound, in all cases a diffuse enlargement of the parotid glands with a cystoids pattern and hyperperfusion was identified.

CONCLUSIONS: Cystoid pattern is associated with different diseases of the parotid glands. It should be known for physicians.

P42 Diagnostic performance of ultrasound guided fine needle aspiration cytology in the assessment of major salivary gland masses: a retrospective analysis

Romain Kohler (Study)

Geneva University Hospital, Radiology, Geneva, Switzerland

Co-Authors: Masterson K, Pache J, Dulguerov P, Becker M

OBJECTIVES: To evaluate the diagnostic performance of ultrasound guided fine needle aspiration cytology (USFNAC) in salivary gland masses.

MATERIALS AND METHODS: The Institutional Ethics Committee approved this retrospective study on a consecutive series of 177 patients addressed to our department for USFNAC of salivary glands lesions. The radiology records of 110 males and 67 females (mean age 59.8 years, range 16–99 years) were reviewed and findings from cytopathological and bacterio-

logical analysis were compared to subsequent histology (n=69), or clinical and radiological follow-up of > 8 months (n=91).

RESULTS: 90.4 % of USFNAC procedures were performed in the parotid and 9.6% were performed in the submandibular glands on an outpatient basis using 22G and 21G needles. No major complications were noted. 90.4% of all samples were diagnostic and 9.6 % were non-diagnostic. In the 160 procedures with diagnostic cytology, the definitive diagnosis was

infectious/inflammatory in 21.9 % (n=35), benign tumors in 56.9% (n=91) and malignant tumors in 21.2 % (n=34) of cases. The sensitivity and specificity for differentiating benign from malignant salivary gland masses were 88.6 % and 97.6 %, respectively. The positive and negative predictive values were 91.2 % and 96.8 %, respectively. With a total of 3 false positive and 4 false negative findings, USFNAC had some

difficulties to differentiate benign tumors from low-grade malignances, mainly mucoepidermoid carcinoma.

CONCLUSIONS: USFNAC is a safe and reliable technique with a high negative predictive value for differentiating benign from malignant salivary gland pathologies.

P43 Non-invasive differentiation of primary parotid gland tumors: does high-resolution dynamic contrast-enhanced MRI offer a solution?

Jasmin D. Busch (Study)

University Medical Center Hamburg-Eppendorf, Department of Diagnostic and Interventional Radiology, Hamburg, Germany

Co-Authors: Treszl A, Bier J, Muenscher A, Adam G, Habermann C

OBJECTIVES: To determine the value of dynamic contrast-enhanced (DCE) magnetic resonance imaging (MRI) with high temporal resolution in differentiating various entities of primary parotid gland tumors.

MATERIALS AND METHODS: 112 consecutive patients with a suspected tumor of the parotid gland were prospectively examined with a DCE sequence using a 1.5 T unit. A single transverse 4mm thick slice with FOV of 200x188mm² was measured with a dynamic gradient echo sequence (TR/TE=15/4.4, $\alpha=50^\circ$, matrix 256x192) with 2.9s/image. A dose of 0.1mmol/kg Gd-DTPA was injected with 2.5ccm/s in the antecubital vein followed by saline. Analyses were performed with an in-house developed semi-automatic software tool. The following parameters were evaluated: bolus arrival time (BAT), tumor blood flow (TBF), tumor blood volume (TBV), volume transfer constant (Ktrans), and the exchange rate constant (Kep). Histological diagnosis was obtained in every patient. For comparison of perfusion parameters, paired two-tailed Student t-test with Bonferroni correction for multiple testing was used.

RESULTS: In all 112 patients a primary parotid gland tumor was confirmed, showing 48 pleomorphic adenoma, 44 Warthin tumors, 5 basal cell adenoma, and 15 carcinomas. BAT showed no significant differences between entities ($p=0.071$ to 0.784), whereas based on TBF and TBV basal cell adenomas differed significantly from all other entities ($p<0.001$ to 0.006). TBF differentiated pleomorphic adenomas significantly from Warthin tumors ($p=0.014$). Additionally, TBF distinguished carcinomas significantly from pleomorphic adenomas ($p=0.008$), but not from Warthin tumors ($p=0.365$). TBV made a significant distinction between carcinomas and Warthin tumors ($p=0.01$). Ktrans and Kep offered no discriminative potential.

CONCLUSIONS: DCE MRI has a non-invasive discriminative potential for differentiation of various entities of primary parotid gland tumors. For improvement of this potential, combination with other MR techniques needs to be evaluated.

P44 Non-invasive differentiation of non-tumorous parotid gland diseases using high-resolution dynamic contrast-enhanced MRI

Christian R. Habermann (Study)

University Medical Center Hamburg-Eppendorf, Department of Diagnostic and Interventional Radiology, Hamburg, Germany

Co-Authors: Treszl A, Bier J, Muenscher A, Adam G, Busch JD

OBJECTIVES: To determine the value of dynamic contrast-enhanced (DCE) magnetic resonance imaging (MRI) with high temporal resolution for differentiating non-tumorous diseases of parotid glands.

MATERIALS AND METHODS: 143 consecutive patients with clinically and sonographically proven non-tumorous diseases of the parotid glands were prospectively examined with a DCE sequence using a 1.5 T unit. A single transverse 4mm thick slice with FOV of 200x188mm² was measured with a dynamic gradient echo sequence (TR/TE=15/4.4, $\alpha=50^\circ$, matrix 256x192) with 2.9s/image. A dose of 0.1mmol/kg Gd-DTPA was injected with 2.5cm/s in the antecubital vein followed by saline. Analyses were performed with an in-house developed semi-automatic software tool. The following parameters were evaluated: bolus arrival time (BAT), parotid blood flow (PBF), parotid blood volume (PBV), volume transfer constant (Ktrans), and the exchange rate constant (Kep). Histological diagnosis was obtained in every patient. For comparison of perfusion parameters, paired two-tailed Student t-test with Bonferroni correction for multiple testing was used.

RESULTS: In all 143 patients a parotid gland disease was confirmed histologically (n=72) or clinically (n=71); (Sjögren syndrome: n=56, sialadenoses: n=39, sialadenitis: n=48). BAT showed no significant differences between entities

(p=0.0128 to 0.582), whereas based on PBF discrimination between sialadenitis and Sjögren syndrome is possible (p=0.02). PBV differentiated not only sialadenitis and Sjögren syndrome (p<0.001), but also sialadenitis and sialadenoses (p=0.002). A differentiation between was not possible based on PBV (p=0.619). Ktrans and Kep offered no discriminative potential.

CONCLUSIONS: DCE MRI has a non-invasive discriminative potential for differentiation of non-tumorous diseases of parotid glands. For improvement of this potential, combination with other MR techniques needs to be evaluated.

CASES

P45 Reparative granuloma post-stapedectomy in patients with otosclerosis: distinctive and unusual imaging appearances.

Juveria Siddiqui (Case report)

Royal National Throat, Nose and Ear Hospital, Otology, London, United Kingdom

Co-Authors: Adjei-Gyamfi Y, Dudau C, Beale T, Saeed Sh

SUMMARY: Reparative granuloma is a rare complication occurring in around 1% of otosclerosis patients post stapedectomy. It usually occurs 1–2 weeks after surgery, with patients presenting with either progressive or sudden sensorineural deafness, although vertigo and tinnitus may occur. It is thought to occur as a reaction to the stapes prosthesis. Post-operative infection is amongst the differentials at this stage. A presentation of new-onset deafness post stapedectomy mandates computed tomography (CT) scanning of the petrous temporal bones. Magnetic resonance imaging (MRI) of the brain with high resolution images through the posterior fossa and temporal bones pre and post gadolinium is recommended to assess any dural or intracranial involvement and monitor response to treatment. Conservative management of the condition involves steroids and antibiotics. However, many advocate early surgical intervention

to remove both prosthesis and granuloma. We report two cases of post-operative reparative granuloma in patients with otosclerosis, presenting with unilateral sensorineural hearing loss two weeks after ipsilateral stapedectomy. They highlight the CT and MRI features that suggest the diagnosis. The CT scan appearances are distinctive with an irregularly expanded bony labyrinth (cochlea and semicircular canals), focal areas of lucency in the adjacent otic capsule and soft tissue filled channels leading from the opacified middle ear cleft to the bony labyrinth. The MRI confirms soft tissue of similar signal intensity and enhancement characteristics both within the middle ear cleft and the eroded otic capsule and involved cochlea and semicircular canals. MRI also demonstrates extension into the internal auditory canal and dural enhancement not visible on CT.

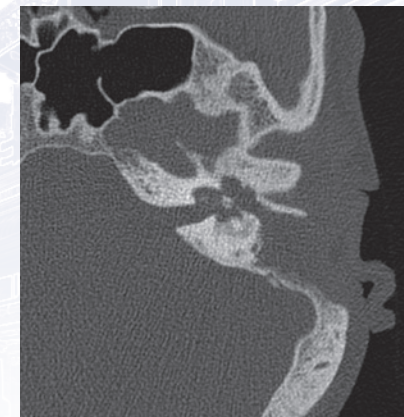


Figure 1: Axial CT temporal bone demonstrating erosion into the cochlea and vestibule with a completely opacified middle ear cleft and mastoid cavity.

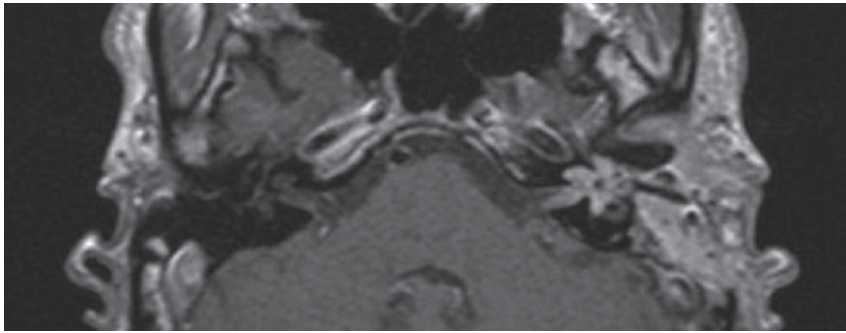


Figure 2: Axial T1 post contrast MR demonstrating similar enhancing soft tissue within both middle ear cleft mastoid cavity, cochlea, vestibule, lateral SCC and IAC.

Subsequent re-exploration of the regions demonstrated tympanomastoid granuloma. Histopathology of middle ear biopsies confirmed chronically inflamed granulation tissue in keeping with reparative granuloma.

TAKE HOME POINTS: Reparative granuloma is a rare complication in otosclerosis patients post stapedectomy. New deafness post stapedectomy mandates an urgent CT scan of the petrous temporal bones. In these cases, CT revealed

an irregularly expanded bony labyrinth, focal lucency of the otic capsule, and soft tissue filled channels leading from the opacified middle ear cleft to the bony labyrinth MRI of the brain including the posterior fossa and temporal bones pre- and post contrast is indicated to assess dural or intracranial involvement. In these cases, MRI confirmed the CT findings but also revealed extension into the internal auditory canal and dural enhancement not visible on CT.

P46 Cholesteatoma: A rare differential diagnosis of intracranial masses

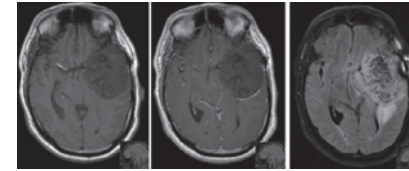
Stephan Niestroj (Case report)

Asklepios Klinik St. Georg, Radiologie, Hamburg, Germany

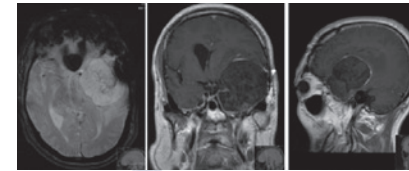
Co-Authors: Schwabe J, Manthei G, Terborg C, Kivelitz D

SUMMARY: Acquired cholesteatomas are benign, but invasive growing tumors, that originate from proliferating keratinizing squamous cells. An underlying chronic inflammatory process seems to be the main factor in the etiology of acquired cholesteatomas (comprised by a stratified ep-

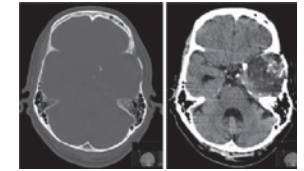
ithelium-lined sac filled with exfoliating keratin debris). Post-traumatic cholesteatomas are rare complications following skull fractures, that may develop even decades after the traumatic event and may present with aggressive intracranial extension. picture



MRI T1 T1 with contrast T2



MRI T2* T1 with contrast T1 with contrast



Non-contrast CT

Non-contrast CT: heterogenous left-side middle fossa intracranial mass with intrinsic coarse calcifications and aggressive skull base erosion.

MRI: Well-circumscribed heterogenous T1-hypointense, T2-midly hyperintense and T2* hyperintense mass with peripherally enhancing pseudo-capsule and associated perilesional edema. The T1- and T2- hypointense intralesional foci represent old hemosiderin deposits related to prior hemorrhage.

TAKE HOME POINTS: The acquired cholesteatoma is a rare differential diagnosis of intracranial space-occupying lesions, characterized by a large spectrum of imaging findings, the most important of which being its overall non-enhancing feature. The presence of intrinsic foci of enhancement or an enhancing capsule are secondary to the presence of granulation tissue. Because of its slow growth, late neurological symp-

toms may occur and the diagnosis is often made only when the tumor reaches a substantial size. Erosions of the skull base and the compression of the surrounding vascular structures are typical complications. In the setting of prior head trauma and an intracranial space-occupying lesion with aggressive bone changes, the diagnosis of acquired cholesteatoma should be excluded.

P47 Osteolysis of the skull base mimicking M. Gorham-Stout – A case report

Carolin Gramsch (Case report)

Universitätsklinikum Essen, Institut für Diagnostische und Interventionelle Radiologie und Neuroradiologie, Essen, Germany

Co-Authors: Müller O, le Saout Chapot V, Schlamann M

SUMMARY: A 23-year-old male patient presented with a history of intermittend and aggravated headache and nuchalgia. Anamnesis and first blood tests did not reveal any underlying disease. Cranial computed tomography (CCT) showed an osteolytic process of the skull base with subtle marginal hypersclerosis and Magnetic Resonance Imaging (MRI) presented a contrast-enhanced necrotic mass of the clivus.

As osteolytic metastasis in this young patient seemed to be implausible and extended serologic examinations excluded endocrinological causes as well as various infections, including tuberculosis first of all M. Gorham-Stout was assumed. However marginal hypersclerosis cast doubt on that diagnosis. Finally endoscopic transsphenoidal biopsy of the clivus was initiated and revealed a granulomatous infection caused

by *Aspergillus oryzae*. Systemic fungal infection was ruled out because serological examinations for aspergillus antigen were negative. Moreover additional bioptic samples could screen out an infection deriving from the paranasal sinuses. Thus finally the absolute rarity of a bone-derived *Aspergillus* granuloma without serotyping in an immuno-competent patient was diagnosed and oral

antifungal therapy with voriconazol was started.

TAKE HOME POINTS: This case illustrates the importance of a precise description and analysis of MR findings in osteolysis, because the subtle marginal hypersclerosis was the initial key to diagnosis and therapy.

P48 Chondrosarcoma of the base of skull

Tomislav Stavric (Case report)

KBC Bezanijaska Kosa, Radiology,
Belgrade, Serbia

Co-Authors: Medan A Jovanovic-Stavric I

SUMMARY: Chondrosarcomas of the base of skull are rare intracranial malignancy, accounting for a very small proportion of all chondrosarcomas of head and neck, commonly incidentally detected, typically localised off midline, often with signs of intracranial extension locally. The aim of the study was to demonstrate a role of native and contrast enhanced CT and MRI ex-

amination in diagnosing and further evaluation of our patient with recidivant chondrosarcoma of clivus and sella turcica unilaterally. After surgical treatment, tumour relapses parasellar in cavernous sinus with inclusion of ACI, and intracranial into prepontine cistern, cerebellopontine angle and petrose bone, with functional impairment of V, VII and VIII cranial nerve.

P49 Lipoblastoma of the nasal cavity

Eva Klintström (Case report)

University Hospital, County Council of Östergötland, Radiology Department,
Linköping, Sweden

Co-Authors: Kovacovics B

SUMMARY: Lipoblastoma is a rare benign mesenchymal tumour of embryonal fat that may occur in newborns and in small children. We describe a case where a two months old girl presented with a mass in the right nasal cavity. She was referred to the Radiology Clinic at the University Hospital in Linköping because of difficulty in breathing and feeding. A MRI

examination was performed to exclude an encephalocele before the operation procedure. The MRI showed a mass consisting mainly of fat in the right nasal cavity. Connection with the brain could be excluded. The radiological diagnosis was lipoblastoma. The tumour was inserted to the nasal septum and could easily be removed in two pieces during surgery. The

nasal conchae on the right side were small but otherwise normal. The nasal breathing was improved immediately after the surgery and the healing was uneventful. The tumour was sent for histopathological examination and the primary diagnosis was lipoblastoma. Another possible

histopathological diagnosis was mesenchymal hamartoma.

TAKE HOME POINTS: In small children, MRI is the modality of choice imaging intranasal masses and their relations to the intracranial cavity.

P50 Clear cell odontogenic carcinoma with multiple lung metastases and late recurrence

Eva Klintström (Case report)

University Hospital, County Council of Östergötland, Radiology Department,
Linköping, Sweden

Co-Authors: Kovacovics B, Warfvinge G

OBJECTIVES: Clear-cell odontogenic carcinoma (CCOC) is a rare and locally aggressive malignancy first described by Hansen et al in 1985. The tumour is known to recur and having capacity to metastasize to distant sites, most frequently the lungs. Some articles describe perineural tumour spread. The lesion has a peak incidence in the 5-7th decades with the anterior part of the mandible most frequently affected. Review articles describe that ameloblastoma is the primary diagnosis in 29 % of the cases.

MATERIALS AND METHODS: A case where the tumour occurred in an 8 year old girl is described. At the first visit to the oral surgeon a panoramic radiograph showed inferiorly displaced right lower second premolar. The girl had complained of right mild facial pain and swelling. The lesion was first diagnosed as an ameloblastoma and recurred several times. A recurrence, four years from the first operation, displayed an altered histological pattern and was diagnosed as CCOC. The lesion was imaged with multislice computed tomography (MSCT) and magnetic resonance imaging (MRI) before the resection of the right mandible body. The resection margins were at histopathological examination considered tumour-free. An iliac crest transplant was performed and the healing was clinically uneventful.

RESULTS: Multiple lung metastases were diagnosed when the girl was 15 and she underwent chemotherapy treatment. PET-CT of the neck, thorax and abdomen, not visualizing the mandible, showed no increased FDG uptake in the pulmonary nodules. The nodules increased in size despite of several cycles of chemotherapy. At a clinical check up, at the age of 20, the girl felt a facial swelling on the right side. MSCT and MRI showed a soft tissue mass infiltrating the masticator muscles and destructing the mandible ramus. The centre of the lesion was located at the mandible foramen suggesting the possibility of perineural tumour spread. MRI showed no intracranial perineural tumor spread.

CONCLUSIONS: CCOC can occur in young children and are often primarily diagnosed as ameloblastomas. Several modalities are required for the diagnosis and the images have to be evaluated also for perineural tumour spread and lung metastases. Literature describing perineural tumour spread of CCOC is reviewed.

P51 Orbital abscess as a result of acute frontal sinusitis and ethmoiditis

Theodosia Kontaki (Case report)

«Mamatseio» General Hospital, Radiology,
Kozani, Greece

Co-Authors: Tziola M, Grigoriadis G, Markou A, Kougias L, Pozoukidis C

OBJECTIVES: Orbital cellulitis and abscess formation are uncommon complications of sinusitis. Early diagnosis and treatment are important, in order to prevent blindness and intracranial complications. We present a case of an orbital abscess, as a result of acute sinusitis.

MATERIALS AND METHODS: A 21-year-old woman presented with a 9-day history of headache and a 5-day history of right orbital pain, periorbital swelling, right nasal discharge and progressive deterioration of vision on the right side. The patient was febrile (temperature 38.2 °C), white blood cell count was 12,700/L and CRP was 3.2 mg/dL.

RESULTS: Contrast enhanced MDCT of the sinuses and orbits (with sagittal and coronal reconstructed images) showed right frontal sinusitis and ipsilateral ethmoiditis, smooth erosion

of the superior-medial orbital wall, as well as right orbital abscess. There were no intracranial complications. The patient underwent surgical drainage of the right frontal and ethmoid sinuses and also drainage of the orbital abscess, combined with intravenous antibiotics administration. The postoperative period was uneventful, with progressive resolution of orbital and sinus symptoms.

CONCLUSIONS: Acute orbital inflammation is secondary to sinusitis in about 70% of cases and the maxillary, ethmoid and frontal sinuses may all be involved. MDCT scan of the sinuses and orbits with intravenous contrast administration, allows accurate localization of the sinus infection, bone erosion and usually enables an accurate grading of the orbital inflammation. Treatment should be commenced as soon as the diagnosis has established.

P52 Rapidly evolving large extracranial vertebral artery pseudoaneurysm in Behcet's disease

Rao Sibir (Case report)

Baylor College of Medicine, Radiology,
Houston, Texas, USA

Co-Authors: Bhanusali N, Moron F, Benndorf G

OBJECTIVES: Behcet's disease is a multisystem chronic autoimmune disease of unknown etiology with a wide spectrum of symptoms and organ system involvement. Behcet's vasculitis usually affects veins of all sizes with superficial thrombophlebitis and thrombosis of major vessels (1). Arterial manifestation, particularly of the

extracranial vertebral arteries is rare. We report a rare case of a patient with Behcet's disease who presented with bilateral spontaneous vertebral artery pseudoaneurysms.

MATERIALS AND METHODS: A 26-year-old African American female with Behcet's disease initially presented with radiating left neck and arm pain. A 6mm left spontaneous vertebral artery (VA) pseudoaneurysm of the V2 segment was found on computed tomography angiography (CTA) and was managed conservatively with steroids and medical anticoagulation. She returned four months later due to new onset right neck and arm pain with accompanying weakness. A second, new, 1.2x1.6x0.8 cm right VA (V1 segment) pseudoaneurysm was identified on CTA and confirmed by angiography. Over four days, the patient developed escalating right upper extremity sensory and motor deficits with rapid enlargement of the right VA pseudoaneurysm. Repeat angiography prior to the planned endovascular treatment revealed subtotal occlusion of the right VA by the enlarging pseudoaneurysm. Given the large size of the pseudoaneurysm along with the likely fragility of the vessel wall, parent vessel occlusion was pursued rather than stenting. A microcatheter was navigated into the distal most portion of the patent proximal right vertebral artery segment just proximal to the pseudoaneurysm at C6 and multiple detachable coils (Codman Neurovascular; Raynham, Massachusetts) were deployed.

RESULTS: Endovascular coil occlusion of the remaining right proximal vertebral arterial inflow was performed successfully. Post-treatment, retrograde reconstitution of the distal intracranial right vertebral artery was visualized via cervical collaterals and retrograde filling from the left vertebral artery. Patient was started on high dose prednisone and counseled on compliance. Follow-up post-procedure angiogram at four months showed complete coil occlusion of the right VA and decreased size of the left VA. Clinically, the patient showed improvement of pain to baseline and normal sensory-motor neurologic exam.

CONCLUSIONS: This case is notable for its presentation in an African American patient, the unusual location and bilaterality of the vertebral artery pseudoaneurysms, and the rapidity of its growth. In this rare case, Behcet's disease presented with a rapidly enlarging pseudoaneurysm of the cervical arterial circulation, which warranted endovascular management in combination with optimized medical management of the underlying disease.

P53 Prevertebral tendinitis

Dominik Schramm (Case report)

Martin Luther University Halle/Wittenberg, Faculty of Medicine / Department of Radiology,
Halle, Germany

Co-Authors: Kösling S, Glien A

OBJECTIVES: Prevertebral tendinitis is a rare, mostly acute disease which is relatively unknown among radiologists. Also sub-acute courses have been described. Although the aetiology is still unexplained, it is assumed that the disease is caused by an inflammatory foreign body reaction due to calcium hydroxyapatite deposits

in the tendon of the longus colli muscle. There are some suggestions that repetitive trauma, recent injury, tissue necrosis, or ischemia may play a role in pathogenesis. To our best knowledge 83 cases have been published until now. By two cases we present clinical signs, the appearance on imaging and therapeutic options.

Patients complain of rapidly developing severe cervical pain, stiff neck and dysphagia leading often to emergency investigations. Sometimes, mild fever does occur. Laboratory tests show slightly increased inflammatory parameters (leucocytosis, C-reactive protein). From clinical point of view there are several differential diagnoses: infectious spondylitis, retropharyngeal abscess or phlegmon, dissection of vessels, traumatic injury and meningitis. Imaging may help in the differentiation if the appearance of the disease is known. Most helpful is the identification of anteriorly below the atlas median or para-median located amorphous calcifications (best seen on CT) and of a fluid collection without a rim enhancement in the superior retropharyngeal space (MRI or CT). An edema of the prevertebral muscles has been described in the literature too. Especially in absent calcifications the disease can be confused with a retropharyngeal abscess. The latter is more space-occupying, shows usually a rim enhancement and has to

be treated surgically. Prevertebral tendinitis is a self-limiting disease that usually resolves within about two weeks. Treatment with non-steroidal anti-inflammatory drugs or steroids may shorten the duration.

TAKE HOME POINTS: Prevertebral tendinitis is a rare, inflammatory process, which affects the cervicothoracic prevertebral muscles. Clinically, it can be misdiagnosed as retropharyngeal abscess, traumatic injury or infectious spondylitis. The diagnosis is made radiographically by an amorphous calcification anterior to C1/C2 and retropharyngeal fluid/ soft tissue swelling. It is a self-limiting disease that usually resolves within about two weeks. Treatment with non-steroidal anti-inflammatory drugs or steroids may shorten the duration.

Treatment with non-steroidal anti-inflammatory drugs or steroids may shorten the duration.

P54 Spontaneous idiopathic cervical surgical emphysema and pneumomediastinum: a unique case?

Juveria Siddiqui (Case report)

Royal National Throat, Nose and Ear Hospital, Otolaryngology, London, United Kingdom

Co-Authors: Jaberoo MC, Lingam R, Farrell R

SUMMARY: Spontaneous surgical emphysema in the neck, mediastinum and thorax is a phenomenon that is usually found to be secondary to a predisposing factor; causes include traumatic rupture of a viscus, or an abscess or collection colonised by a gas-producing organism. We present the case of an eighteen year old girl with spontaneous surgical emphysema of unknown origin. The patient, who was otherwise fit and well, had a three day history of coryzal symptoms, but no history of coughing, vomiting, straining, foreign body ingestion or neck trauma. She was clinically well and afebrile. There was no

clinical or biochemical suggestion of abscess in the region. Clinically, there was mildly palpable bilateral supraclavicular surgical emphysema; surgical emphysema was confirmed on the lateral soft tissue neck radiograph (figure 1).

The full extent of this was only seen on IV contrast enhanced CT scanning of the neck and thorax, with extensive surgical emphysema in the neck and the mediastinum (figure 2). In the neck it was predominantly in the lower neck and extending superiorly in the retropharyngeal space to the level of the nasopharynx.



Figure 1: the lateral soft tissue neck radiograph demonstrating surgical emphysema in the soft tissues of the lower neck.

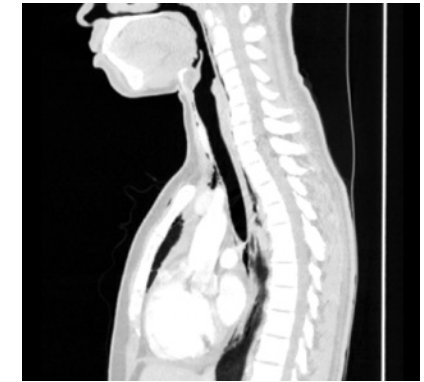


Figure 2: IV contrast-enhanced CT neck and thorax in the sagittal plane, demonstrating the extent of surgical emphysema from the nasopharyngeal region superiorly to the posterior mediastinum inferiorly.

In the mediastinum, air was seen predominantly in the superior and middle mediastinum, tracking down inferiorly in the posterior mediastinum towards the gastroesophageal junction.

The pockets of air were not associated with fluid or collection. No obvious foreign body was noted within the oesophagus. The pharynx and larynx were clear. The lungs were clear. No identifiable source was seen. There was no visible compression on vital structures. The surgical emphysema resolved with conservative management, and follow up, the patient is well with no palpable residual surgical emphysema. Although cases of spontaneous cervical surgical emphysema have been described, all reported cases have had a known predisposing risk factor, for example, coughing, vomiting, straining at childbirth. One case was described after diving. Surgical decompression has been performed in some of these cases. No idiopathic cases were found in our search.

TAKE HOME POINTS: We describe a case of idiopathic spontaneous cervical surgical emphysema which resolved conservatively; this, to our knowledge is a unique case. This case emphasises that in a patient with clinical cervical surgical emphysema despite a lack of a predisposing risk factor, urgent imaging should be sought to assess the extent of the condition, and its effects on vital structures. Urgent surgical decompression may become necessary if critical compression on vital structures has occurred.

ACKNOWLEDGEMENT

We thank warmly the following companies for their support as Sponsor of the ESHNR 25th Congress and Refresher Course:





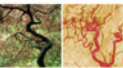
The Power of Contrast

Radiology & Interventional

medRAD
is part of Bayer HealthCare

Gadobutrol
Gadovist® 1.0
mmol/ml

Gadovist® 1.0 mmol/mL solution for injection. Composition: 1 mL solution for injection contains 604.72 mg gadobutrol (equiv. 1.0 mmol) as active ingredient. **Excipients:** calcobutrol sodium, tromethamol, hydrochloric acid, water for injections. **Indications:** This medicinal product is for diagnostic use only. Gadovist® 1.0 is indicated in adults, adolescents, and children aged 2 years and older for: Contrast enhancement in cranial and spinal magnetic resonance imaging (MRI), contrast enhanced MRI of liver or kidneys in patients with high suspicion or evidence of having focal lesions to classify these lesions as benign or malignant, contrast enhancement in magnetic resonance angiography (CE-MRA). **Contraindications:** Hypersensitivity to the active substance or any of the excipients. **Special warnings and precautions for use:** While injecting Gadovist into veins with a small lumen there is the possibility of adverse effects such as reddening and swelling. The usual safety requirements for magnetic resonance imaging, especially the exclusion of ferromagnetic materials, also apply when using Gadovist. Hypersensitivity reactions, including anaphylactoid reactions ranging to shock, have been observed after administration of Gadovist. To be able to react immediately to an emergency, medicinal products and equipment (e.g. endotracheal tube and respirator) should be within hand reach. Hypersensitivity reactions are not predictable, however in patients with an allergic disposition hypersensitivity may occur more often than in patients without such a disposition. In rare cases delayed anaphylactoid reactions (after hours to days) have been observed. **Severe cardiovascular disease:** In patients with severe cardiovascular disease Gadovist should only be administered after careful risk benefit assessment because only limited data are available so far. Gadovist should be used with special care in patients: 1.) with known congenital long QT syndrome or a family history of congenital long QT syndrome; 2.) with known previous arrhythmias after taking medicinal products that prolong cardiac repolarisation; 3.) who are currently taking a medicinal product that is known to prolong cardiac repolarisation e.g. a Class III antiarrhythmic (e.g. amiodarone, sotalol). The possibility that Gadovist may cause torsade de pointes arrhythmias in an individual patient cannot be excluded. **Hypokalemia:** Gadovist should not be used in patients with uncorrected hypokalemia. **Impaired renal function:** Prior to administration of Gadovist, it is recommended that all patients are screened for renal dysfunction by obtaining laboratory tests. There have been reports of nephrogenic systemic fibrosis (NSF) associated with use of some gadolinium-containing contrast agents in patients with acute or chronic severe renal impairment (GFR < 30 mL/min/1.73m²). Patients undergoing liver transplantation are at particular risk since the incidence of acute renal failure is high in this group. As there is a possibility that NSF may occur with Gadovist, it should therefore only be used in patients with severe renal impairment and in patients in the perioperative liver transplantation period after careful risk/benefit assessment and if the diagnostic information is essential and not available with noncontrast enhanced magnetic resonance imaging (MRI). Haemodialysis shortly after Gadovist administration may be useful at removing Gadovist from the body. There is no evidence to support the initiation of haemodialysis for prevention or treatment of NSF in patients not already undergoing haemodialysis. **Elderly:** As the renal clearance of gadobutrol may be impaired in the elderly, it is particularly important to screen patients aged 65 years and older for renal dysfunction. **Seizure disorders:** Like with other gadolinium containing contrast agents special precaution is necessary in patients with a low threshold for seizures. **Undesirable effects:** Following adverse reactions have been observed in clinical trials. Uncommon (≥ 1/1,000 to < 1/100): Headache, dizziness, paresthesia, dysgeusia, nausea, vasodilatation, injection site pain, injection site reaction. Rare (≥ 1/10,000 to < 1/1,000): Anaphylactoid reaction, parosmia, hypotension, dyspnoea, vomiting, urticaria, rash. Following additional adverse reactions have been reported from postmarketing spontaneous reporting: Rare (≥ 1/10,000 to < 1/1,000): Cardiac arrest, tachycardia, loss of consciousness, convulsion, conjunctivitis, eyelid oedema, respiratory arrest, bronchospasm, cyanosis, oropharyngeal swelling, cough, sneezing, face edema, hyperhidrosis, pruritus, erythema, circulatory collapse, flushing, feeling hot, malaise, anaphylactoid shock. **Additional safety information:** Short-lasting mild to moderate feelings of coldness, warmth or pain at the injection site have been uncommonly observed in association with the venous puncture or contrast medium injection. On paravascular injection Gadovist may cause tissue pain lasting up to several minutes. Hypersensitivity reactions (e.g. urticaria, rash, vasodilatation) have been uncommonly reported and were mostly of mild to moderate intensity. In rare cases anaphylactoid reactions ranging to shock may occur. Delayed anaphylactoid reactions (after hours to days) have been observed rarely. Patients with an allergic disposition suffer more frequently than others from hypersensitivity reactions. Isolated cases of renal impairment or renal impairment aggravation have been reported. Isolated cases of nephrogenic systemic fibrosis (NSF) have been reported with Gadovist. **Date of revision of text:** January 2012 **Please note:** for current prescribing information refer to the package insert and/or contact your local Bayer HealthCare organisation. Bayer Pharma AG, 13342 Berlin, Germany. Adverse reactions can be reported to GPV.CaseProcessing@bayer.com



Innovative Contrast Agents for Medical Imaging



www.guerbet.de

Guerbet | 
Contrast for Life

© escapades